



CORROSION BEHAVIOUR OF METALS IN ARTIFICIAL URINE IN PRESENCE OF SODIUM CHLORIDE

**R. Nagalakshmi^[a], S. Rajendran^[b,c], J. Sathiyabama^[b],
M. Pandiarajan^{[b]*} and J. Lydia Christy^[d]**

Keywords: Mild steel, nickel –Ti super elastic alloy, Artificial Urine, sodium chloride, implants, biomaterials

Corrosion resistance of two metals namely mild steel (MS), Nickel Titanium super elastic alloy has been evaluated in artificial urine in the absence and presence of sodium chloride. Potentiodynamic polarization study has been used to investigate the corrosion behaviour of these metals. The order of corrosion resistance of metals in artificial urine, in the absence and also in the presence of sodium chloride was Ni-Ti super elastic alloy > mild steel.

*Corresponding Authors

*E-mail: pandiarajan777@gmail.com

- [a] Department of chemistry, Aarupadai Veedu Institute of technology, Chennai-603110, Tamilnadu, India. Email: nagalakshmirajan@gmail.com
- [b] PG and Research Department of Chemistry, GTN Arts College, Dindigul-624 005, Tamilnadu, India, E-mail: pandiarajan777@gmail.com
- [c] Research Centre RVS School of Engineering and Technology, Dindigul -624 005, Tamilnadu, India, E-mail: srmojany@sify.com
- [d] Department of Chemistry, VSB Engineering College Karur-639 111, Tamilnadu, India

Introduction

Titanium metal and its alloys are used in dental and orthopaedic implants on account of their excellent corrosion resistance, biocompatibility and osseointegration behaviour.¹⁻³

Commercially pure titanium (CP-Ti) is widely used as an implant material. The biocompatibility and corrosion resistance of the titanium metals the result of passive TiO₂ films of thickness 2–6 nm formed on the titanium surface.⁴⁻⁸ Many studies have been reported⁹⁻¹³ to understand the corrosion mechanism of pure titanium in different biological media. Various surface modifications like anodic oxidation treatments,¹⁴ electrochemical treatments,¹⁵ sandblasting,¹⁶ carbide coatings,¹⁷ laser nitriding,¹⁸ electrolytic polishing,¹⁹ etc., on CP-Ti implants have been carried out to improve their corrosion resistance. The above techniques have shown to improve the corrosion resistance of CP-Ti. But the strength of these implants still remains an issue of concern. Stainless steels, titanium alloys and cobalt alloys are commonly used as biomaterials.¹⁹⁻²⁵ Now a days NiTi shape memory alloys are also introduced to clinical practice. The major advantage of these biomaterials refers to their unique properties, i.e. a thermal shape memory effect and a super elasticity. When shape memory alloys are considered as candidates to be applied in medical devices, they must be able to fulfil functional requirements related not only to their mechanical reliability but also to their chemical reliability (in vivo degradation, decomposition and dissolution, corrosion, etc.) and their biological reliability

incompatibility, cytotoxicity, carcinogenicity, anti-thrombogenicity, antigenicity, etc. A great body of research was done to understand the mechanical and physicochemical properties to this extraordinary biomaterial and introduce it to clinical practice.²⁶⁻³³

In the present study commercially available sodium chloride was used. The present work was undertaken to study the corrosion behaviour of two metals namely mild steel (MS), Nickel-titanium super elastic alloy in artificial urine, in the absence and presence of sodium chloride by polarization study. Corrosion parameters such as corrosion potential, corrosion current and linear polarization resistance have been derived from these studies.

Materials and Methods

Two metals namely mild steel (MS), Nickel Titanium super elastic alloy were chosen for the present. The composition of mild steel was (wt %): 0.026S, 0.06P, 0.4 Mn, 0.1 C and balance iron.³⁴ The composition of Ni-Ti super elastic alloy was (wt%) Ni 55.5, and balance Ti.³⁵ The metal specimens were encapsulated in Teflon. The surface area of the exposed metal surface was 1 cm². The metal specimens were polished to mirror finish and degreased with trichloroethylene. The metal specimens were immersed in artificial urine (AU),³⁶ whose composition was: Solution A: CaCl₂.H₂O-1.765 g L⁻¹, Na₂SO₄-4.862 g L⁻¹, MgSO₄.7H₂O - 1.462 g L⁻¹, NH₄Cl - 4.643 g L⁻¹, KCl- 12.130 g L⁻¹. Solution :NaH₂PO₄.2H₂O - 2.660 g L⁻¹, Na₂HPO₄- 0.869 g L⁻¹, C₆H₅Na₃O₇.2H₂O - 1.168 g L⁻¹, NaCl -13.545 g L⁻¹. The pH of the solution was 6.5.³⁷ Just before the experiment, equal volumes of A and B were mixed and used as artificial urine.

In electrochemical studies the metal specimens were used as working electrodes. Artificial urine (AU) was used as the electrolyte (10 ml). The temperature was maintained at 37±0.1 °C. Commercially available sodium chloride was used in this study 50 ppm and 100 ppm of sodium chloride was dissolved in artificial urine.

Potentiodynamic polarization

Polarization studies were carried out in a CHI-Electrochemical workstation with impedance, Model 660A. A three electrode cell assembly was used. The working electrode was one of the two metals. A saturated calomel electrode (SCE) was the reference electrode and platinum was the counter electrode. From the polarization study, corrosion parameter such as corrosion potential (E_{corr}), Corrosion current (I_{corr}) and Tafel slopes (anodic = b_a and cathodic = b_c) were calculated.

Result and Discussion

Polarization Study

The polarization curves of mild steel immersed in Artificial Urine (AU) in the absence and presence of sodium chloride are shown in Figs 1 to 3. The corrosion parameters namely LPR , I_{corr} , E_{corr} , Tafel slopes (b_c = cathodic, b_a = anodic) are given in Table.1 when corrosion resistance of a metal in a medium increases, LPR (Linear polar resistance) value increases and corrosion current decreases.³⁸⁻⁴⁸

Table 1. Corrosion parameters of MS immersed in AU in absence and presence of sodium chloride obtained by polarization study.

System	E_{corr} mV*	b_c mV**	b_a mV**	LPR $\Omega \text{ cm}^2$	I_{corr} A cm^{-2}
AU	-0.651	183	208	11415	3.69×10^{-6}
AU+A	-0.697	146	207	8850	4.19×10^{-6}
AU+B	-0.681	162	220	7793	5.19×10^{-6}

AU=Artificial Urine; A=50ppm NaCl; B=100ppm NaCl; *mV vs SCE; ** mV in one decade.

It is observed from Table.1 that when 50ppm of sodium chloride is added to AU, the LPR value decreases from 11415 to 8850 ohmcm^2 . Correspondingly the corrosion current (I_{corr}) increases from 3.69×10^{-6} to 4.19×10^{-6} A cm^{-2} . When 100 ppm of sodium chloride is added to AU, the LPR value further decreases to 7793 ohm cm^2 and the corrosion current (I_{corr}) increases to 5.19×10^{-6} A cm^{-2} . In general it is observed that the corrosion resistance of MS in AU decreases in the presence of sodium chloride.

It is observed from the table that the corrosion potential shifts to cathodic side (more negative) in the presence of sodium chloride. Hence it is concluded that in presence of sodium chloride, the cathodic reaction is controlled predominantly.

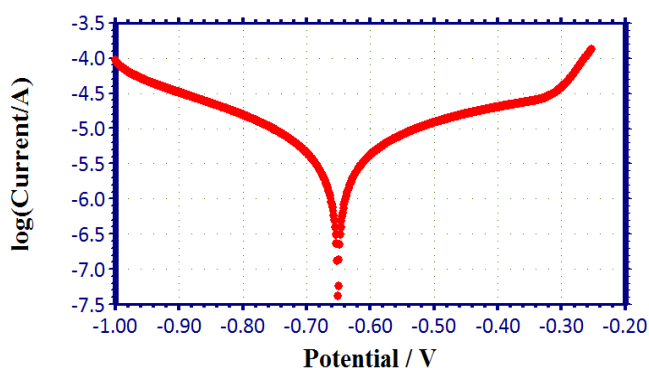


Figure 1. Polarization curves of MS is immersed in AU

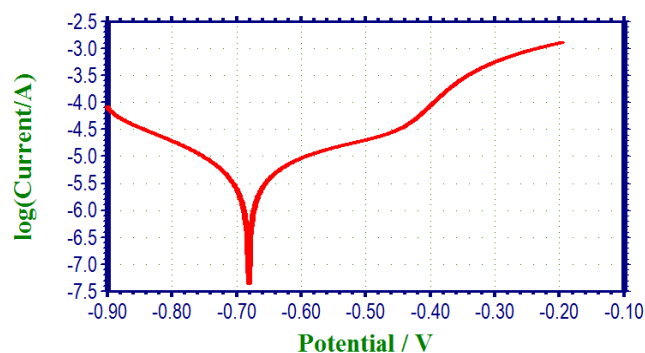


Figure 2. Polarization curves of MS is immersed in AU + 50ppm sodium chloride

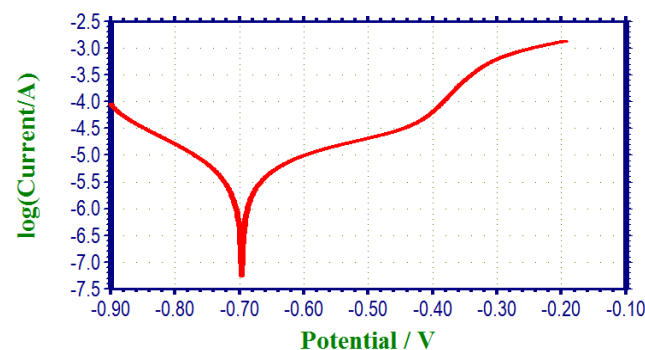


Figure 3. Polarization curves of MS is immersed in AU + 100ppm sodium chloride

Corrosion resistance of Ni-Ti superelastic alloy in AU in the presence of sodium chloride

The polarization curves of Ni-Ti super elastic alloy immersed in AU in the absence and presence of sodium chloride are shown in Fig. 8 The corrosion parameters namely LPR , I_{corr} , E_{corr} , Tafel slopes (b_c = cathodic, b_a = anodic) are given in Table.2. The polarization curves are shown in 4, 5 and 6.

Table 2. Corrosion parameters of Ni-Ti superelastic alloy immersed in AU in absence and presence of sodium chloride obtained by polarization study.

System	E_{corr} mv*	b_c mv**	b_a mv**	LPR $\Omega \text{ cm}^2$	I_{corr} A cm^{-2}
AU	-0.432	124	208	1.84×10^7	1.84×10^{-9}
AU+A	-0.493	121	304	1.93×10^7	1.95×10^{-9}
AU+B	-0.503	121	368	2.29×10^7	1.73×10^{-9}

AU=Artificial Urine; A=50ppm NaCl; B=100ppm NaCl; *mV vs SCE; ** mV in one decade.

It is observed from Table.2 that when 50 ppm of sodium chloride is added to AU, the LPR value increases from 1.84×10^7 to 1.93×10^7 $\Omega \text{ cm}^2$. Correspondingly the corrosion current (I_{corr}) decreases from 1.84×10^{-9} to 1.95×10^{-9} A cm^{-2} . When 100ppm of sodium chloride is added to AU, the LPR value further increases to 2.29×10^7 ohmcm^2 and the corrosion current (I_{corr}) decreases to 1.73×10^{-9} A cm^{-2} . In general it is observed that the corrosion resistance of Ni-Ti superelastic alloy in AU increases in the presence of sodium chloride.

It is observed from the table that the corrosion potential shifts to cathodic side (more negative) in the presence of sodium chloride. Hence it is concluded that in presence of sodium chloride, the cathodic reaction is controlled predominantly.

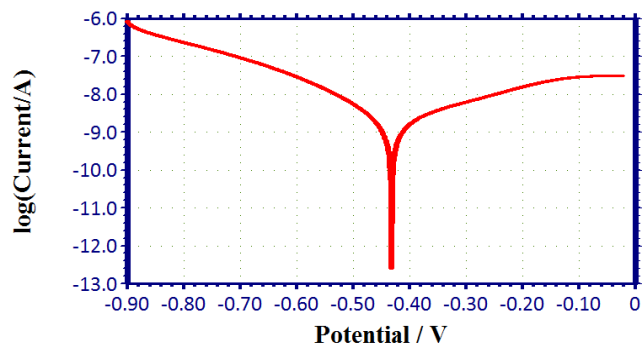


Figure 4. Polarization curves of Ni-Ti Super elastic is immersed in AU

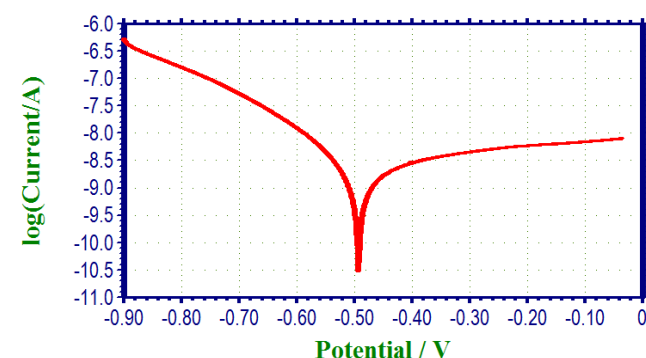


Figure 5. Polarization curves of Ni-Ti Super elastic is immersed in AU+50ppm sodium chloride

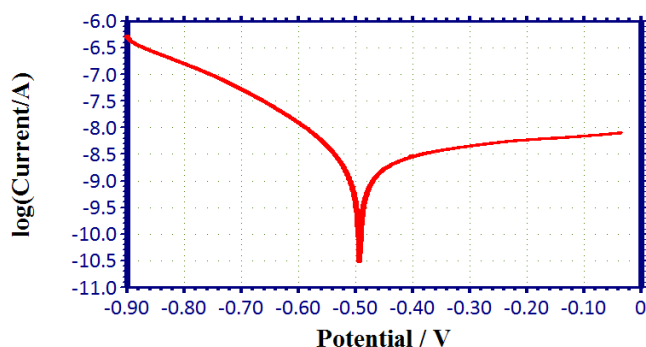


Figure 6. Polarization curves of Ni-Ti Super elastic is immersed in AU+100ppm sodium chloride

Conclusions

The corrosion behaviour of two metals namely mild steel (MS), Nickel-titanium super elastic alloy have been studied in artificial urine in the absence and presence of sodium chloride. Polarization has led to the following conclusions.

In the absence and presence of 50 ppm, 100 ppm of sodium chloride, the order of corrosion resistance was: Ni-Ti super elastic alloy > Mild steel.

Ni-Ti superelastic alloy was more corrosion resistant in the presence of sodium chloride than in its absence.

Mild steel was less corrosion resistant in the presence of sodium chloride than in its absence.

ACKNOWLEDGEMENT

The authors are thankful to their Managements and St,Joseph's Research and Community Development Trust, Dindigul, India for their help and encouragement.

References

- ¹Hobo, S., Ichida, E. and Garcia, L. T., *Osseointegration and Occlusal Rehabilitation*, (Ed) I. Quintessence Publishing, Tokyo, Japan, **1989**,
- ²Rubin, L. R., *Biomaterials in Reconstructive Surgery*, C. V., Mosby Company, St. Louis, **1983**, p.158
- ³Albrektsson, T., *CRC Critical Reviews in Biocompatibility*, **1984**, 1, 53,
- ⁴Esposito, M., Lausmaa, J., Hirsch, J. M. and Thomsen, P., *J. Biomed. Mater. Res.*, **1999**, 48, 55.
- ⁵Lopez, M. F., Jimenez, J. A., and Gutierrez, A., *Electrochim. Acta*, **2003**, 48, 1395.
- ⁶Strietzel, R., Hosch, A., Kalbfleisch, H., and Buch, D., *Biomaterials*, **1998**, 19, 1495
- ⁷Dearnley, P. A., Dahm, K. L., and Cimenoolu, H., *Wear*, **2003**, 256, 469.
- ⁸Velten, D., Biehl, V., Aubertin, F., Valeske, B., Possart, W. and Brems, J., *J. Biomed. Mater. Res.*, **2002**, 59, 18.
- ⁹Mabilleau, G., Bourdon, S., Joly-Guillou, M. L., Filmon, R., Baslé, M. F and Chappard, D., *Acta Biomater*, **2006**, 2, 121.
- ¹⁰Clark, G. C. F. and Williams, D.F., *J. Biomed. Mater. Res*, **1982**, 16, 1250.
- ¹¹Contu, F., Elsener, B. and Hohni, H., *J. Biomed. Mater. Res.*, **2002**, 62, 412.
- ¹²Ibris, N., and Rosca, J. C. M., *J. Electroanal. Chem*, **2002**, 526, 53.
- ¹³Choubey, A., Basu, B., and Balasubramanian, R., *Trends Biomater. Artif. Organs*, 2005, 18, 64.
- ¹⁴Song, H-J., Kim, M-K., Chun Jung-G., Sook Vang-M. and Joon Park-Y., *Surf. Coat. Tech.* **2007**, 201, 8738.
- ¹⁵Masmoudi, M., Assoul, M., Wery, M., Abdelhedi, R., El Halouani, F. and Monteil, G., *Appl. Surf. Sci.* **2006**, 253, 2237.
- ¹⁶Jiang, X. P, Wang, X. Y., Li, J. X., Li, D. Y., Man, C-S., Shepard, M. J. and Zhai, T., *Mater. Sci and Eng., A.*, 2006, 429, 30.
- ¹⁷He L., Zhang, X. and Tong, C., *Surf. Coat. Tech.*, 2006, 200, 3016.
- ¹⁸Carpene, E., Shinn, M., and Schaaf, P., *Appl. Surf. Sci.*, 2005, 247, 307.
- ¹⁹Guilherme, A.S., Henriques, G.E.P., Zavanelli, R.A., and Mesquita, M.F., *J.Prosth. Dent.*, **2005**, 93, 378.
- ²⁰Paszenda, Z., Tyrlik-Held, J., Marciniak, J., Wodarczyk, A *Achievements in Mechanical and Materials Engineering 2000*, Gliwice-Sopot-Gdansk, **2000**, 425.
- ²¹Szewczenko, J., Marciniak, J., *J. Mater. Process. Technol.*, **2006**, 175, 404.
- ²²Walke, W., Paszenda, Z., Tyrlik-Held, J., *J. Achiev. Mater. Manuf. Engg.* **2006**, 16, 74.
- ²³Chrzanowski, W., *J. Achiev. Mater. Manuf. Engg*, **2006**, 18, 67.

- ²⁴Krasicka-Cydzik, E., Kowalski, K., Glazowska, I., *J. Achiev. Mater. Manuf. Engg.*, **2006**, 18, 147.
- ²⁵Krauza, A., Zibowicz, A., Marciniak, J., *J. Achiev. Mater. Manuf. Engg.*, **2005**, 13, 355.
- ²⁶Shabalovskaya, S.A., *BioMed. Mater. Eng.*, **2002**, 12, 69.
- ²⁷Gil, F.J., Planell, J.A., *Proc. Instn. Mech. Engrs.*, **1998**, 212, 473.
- ²⁸Yang, H., Qian, L., Zhou, Z., Ju, X., Dong, H., *Tribology Lett.*, **2007**, 25, 215.
- ²⁹Chu, C. L., Chung, C. Y., Chu, P. K., *Mater. Sci. Eng., A*, **2006**, 417, 104.
- ³⁰Wang, J., Li, N., Rao, G., Han, E., Ke, W., *Dental Mater.*, **2007**, 23, 133.
- ³¹Wong, M. H., Cheng, F. T., Pang, G. K. M., Man, H. C., *Mater. Sci. Eng., A*, **2007**, 448, 97.
- ³²Michiardi, A., Aparicio, C., Planell, J. A., Gil, F. J., *Surf. Coat. Tech.* **2007**, 201, 6484.
- ³³Ju, X., Dong, H., *Surf. Coat. Technol.*, **2006**, 201, 1542.
- ³⁴Arockiaselvi, J., Rajendran, S., Ganga Sri, V., John, A., Narayanasamy, B., *Port. Electrochem. Acta.* **2009**, 27, 1.
- ³⁵Kaczmarek, M., *Achiev. Mater. Manuf. Eng.*, **2007**, 28(5), 269.
- ³⁶Przondziono, J., Walke, W., *J. Achiev. Mater. Manuf. Eng.*, **2009**, 35(1), 21.
- ³⁷Kajzer, W., Krauze, A., Walke, W., Marciniak, J., *J. Achiev. Mater. Manuf. Eng.*, **2006**, 18, 115.
- ³⁸Kavipriya, K., Sathiyabama, J., Rajendran, S. and Krishnaveni, A., *Int. J. Adv. Eng. Sci. Technol.*, **2012**, 2(2), 106.
- ³⁹Manimaran, N. and Rajendran, S., Manivannan, M. and Saranya, R., *J. Chem. Biol. Phys. Sci.*, **2012**, 2(2), 568.
- ⁴⁰Sahaya Raja, A. S. and Rajendran, S., *J. Electrochem. Sci. Eng.* **2012**, 2, 91.
- ⁴¹Benita Sherine, A., Jamal Abdul Nasser, A., and Rajendran, S., *Int. J. Adv. Eng. Sci. Technol.*, **2010**, 2(4), 314.
- ⁴²Leema Rose, A., Regis, P. P. A., Rajendran, S. Selvarani, F. R., Krishnaveni, S. A., *Zastit. Mater.*, **2010**, 51(4), 221
- ⁴³Sahayaraj, W. J., Rajendran, S., Muthu Megala, T.S., John, A. A., *Zastit. Mater.*, **2010**, 51(4), 232.
- ⁴⁴Benita Sherine, H., Jamal Abdul Nasser, A., Rajendran, S., *J. Electrochem. Soc. India*, **2009**, 58, 30.
- ⁴⁵Rajendran, S., Brigita, V. A., Manivannan, J., Jeyasundari, J., *Port. Electrochemica Acta.*, **2009**, 27(5), 555.
- ⁴⁶Nithiya, A., Rajendran, S., *Bulg. Chem. Ccommun.*, **2010**, 42(2), 119.
- ⁴⁷Rajendran, S., Uma, V., Krishnaveni, A., Jeyasundari, J., Shyamaladevi, B. and Manivannan, M., *Arab. J. Sci. Eng.* **2009**, 34(2), 147.
- ⁴⁸Anbarasi, M. C., Rajendran, S., Vijaya, N., Manivannan, M., and Shanthi, T., *The Open Corros. J.*, **2011**, 4, 40.

Received: 29. 11. 2012.

Accepted: 02. 01. 2013.



CHROMATOGRAPHY OF BEER

Tibor Cserhádi^[a] and Mária Szógyi^[a]

Keywords: gas chromatography, high performance liquid chromatography, dark and pale beers, beer specialities.

The objectives of the review are the collection, concise description and evaluation of the various chromatographic techniques used for the separation and quantitative determination of macro- and microcomponents present in beers.

Corresponding Authors

E-mail: szogyim@t-online.hu

[a] Research Center for Natural Sciences, Hungarian Academy of Sciences, Budapest, Hungary

Introduction

Beer is a popular beverage all over the world. It has been established many times that the moderate consumption of beer exerts favourable influences on human's health such as nutritional benefits, anti-mutagenic and anti-carcinogenic effects, reduction of cardiovascular diseases, hypolipidemic effect, stimulation of immune system, anti-osteoporosis effect and the reduction of the risk of dementia. It has been also found that the excessive consumption of beer may result in health disorders, allergy induction, increase in the plasma concentration of uric acid, mutation and induction of cancer, increase of the risk of dementia, obesity and social misbehaviour.^{1,2}

Gas chromatography (GC)

Gas chromatographic methods are generally applied for the separation and quantitative analysis of volatile and semi-volatile compounds. As beers contain volatile compounds of both natural and synthetic origin GC separation technologies found application in the investigation of the micro- and macro-components of beers. Headspace solid phase microextraction (HS-SPME) followed by gas chromatography mass spectrometric detection (GC-MS) was used for the study of the correlation between quantitative sensorial descriptors and chromatographic signals. Sensorial descriptors were estimated by conventional descriptive analyses (QDA). Genetic algorithm (GA) and ordered predictors selection (OPS) were applied as tools of selection of variables. The calculations revealed that the combination of sensorial descriptors and chromatographic signals can be successfully employed for the evaluation of foods and beverages.³

The maximum ethanol concentration in blood was measured after forced consumption of non-alcoholic beer. The investigations were carried out with headspace gas chromatography-flame ionization detection (HS-GC-FID). The limit of detection (LOD) was 0.0000 g L⁻¹, the maximum concentration of ethanol in blood was 0.0056 %. The investigations indicated that forensic implications cannot be expected from the consumption of non-alcoholic beer.⁴ The aroma stability of beers under different storage conditions was investigated by HS-SPME/GC-MS and the

influence of the extraction conditions on the efficacy of extraction was studied in detail. The data were evaluated by linear regression analysis. The calculations revealed that the sample volume (V) and extraction temperature (T) exert the highest impact on the extraction yield. The effect of storage temperature and the length of storage on the volatile profile was also determined. The measurements indicated that both the length and temperature of the storage influence the aroma profile of beers.⁵ GC-olfactometry, GC-MS, and GC combined with pulsed flame photometric detection were employed for the study of the occurrence of polyfunctional thiols in sorghum beer. Target compounds were selectively extracted with p-hydroxymercuribenzoic acid. It was established that the application of *Vernonia amygdalina* influences considerably the character of beer.⁶ A novel dispersive liquid-liquid microextraction (DLLME) coupled with GC-MS were employed for the separation and quantitative determination of 18 biogenic amines in beers. It was found that the simultaneous extraction/derivatization of the amines results in a fast and simple extract enrichment. The extracting agent consisted of acetonitrile (dispersive solvent; 1.0 mL), toluene (extracting solvent; 325 µL), and isobutyl chloroformate (derivatizing agent; 25 µL). The recoveries ranged from 72 to 113 %. The inter-day and intra-day precision was 13 and 14 %, respectively. LOD was always lower than 2.9 µg L⁻¹. It was established that the putrescine, tyramine, dimethylamine, cadaverine, pyrrolidine, and 1,3-diaminopropane were the dominant biogenic amines in beers.⁷ The newest results in the theory and practice of the application of GC-olfactometry (GC-O) of alcoholic beverages have been previously discussed. The principles of GC-O methodology, sample preparation techniques, data collection procedures, GC instrumentation and other analytical conditions have been explained in detail. Examples for the analysis of alcoholic beverages such as wine, beer and spirits are presented.⁸

High performance liquid chromatography (HPLC)

Natural components

The allergy to beer has been extensively investigated. It has been established that in the majority of cases beer allergy was correlated with the hypersensitivity to the non-specific lipid transfer protein (LTP). The immun reactive LTP was separated by HPLC. The measurements indicated that allergy to beer considerably depends on the type and on the character of brewing process.⁹ The cause of the rapid deterioration of flavour of beer has been intensively

investigated using HPLC technologies. It was established that this procedure may be due to the vulnerability of iso-alpha-acids to the light, the oxidation of iso-alpha acids. The stability of beers can be improved by adding phenolic compounds with antioxidant properties, addition of pure stereoisomers cis-iso-alpha acids or their reduced species, or use of riboflavin-binding proteins.¹⁰ Real degree of fermentation (RDF) is an important characteristic of brewhouse performance. The relationship between RDF and the properties of malted barley starch has been intensively investigated. The molecular size distribution was determined with high performance size exclusion chromatography (HPSEC). Target compounds were detected with multi-angle laser light scattering. The data were analysed by various multivariate mathematical-statistical methods such as cluster analysis, analysis of variance, principal component analysis. Starch properties explained the 86% of the RDF variance suggesting that other malted barley constituents may influence the relationship.¹¹

A simple and rapid analytical method was developed for the determination of 9 heterocyclic amines in beer and beer-like drinks. Measurements were carried out by employing hydrophilic interaction liquid chromatography-mass spectrometry. The recoveries of the measurements varied between 72-123 % for pilsner beer and 61-96 % for dark beer. As heterocyclic amines were not detected in the samples it was concluded that the health risk due to heterocyclic amines in beers and beer-like drink is extremely low (English abstract).¹² Dispersive liquid-liquid microextraction (DLLME) followed by LC with fluorometric detection has been employed for the analysis of thiamine (vitamin B-1) in foods. Derivatization was carried out by the oxidation of thiamine with ferricyanide at pH 13 to form fluorescent thiochrome. DLLME method was carried out by mixing 0.5 mL acetonitrile (dispersing agent) containing 90 μL of tetrachloroethane (extraction solvent). The mixture was added to 24 % of sodium chloride. Phase separation was achieved by centrifugation and the sedimented phase was analyzed by HPLC. LOD was 0.09 ng mL^{-1} , relative standard deviation was 3.2 %. It was established that the method can be applied for the analysis of thiamine monophosphate and thiamine pyrophosphate after acidic and enzymatic treatments. The procedure was successfully employed for the determination of thiamine in various foods and food products such as beer, brewer's yeast, honey, baby foods, infant formulas, fermented milk, cereals, and purees. Before HPLC analyses solid samples were hydrolysed with trichloroacetic acid. It was found that the results obtained by analyzing certified reference material were in excellent agreement with the certified value.¹³

A method using derivatization followed by RP-HPLC was developed for the determination of diacetyl an important flavour compound. Because of its importance as flavour compound and its impact on human health a considerable number of chromatographic method have been developed and applied for their determination in beers. A new method based on the derivatization of diacetyl and the subsequent separation of the derivatized product has been published. Diacetyl was derivatized with 4-nitro-o-phenylenediamine (NPDA) at 45°C, for 20 min, at pH 3. The resulting 6-nitro-2,3-dimethylquinoxaline was separated on a RP18 column.

Target compound was detected at 257 nm. LOD was 0.0008 mg L^{-1} , the recoveries ranged 94-99.0 % The relative standard deviation range was 1.20-3.10 %. The

concentration of diacetyl in the samples varied between 0.034 – 0.110 mg L^{-1} . Because of the excellent separation capacity, linearity and good repeatability the method was proposed for the determination of diacetyl in beer samples.¹⁴ An automatic headspace in-tube extraction (ITEX) method was employed for the determination of acetaldehyde, ethyl acetate, diacetyl, and other volatile compounds in wine and beer. The optimization process established that the vial and sample sizes and the trapping material are most important parameters of the accuracy of the method. Small 2 mL vials containing a very small amount of sample (20 μL of 1:10 diluted sample) and a trap filled with 22 mg Bond Elut ENV was applied. The effective extraction required 100 x 0.5 mL pumping strokes at 60 °C. Determination coefficients were over 0.995, the repeatability was better than 7 %, and reproducibility was lower than 8.3%. It was stated that the method can be used for the investigation of volatile compounds in complicated matrices.¹⁵ The influence of immobilized matrix on the fermentation process has been studied in detail and the results were compared with the results obtained with the results of traditional brewing. Cell microencapsulated technology was applied as a new brewing technique. Cell were microencapsulated in alginate. The investigated parameters included glucose concentration, cell multiplication, cell viability, specific gravity, pH, Brix, and ethanol. Fermentation processes were followed by both sensorial and instrumental methods (gas chromatography). No significant differences were found between the sensory characteristics of the beers brewed by the traditional and modern technologies. Although the profile of the headspace compounds were different it does not influenced the sensorial character of the beers.¹⁶ It has been previously established that the yeast (*Saccharomyces cerevisiae*) and lactic bacteria are able to accumulate and biotransform inorganic selenium into organo Se compounds. Selenium biotransformation was followed during brewing by using *S. cerevisiae* and *Saccharomyces uvarum* for Ale and Lager fermentations, respectively. Se-enriched beer was produced by adding sodium selenite (0.02, 1.0, 2.0, 10.0 and 20 $\mu\text{g mL}^{-1}$). The fermentation brew contained yeast, malt extract and water. Target compounds were separated by HPLC-ICP-MS and anion exchange HPLC. It was established that selenomethionin was the most frequent organo Se compound found during the investigations.¹⁷ The concentration of biogenic amines (BA) and polyamines (PA) were determined in alcoholic and non-alcoholic beer in the Czech Republic. The measurements established that the concentration of histamine, phenylethylamine and tryptamine was very low in the samples. The amount of the PA spermine and spermidine was also low. However, the total amount of BA and PA exceeded the "healthy" level of 100 mg L^{-1} .¹⁸ A new method was developed for the removal of volatile compounds from complicated accompanying matrices. Nitrogen gas stripping combined with high vacuum (NSHV) was employed for the removal of volatile components without the application of heat. It was established that the efficacy of the method is higher than that of the traditional rotary evaporation. The application of the new method was proposed for the removal of volatile compounds from beer and possibly other liquid samples as well.¹⁹ The production of eight biogenic amines (BAs) (histamine, tyramine (TYR), tryptamine, putrescine, cadaverine (CAD), phenylethylamine, spermine and spermidine) by 81 lactic acid bacteria (LAB) strains (*Lactobacillus*, *Lactococcus*, *Leuconostoc*, *Enterococcus*,

Pediococcus, *Tetragenococcus* and *Bifidobacterium*) was investigated. It was established that contaminating LAB can increase the concentration of CAD and TYR in beer.²⁰ The new extraction technique gas diffusion microextraction (GDME) has been employed for the determination of methylamine, dimethylamine and ethylamine in beers and other fermented beverages. Amines were extracted with GDME, and derivatised with phenyl isothiocyanate (PITC). Target compounds were analysed by HPLC using UV detection. LOD was between 12 – 46 $\mu\text{g L}^{-1}$, LOQ ranged from 39 to 153 $\mu\text{g L}^{-1}$. Because its simplicity GDME was proposed for the extraction of aliphatic amines in fermented beverages.²¹ The influence of the different beers on the mechanism of gastric acid secretion has been studied in detail. Organic acids and bitter compounds were separated by HPLC-DAD and UPLC-MS/MS. It was found that ethanol, and organic acids such as succinic acid, malic acid, and citric acid influence the gastric acid secretion. It was further established that the bitter acids such as alpha-, beta-, and iso-alpha acids play a considerable role in the regulation of gastric acid secretion.²²

Environmental pollutants

A triple quadruple LC-MS/MS method was developed for the determination of the *Fusarium* mycotoxins deoxynivalenol (DON), 3-acetyl-DON (3-ADON) and the conjugated mycotoxin deoxynivalenol-3-glucoside (D3G). Before HPLC analysis the samples were degassed, the matrix compounds were precipitated and the dried rests were dissolved in the solvent. The relative standard deviation of the measurements were 4-16 %. Recoveries for DON, D3D and 3-ADON were 60-90, 39-69 and 96-124 %, respectively. It was established that beers contain in average 6.6 $\mu\text{g L}^{-1}$ DON and D3G, while 3-ADON was not detected. The occurrence of mycotoxins together with endotoxins was investigated in indigenous banana beer. The measurements prove the presence of both mycotoxins and endotoxins causing health risk for consumers.²³ The influence of unmalted barley on the oxidative stability of wort and beer has also been investigated by GC-MS. The results indicated that the addition of barley increased the oxidative beer stability.²⁴ GC-MS method was applied for the determination of the effect of wood aging on beer flavor and the concentration of monophenols. The investigation indicated that the addition of oak chips modified considerably the flavor profile of the beer. The woody, vanilla-like, spicy, and smoky aroma increased. The concentration of monophenols as vanillin, acetovanillone, syringaldehyde, acetosyringone, guaiacol, ethylguaiacol, eugenol, thymol, and salicylaldehyde were also elevated. Both sensory effects and monophenol concentrations were correlated with the origin and toasting degree of the oak chips applied.²⁵ The concentration of phenolic compounds and their antioxidant activity in barley and malt extract were investigated by liquid chromatographic technologies. Barley and malt were extracted with ethyl acetate and the component of the extracts were separated with RP-HPLC. Detection was carried out on two wavelengths one for the detection of phenolic compounds the other for the reduced form of the radical cation 2,2'-azinobis(3-ethylbenzothiazoline-6-sulfonic acid) (ABTS). It was found that prodelphinidine 83 and procyanidin B3 are responsible for the overwhelming majority of the antioxidant activity. It was further established that malting and brewing markedly

decreases both the concentration and antioxidant activity of phenolic compounds.²⁶ The effect of mashing technology processes on the composition and quantity of phenolic compound was investigated by HPLC, and by other two electron spin resonance method. The measurements indicated that the concentration of polyphenols decreases during the mashing process.²⁷ HPLC/MS combined with clean upon immunoaffinity column was employed for the determination of aflatoxins B1, B2, G1 and G2 in brewing raw material and beer. LOD ranged 0.04 – 0.12 $\mu\text{g kg}^{-1}$ in barley and malt, 0.08 – 0.58 $\mu\text{g kg}^{-1}$ in hops, 0.04 – 0.12 $\mu\text{g kg}^{-1}$ in brewers' yeast, and spent grains, and 1.5 – 4.7 ng L^{-1} in beer. LOQ varied from 0.13 – 0.39 $\mu\text{g kg}^{-1}$ in barley and malt, 0.25 - 1.94 $\mu\text{g kg}^{-1}$ in hop samples, 0.13 – 0.39 $\mu\text{g kg}^{-1}$ in brewers yeast and spent grains, and 5.1 – 15.2 $\mu\text{g L}^{-1}$ in beer. It was established that the aflatoxin levels did not exceed the maximum allowable limit set by the European Union²⁸. The formaldehyde level in beers was also measured by HPLC. The target molecule was preconcentrated with the cloud point extraction method. Formaldehyde was complexed with 2,4-dinitrophenylhydrazine in an aqueous solution of the nonionic surfactant Triton X-114. The target compound was concentrated at the temperature of 60°C. LOD was 0.7 ng mL^{-1} . The concentration of formaldehyde ranged 172-385 ng mL^{-1} . This new sensitive and rapid procedure was proposed for the determination of formaldehyde in beer.²⁹ The occurrence of Ochratoxin A (OTA) in various manufactured food products has been investigated. Samples were prepurified on an immunoaffinity column (IAC). Separation and quantitative determination was carried out by HPLC-FD, and confirmed with LC-ESI-MS/MS. Recoveries were between 78.3 – 103.3 %. RSDs (relative standard deviations) was 2.1 – 4.3 %. It was concluded from the data that the consumption of the food products investigated present no risk to consumers³⁰. The concentration of OTA was measured in various foods and food products such as composite samples of cereal-based baby foods, beer, breakfast cereals (corn and rice and wheat based), loaf bread, peanuts, and pistachios. Samples were pretreated by liquid-liquid extraction followed by separation on immunoaffinity column and HPLC measurements. The results indicated that the median estimated daily intake of OTA through the foodstuffs were below the latest provisional (PTDIs) tolerable daily intakes recommended by the Food Safety Authority (EFSA) in 2006 and the Joint FAO/WHO Expert Committee on Food Additives (JECFA).³¹ Plasma ochratoxin A levels were determined in men and women in the Molise region Italy. The relationship between the concentration of ochratoxin A in plasma and some physicochemical parameters such as dietary habits, specific disease risk biomarkers (body mass index) (BMI), C-reactive protein (CRP), cardiovascular risk score were calculated. The amount of ochratoxin A in plasma was evaluated by HPLC. CRP was measured by a latex particle enhanced immunoturbidimetric assay. LOD was 25 ng L^{-1} , the mean \pm standard deviation was 0.229 \pm 0.238 ng mL^{-1} . The investigations revealed that cereals, wine, beer and jam/honey influence the level of OTA in plasma. It was further established that the positive correlation between OTA and CRP suggests a possible role of OTA in inflammation and in the genesis of cardiovascular diseases and cancer.³² A novel method was developed for the separation and quantitative determination of chloroacetic, bromoacetic and iodoacetic acids in alcoholic beverages. Monohalogenic acids (m-HAAS) were extracted using static headspace extraction and were esterified to increase their

volatility. It was stated that the method is suitable for the detection of monohalogenated acids at the concentration of $\mu\text{g L}^{-1}$.³³ Formaldehyde was classified as carcinogenic to humans. It can cause leukemia and nasopharyngeal cancer. The exposure to formaldehyde in alcoholic beverages has been discussed in detail. It was concluded that formaldehyde in alcoholic beverages cause a negligible risk for consumers, the main risk factors are ethanol and acetaldehyde.³⁴ SPME using on-fibre derivatization was applied for the analysis of furfural in infant formulas, beers and vinegars. The poly(dimethylsiloxane)divinylbenzene (PDMS/DVB) fibre was employed and O-2,3,4,5,6-(pentafluorobenzyl)-hydroxylamine hydrochloride (PHBFA) was loaded onto the fibre. Food samples of 2 mL were placed in a glass vial. SPME was carried out at 80 °C for 20 min under magnetic stirring. SPME fibre was desorbed at the injection port of GC/MS. The method detection limits (MDLs) were lower than 5%. Recoveries were $100 \pm 5\%$, MDLs ranged from 3.09 to 14.05 $\mu\text{g L}^{-1}$.³⁵ HPLC combined with UV detection and triple quad MS was applied for the separation and quantitative determination of the Maillard reaction product 6-(2-formyl-1-pyrrolyl)-l-norleucine (formyline). This new pyrrole amino acid resulted from the reaction of free and protein-bonded lysine residues with the 1,2-dicarbonyl compounds such as 3-deoxyxypentosone, pentose sugars, and degradation products of disaccharides. Formyline and its structural analog pyrroline were detected in enzymatically hydrolyzed food matrices (milk and whey products, breakfast cereals, pasta, and bakery products). It was further established that formyline and pyrroline are constituents of beer proteins.³⁶ A GC/MS method was employed for the determination of ethyl carbamate (EC) in fermented foods and beverages. It was established that rice wines contained up to $515 \pm \mu\text{g kg}^{-1}$ ethyl carbamate; rice cooking wine $206 \pm 87 \mu\text{g kg}^{-1}$; white spirits, wine and beer $72 \pm \mu\text{g kg}^{-1}$; Soy sauces and vinegars contained also EC in the concentration of $47 \pm 27 \mu\text{g kg}^{-1}$. EC was determined in normal sufu ($63 \mu\text{g kg}^{-1}$) and in red sufu ($182 \mu\text{g}$).³⁷

HOP

High speed counter-current chromatography (HSCCC) and HPLC were applied for the separation of xanthohumol (XN) and related prenyl flavonoids from the hops (*Humulus lupulus L.*). The solvent system employed for the analysis of XN consisted of n-hexane-ethyl acetate-methanol-water 5; 5; 4; 3. It was established that the method can be successfully used for the isolation of XN from hop extract. The purity of XN was over 95%, the yield of the extraction was 96.60%. UV, H1 NMR, and C13 NMR technologies were applied for the elucidation of the exact structure of XN.³⁸

Electrically driven systems

Capillary zone electrophoresis (CZE) has been used for the analysis of compositional carbohydrates in polysaccharides and foods. The method made possible the simultaneous determination of thirteen reducing carbohydrate such as aldohexose, aldopentose, maltose and lactose. Analytes were derivatized with 1-phenyl-3-methyl-5-pyrazolone (PMP). The conditions of the CZE measurement were: background electrolyte 175 mM borate buffer (pH 11.0), organic modifier: methanol; detection 245

nm. The quantitative recoveries of compositional carbohydrates in the samples were between 93.2 – 104.0 %, the RSD values varied between 2.9% - 4.9 %. The method was proposed for the quality control of reducing carbohydrates in food analysis. A thin-layer electrochemical flow cell coupled with capillary electrophoresis with contactless conductivity detection (EC-CE-C⁴D) was employed for the derivatization and quantification of aliphatic alcohols (ethanol, 1-propanol, 1-butanol, and 1-pentanol). The simultaneous electrooxidation of the analytes were carried out on a platinum working electrode in acid medium. The analysis time was 2.5 min., the LOD was $5 \times 10^{-5} \text{ mol L}^{-1}$. It was established that no significant differences can be found between the results obtained with the new method and those obtained by the traditional GC/MS procedure.³⁹

The volatile compounds of hop were analysed by a headspace (HS)-trap method followed with GC-MS. The investigations revealed that steam distillation is not suitable for the preconcentration of thermolabile compounds, such as caryophyllene oxide. It was stated that the HS-trap procedure is fast and sensitive, requires small sample volume and minimal sample preparation steps.⁴⁰ Headspace solid-phase microextraction followed with GC/MS was employed for the determination of the terpenoid (monoterpenes and sesquiterpenes) metabolic pattern of hop-essential oil. The parameters of the extraction (type of fiber coatings, extraction temperature, extraction time, ionic strength, and sample agitation) were optimized: analytes were extracted for 30 min at 40 °C using a 50/30 μm divinylbenzene/carboxene/polydimethyl siloxane coated fiber. The measurements established that hop essential oil contained 56.1 % monoterpenes (13 compounds); 39.9 % sesquiterpenes (10 compounds); 1.41 % oxygenated monoterpenes (3); 0.04 % hemiterpenes (1). The main metabolites were identified as monoterpene β -myrcene ($53.0 \pm 1.1\%$); and cyclic sesquiterpenes, α -humulene ($16.6 \pm 0.8\%$); β -caryophyllene ($14.7 \pm 0.4\%$). It was further proposed that hop essential oil can be applied as a powerful biosource of terpenoid metabolites.⁴¹

Abbreviations

ABTS	2,2'-azinobis(3-ethylbenzothiazoline-6-sulphonic acid)
BA	biogenic amines
BMI	body mass index
CAD	cadaverine
CRP	C-reactive protein
CZE	capillary zone electrophoresis
EC	ethyl carbamate
EFSA	European Food Safety Authority
DLLME	dispersive liquid-liquid microextraction
DON	deoxyvalenol
D3G	deoxyvalenol-3-glucoside
FID	flame ionization detector
FD	fluorescence detection
GA	genetic algorithm
GC	gas chromatography

GC-MS	gas chromatography with mass spectrometric detection
GC-O	gas chromatography-olfactometry
GDME	gas-diffusion microextraction
HPLC	high performance liquid chromatography
HPLC-DAD	high performance liquid chromatography diode array detection
HPSEC	molecular size distribution
HS	headspace
HSCCC	high-speed counter-current chromatography
HS-SPME	headspace solid phase microextraction
IAC	immunoaffinity column
JECFA	Joint FAO/WHO Expert Committee on Food Additives
LAB	lactic acid bacteria
LC-MS/MS	quadruple LC-MS/MS
LOD	limit of detection
LOQ	limit of quantitation
LTP	non-specific lipid transfer protein
MDLs	method detection limits
NSHV	nitrogen gas stripping coupled with high vacuum
OTA A	ochratoxin A
OPS	ordered predictors selection
QDA	quantitative descriptive analysis
PMP	1-phenyl-3-methyl-5-pyrazolone
PA	polyamines
PDMS/DVB	poly(dimethylsiloxane)/divinylbenzene
PFBHA	O-2-3-4-5-6-(pentafluorobenzyl) hydroxylamine hydrochloride
RDF	real degree of fermentation
RSD	relative standard deviation
SPME	solid-phase microextraction
T	extraction temperature
TRY	tyramine
UPLC	ultra performance liquid chromatography
V	sample volume
XN	xanthohumol

References

- Malachova, A., Varga, E., Schwartz, H., Krska, R., Berthiller, F. *World Mycotox. J.* **2012**, *5*, 261-270.
- Sohrabvandi, S., Mortazavian, A. M., Rezaei, K., *Int. J. Food Prop.*, **2012**, *15*, 350-373.
- Da Silva, G. A., Maretto, D. A., Bolini, H. M. A., Teofilo, R. F., Augusto, F., Poppi, R., *J. Food Chem.*, **2012**, *134*, 1673-1681.
- Thierauf, A., Perdekamp, M. B., Auwarter, V., *Rechtsmedizin* **2012**, *22*, 244-247.
- Wang, T., Yang, X., Wang, D., Jiao, Y., Wang, Y., Zhao, Y. *Carbohydr. Polym.* **2012**, *88*, 754-762.
- Rodríguez-Bencomo, J. J., Muñoz-González, C., Martín-Álvarez, P. J., Lazaro, E., Mancebo, R., Castane, X., Pozo-Bayón, M. A., *Food Anal. Meth.* **2012**, *5*, 1386-1397.
- Lyumugabe, F., Gros, J., Thonart, P., Colline, S. *Flav. Fragr. J.* **2012**, *27*, 372-377.
- Almeida, C., Fernandes, J. O., Cunha, S. C., *Food Control*, **2012**, *25*, 380-388.
- Plutowska, B., Wardenecki, W., *Alc. Bever.: Sens. Eval. Consum. Res.* **2012**, *225*, 101-130
- Quercia, O., Zoccatelli, G., Stefanini, G. F., Mistrello, G., Amato, S., Bolla, M., Emiliani, F., Asero, R. *Allergy* **2012**, *67*, 1186-1189.
- Caballero, I., Blanco, C. A., Porras, M., *Trends Food Sci. Technol.*, **2012**, *26*, 21-30.
- Patindol, J., Mendez-Montealvo, G., Wang, Y. J., *Starch-Starke* **2012**, *64*, 517-523.
- Kakigi, Y., Yamashita, A., Icho, T., Mochizuki, N., *Bunseki Kagaku*, **2012**, *61*, 391-396.
- Vinas, P., Lopez-Garcia, I., Bravo-Bravo, M., Briceno, M., Hernandez-Cordova, M. *Anal. Bioanal. Chem.*, **2012**, *403*, 1059-1066.
- Li, P.L., Zhu, Y.C., He, S., Fan, J.K., Hu, O.B., Cao, Y.S., *J. Agr. Food Chem.*, **2012**, *60*, 3013-3019.
- Zapata, J., Mateo-Vivaracho, L., Lopez, R., Ferreira, V. *J. Chromatogr. A.*, **2012**, *1230*, 1-7.
- Almonacid F. S., Najera, A. L., Young, M. E., Simpson, R. J., Acevedo, C. A., *Food Bioproc. Technol.*, **2012**, *5*, 750-758.
- Sanchez-Martinez, M., Maria da Silva, E.G.P., Perez-Corona, T., Camara, C., Ferreira, S.L.C., Madrid, Y., *Talanta*, **2012**, *88*, 272-276.
- Bunka, F., Businsky, P., Cechova, M., Drienowsky, V., Pachlova, V., Matoulkova, D., Kuban, V., Bunkova, L., *J. Inst. Brewing*, **2012**, *118*, 213-216.
- Castro, R. F., Ross, C. F., *J. Am. Soc. Brew. Chem.*, **2012**, *70*, 137-141.
- Lorencova, E., Bunkova, L., Matoulkova, D., Drab, V., Pleva, P., Kuban, V., Bunka, F., *Int. J. Food Sci. Technol.*, **2012**, *47*, 2086-2091.
- Valente, I. M., Santos, C. M., Goncalves, L. M., Rodrigues, J. A., Barros, A., *Anal. Meth.* **2012**, *4*, 2569-2573.
- Walker, J., Hell, J., Liszt, K. I., Dresel, M., Pignitter, M., Hofmann, T., Somoza, V., *J. Agr. Food Chem.*, **2012**, *60*, 1405-1412.
- Shale, K., Mukamugena, J., Lues, R.J., Venter, P., *Food Add. Contam. Part A Chem. Anal. Contr. Exp. Risk Assessment* **2012**, *29*, 1300-1306.
- Kunz, T., Muller, C., Mato-Gonzales, D., Methner, F. J., *J. Inst. Brew.*, **2012**, *118*, 32-39.
- Sterckx, F. L., Saison, D., Delvaux, D., *J. Am. Soc. Brew. Chem.* **2012**, *70*, 55-61.
- Leitao, C., Marchioni, E., Bergaentzle, M., Zhao, M. J., Didierjean, L., Miesch, L., Holder, E., Miesch, M., Ennahar, S., *J. Cereal Sci.*, **2012**, *55*, 318-322.
- Jurkova, M., Horak, T., Haskova, D., Culik, J., Cejka, P., Kellner, V., *J. Inst. Brew.*, **2012**, *118*, 230-235.
- Benesová, K., Běláková, S., Mikulíková, R., Svoboda, Z., *Food Control*, **2012**, *25*, 626-630.
- Wang, T., Gao, X. L., Tong, J., Chen, L. G., *Food Chem.*, **2012**, *131*, 1577-1582.
- Wu, J. W., Tan, Y. F., Wang, Y. Q., Xu, R., *Mycopathologia* **2012**, *173*, 199-205.
- Coronel, M. B., Marin, S., Cano-Sancho, G., Ramos, A.J., Sanchis, V. *Food Addit. Contam. A.* **2012**, *29*, 979-993.

- ³²Di Giuseppe, R., Bertuzzi, T., Rossi, F., Rastelli, S., Mulazzi, A., Capraro, J., De Curtis, A., Laccoviello, Pietri, A., *Eur. J. Nutr.* **2012**, *51*, 851-860.
- ³³Cardador, M. J., Gallego, M., *J. Agr. Food Chem.*, **2012**, *60*, 725-730.
- ³⁴Monakhova, Y., Jendral, J., Lachenmeier, D. *Arhiv Hig. Rada Toksikol.*, 2012, *63*, 227-237.
- ³⁵Tsai, S. W., Kao, K. Y., *Int. J. Env. Anal. Chem.*, 2012, 9276-84.
- ³⁶Hellwig, M., Henle, T., *Eur. Food Res. Technol.*, 2012, 235, 99-106.
- ³⁷Wu, P., Pan, X., Wang, L., Shan, X., Yang, D., *Food Control* 2012, *23*, 286-288.
- ³⁸Chen, Q. H., Fu, M. L., Chen, M. M., Liu, J., Liu, X. J., He, G. Q., Pu, S. C., *Food Chem*, **2012**, *132*, 619-623.
- ³⁹Santos, M. S. F., Lopes, F. S., Vidal, D. T. R., Do Lago, C. L., Gutz, I. G. *Chem.*, **2012**, *84*, 7599-7602.
- ⁴⁰Aberl, A., Coelhan, M., *J. Agr. Food Chem.*, **2012**, *60*, 2785-2792.
- ⁴¹Goncalves, J., Figueira, J., Rodrigues, F., Camara, J. S., *J. Sep. Sci.*, **2012**, *35*, 2282-2296.

Received: 29.12.2012.

Accepted: 03.01.2012.



REVIEW ON PERFORMANCE AND AGING KINETICS OF CRUMB RUBBER MODIFIED ASPHALTS

Liu Shu^{[a]*}, Zhang Yongmei^[a] and You Hongjun^[b]

Keywords: performance; aging kinetics; crumb rubber modified asphalt

The present article gives an overview on performance and aging kinetics of matrix and crumb rubber modified asphalts. Three types of asphalts such as crumb rubber modified asphalt, AH-70 and AH-90 have been introduced. Equations related to aging kinetics have also been used in crumb rubber modified asphalt system. The experimental results show that the aging process of two types of asphalts (crumb rubber modified asphalt and AH-70) are of first order kinetics, and the anti-aging performance of crumb rubber modified asphalt is found to be better than that of AH-70.

* Corresponding Author

Fax: 86-24-56860869

E-Mail: youhongjun@hotmail.com

[a] Liaoning Shihua University, Fushun, Liaoning, P.R. China.

[b] SAIT Polytechnic, Calgary, Alberta, Canada.

Introduction

Nowadays a large number of vehicles are required due to rapid growth of the *Chinese* economy; therefore, road material pavement faces serious challenges with respect to *Chinese* upcoming regulations such as rutting, cracking, stripping and decreasing anti-slipping. *Chinese* scientists have been working on improving the performance of road materials in order to meet road development in *China*. Most of asphalts in *China* belong to multi-wax W grade asphalts. Its performance is supposed to be very poor in respect of low adhesive property, high temperature sensitivity, poor heat stability, low thermal crack resistance, easily flowing under the condition of high-temperature and rapidly hardening to become solid under the condition of low-temperature, therefore, it is very difficult for this type of asphalt to meet *Chinese* road design standard. ¹ Crumb rubber is added into asphalts to improve its performance, such as needle penetration, elasticity, ductility and anti-deformation. Its high-temperature stability, anti-cracking and anti-fatigue performance are increased.²

In the present paper, the thermal performance of matrix asphalt and crumb rubber modified asphalt has been compared. Three types of asphalts (crumb rubber modified asphalt, AH-70 and AH-90) have also been studied. Further, aging kinetics equations have also been applied.

Discussion

Comparing the thermal performance between matrix asphalt and crumb rubber modified asphalt ³

Three types of asphalts (No.1, No.2 and No.3) were synthesised by the addition of AH-70 as matrix asphalt and crumb rubber as a modified agent. Its properties were presented in Table 1. The experimental results showed that the performance of asphalt was improved by the addition of crumb rubber. The properties of crumb rubber modified asphalt

satisfied *American* standard. On the other hand, matrix asphalt (AH-70) did not meet *American* standard under the condition of the reaction temperature (163 °C) and the reaction time (5 hours). This proved that crumb rubber improved the performance of asphalt.

Table 2 showed effects of thermal sensitivity on matrix asphalt and crumb rubber modified asphalt. Chen Huiming⁴ introduced the relationship between penetration and temperature. Eqn. (1) was written as follows:

$$\lg P = k + AT \quad (1)$$

where

P	Penetration, 0.1 mm
k	Constant
A	Heat penetration coefficient
T	Temperature, °C

Based on below experimental data, heat penetration coefficient (A) was obtained by using the linear regression method, but its regression coefficient (R) could not be lower than 0.997. T_{800} and $T_{1.2}$ meant equivalent softening point and equivalent brittle point, respectively. The higher T_{800} value was, the higher stability of asphalt can be occurred. Eqn. (2) (T_{800}) and (3) ($T_{1.2}$) were listed as follows:

$$T_{800} = \frac{[2,903 - k]}{A} \quad (2)$$

$$T_{1.2} = \frac{[0.072 - k]}{A} \quad (3)$$

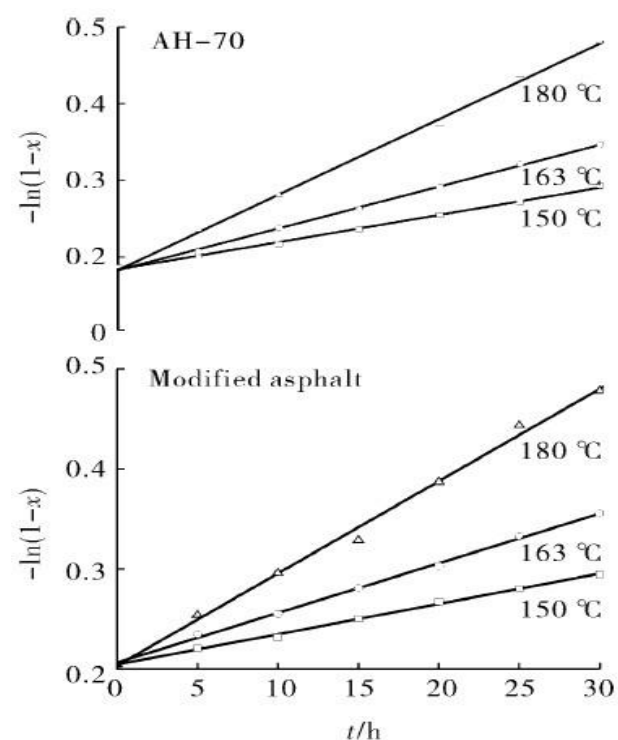
A and k values taken from Eqn. (1). The experimental results presented that when crumb rubber was added into asphalt, the performance of crumb rubber modified asphalt was improved such as penetration (15 °C and 25 °C), T_{800} , $T_{1.2}$, elastic range and penetration index, however penetration values of No.2 and No.3 at 30 °C were lower than that of matrix asphalt. Furthermore, all R values are more than 0.997.

Table 1. Properties of modified and matrix asphalts

Properties	Matrix asphalt	Modified asphalts			American Standard		
	AH-70	No.1	No.2	No.3	ABR-1	ABR-2	ABR-3
Penetration (25°C,100g, 5s)/0.1 mm	69	67	64.5	91.5	25-75	50-100	75-150
Penetration,(4°C, 200 g, 60 s)/0.1 mm	34	36	33	51	>15	>25	>40
Softening point, °C	45.4	54.2	51.5	45.6	>54	>49	>43
Elastic recovery (25°C,10 cm)/%	30	75	70	50	>20	>10	>0
Ductility (4°C)/cm	3	22.5	16.2	21.3	>5	>10	>20
		<i>After 5 hours at 163 °C</i>					
Penetration (4 °C), %	60	81	83	77	>75	>75	>75
Ductility (4°C), %	-	68	63	59	>50	>50	>50

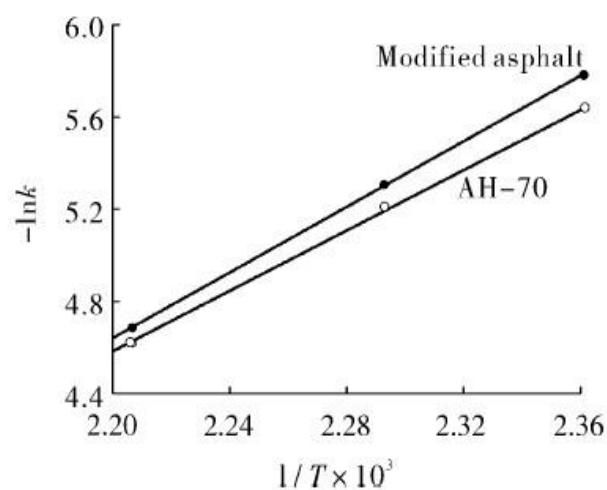
Aging kinetics of AH-70 and crumb rubber modified asphalt

Shi Hongbo⁵ used AH-70 and crumb rubber modified asphalt as feedstocks and studied effects of the aging time on the yields of asphaltene. Two types of aging kinetics parameters and models were obtained. Table 3 presented the relationship between the aging time and the content of asphaltene. The content of asphaltene for No.1 and AH-70 gradually increased with an increase in the aging time at the same reaction temperature.

**Figure 1.** The relationship between $-\ln(1-x)$ and the aging time

Furthermore, the content of asphaltene for No.1 was more than that of AH-70 at the same aging time and reaction temperature. On the other hand, the content of asphaltene for No.1 and AH-70 slowly increased with an increase in the reaction temperature at the same aging time. This proved that the performance of No.1 was better than that of AH-70.

It was supposed that the aging process of asphalt was first order reaction, so $-\ln(1-x)$ was linearly related with the aging time shown in Figure 1. k was the slope of the line. It was very clear that $-\ln(1-x)$ had a significant correlation with the aging time. Furthermore, k value was 0.99762. It was proved that the aging process of asphalt was first order reaction.

**Figure 2.** The relationship between $-\ln k$ and $1/T$

Based on Arrhenius Eqn. (4) and the above experimental data, kinetics parameters of crumb rubber modified asphalt and AH-70 shown in Table 4 were obtained. Figure 2 presented the relationship between $-\ln k$ and $1/T$.

$$\ln k = \frac{E_a}{RT} + \ln A \quad (4)$$

Aging kinetics Eqn. (5) (crumb rubber modified asphalt) and (6) (AH-70) were written as follows:

Table 2. The effect of thermal sensitivity on matrix and crumb rubber modified asphalt

Asphalt	Penetration/ 10 ⁻¹ mm			R	T ₈₀₀	T _{1.2}	Elastic range	Penetration index
	15°C	25°C	30°C					
No.1	28.0	91.5	148.1	0.9988	44.77	-13.24	58.02	-1.26
No.2	20.6	64.5	98.0	0.9976	49.50	-12.17	61.67	-0.88
No.3	22.5	62.5	98.0	0.9995	51.10	-14.79	65.89	-0.45
Matrix asphalt	16.1	61.5	119.0	0.9999	44.20	-4.36	48.56	-2.32

Table 3. The relationship between the aging time and the content of asphaltene

Aging time, h	Content of asphaltene					
	150 °C		163 °C		180 °C	
	No.1	AH-70	No.1	AH-70	No.1	AH-70
0	0.185	0.170	0.185	0.170	0.185	0.170
5	0.198	0.183	0.209	0.187	0.224	0.210
10	0.207	0.195	0.225	0.212	0.256	0.245
15	0.221	0.211	0.245	0.231	0.280	0.275
20	0.235	0.225	0.262	0.253	0.321	0.312
25	0.245	0.238	0.283	0.275	0.358	0.354
30	0.255	0.254	0.299	0.293	0.380	0.382

$$\ln(1-x) = -0.205 - 6.08 \cdot 10^4 e^{-\frac{7116}{T}} t \quad (5)$$

$$\ln(1-x) = -0.186 - 1.82 \cdot 10^4 e^{-\frac{6542}{T}} t \quad (6)$$

where

- k the slope of the line
- R the correlation
- T the reaction temperature,
- K the pre-exponential factor
- E_a the activation energy

Conclusion

Based on the above results and discussion, a comparison of thermal performance of matrix asphalt and crumb rubber modified asphalt has been done. The experimental results showed that the performance of crumb rubber modified asphalt was improved, but penetration values of No.2 and No.3 at 30 °C were lower than that of AH-70. Furthermore, all R values are more than 0.997.

The content of asphaltene for No.1 and AH-70 gradually increased with an increase in the aging time at the same reaction temperature. On the other hand, the content of asphaltene for No.1 and AH-70 slowly increased with an increase in the reaction temperature at the same aging time. The aging process of two types of asphalts (crumb rubber modified asphalt and AH-70) were of first order kinetics reaction.

References

- ¹Dong, C. C. *Utilization of Rubber Resources*, Beijing: Chemical Industry Press, **2003**.
- ²Xiao, P. and Ma, A. Q. *Environ. Protect. Transport.*, **2005**, 26(3), 56.
- ³Shi, H. B., Wang, H. G., Liao, K. J., Yan, F. and Cong, Y. F. *Sci. Technol. Eng.* **2006**, 6(4), 439.
- ⁴Chen, H. M. *Petroleum Asphalt*, **2003**, 17(4), 1.
- ⁵Shi, H. B. and Liao, K. J. *Chinese Synth. Rubber Ind.*, **2007**, 30(1), 26.

Received: 29.11.2012.
Accepted: 04.01.2012.



CORROSION RESISTANCE OF METALS AND ALLOYS IN ARTIFICIAL SALIVA – AN OVERVIEW

R. Saranya^[a], S. Rajendran^{[b,c]*}, A. Krishnaveni^[d], M. Pandiarajan^[b],
and R. Nagalakshmi^[e]

Keywords: corrosion resistance, metals, alloys, artificial saliva, bio-materials.

One of the primary requisites of any metal or alloy that is to be used in the mouth is that it must not produce corrosion products that could be harmful to the body. Some metallic elements that are completely safe in the elemental state can form hazardous or even toxic ions or compounds. Besides, the degradation of the alloy should be limited in order to guarantee its service life. Several metals and alloy have been in dentistry as bracket, band, orthodontic wires it is essential to know the corrosion resistance of this materials in the presence of saliva. The corrosion resistances of these materials have been evaluated by electrochemical studies such as polarization study and AC impedance spectra. The film formed on the metal surface has been analysed by surface analysis techniques such as SEM, EDX, X-ray, and AFM.

* Corresponding Author

- [a] Department of Chemistry, Jayalakshmi Institute of Technology, Thoppur- 636 352, India.
Email: senthilkumar944@gmail.com.
- [b] Corrosion Research centre, PG and Research Department of Chemistry, GTN Arts College, Dindigul- 624005, India.
E-mail: pandirajan777@gmail.com.
- [c] Department of Chemistry, Corrosion Research centre, RVS School of Engineering and Technology, Dindigul 624005, India. E-mail: srmjoany@sify.com.
- [d] Department of Chemistry, Yadava College, Madurai, India.
- [e] Department of Chemistry, Arupadaiveedu Institute of Technology, Chennai-603 110, India.
E-mail: nagalakshmirajan@gmail.com.

researchers (Figure 1). This review article will be a boon to researchers who would like to do research on corrosion behaviour of biomaterials in synthetic body fluids especially in simulated saliva.

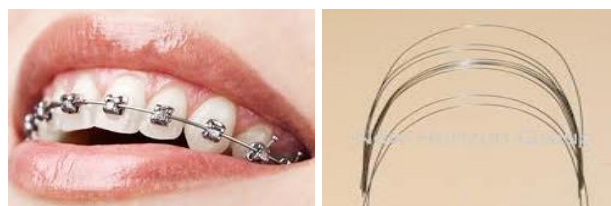


Figure 1. Orthodontic wires

Introduction

Over the past two decades, with the accelerated development of tissue engineering, the demand for a variety of synthetic and natural biomaterials has dramatically increased. Biomaterial sales have already exceeded \$240 million per year and due to the rapid development of biomaterials, the market will only increase in the years ahead for tissue engineering and artificial organ materials. Specifically, costs related to organ replacement account for 8% of all global healthcare spending and by 2040 as much as 25% of the US gross domestic product (GDP) is expected to be related to healthcare. Such demands require unique, better performing biomaterials for regenerative medicine. For example, it is necessary to develop better material mechanical properties and biocompatibility properties. Conventional biomaterials (or those materials with constituent dimensions greater than 1 μm) have not satisfactorily met clinical demands. Researchers, clinicians and other investigators are thus seeking better novel materials to serve as the next generation of tissue engineering and artificial organ materials. Artificial organs, when implanted in body undergo corrosion. Corrosion behaviour of metals and alloys in simulated body fluids has been investigated.¹⁻⁷⁵ Corrosion resistance of metals and an alloy in saliva has attracted the attention of several

Metals and Alloys

Corrosion behaviour of various metals and alloys have been investigated in various synthetic body fluids such as blood plasma, urine and saliva.¹⁻⁷⁵ Titanium metal,^{12,28,46,52,72,73,75} Ni-Cr,^{10,56,57} Ti-Mo,^{4,37} Ni-Ti,^{13,64} Co-Cr,^{14,53,61,63} SS316, MS, MS-Zn,^{23,24} Ti-Ag,^{3,68} Ni-Ti orthodontic wires^{18,27,33} have been used in dentistry.

Medium

Usually corrosion behaviour metals and alloys have been studied in artificial saliva (AS) whose composition is given in Table 1.²³

Table 1. Composition of artificial saliva

KCl	0.4 g/l
NaCl	0.4 g/l
CaCl ₂ ·2H ₂ O	0.906 g/l
NaH ₂ PO ₄ ·2H ₂ O	0.690 g/l
Na ₂ S·9H ₂ O	0.005 g/l
Urea	1 g/l

In some studies aerated and deaerated saliva has been used.^{8,10,46,55} AS containing hydrogen peroxide,⁶ fluoride,^{2,4,6,22,38,43,45,60,73} spirulina,²³ D-Glucose,⁴² electrol,²⁴ physiological solution (ps),^{17,25,40} lactic acid,^{17,51,71} spices extract,²⁹ bacteria,^{33,53} mouthwash,^{34,37} NaF,^{36,39,67,71} citric acid,⁷⁵ Ringer brown solution,^{39,50} have been used.

Temperature

Usually the study is carried out at $37 \pm 1^\circ\text{C}$.

Methods

Weight loss method, polarization study, AC impedance spectra have been used to evaluate the corrosion resistance of various metals and alloys in AS.^{1,4,5,6,7,10,19,20,21,22,23,24,54} The protective film form in the metal surface has been analysed by various surface analysis techniques such as SEM,^{2,6,7,9,21,26,35,36,41,49,59,68,73,75} XRD,^{3,17,68,71} EDX,^{9,14,34,41,59,75} F-test has also been used by some authors.¹¹ Cyclic voltammetry,^{13, 25} AAS,²⁶ and XPS^{3,16,17,25,58,68,71} have also been used.

A list of various materials used in dentistry, the methods used to evaluate the corrosion resistance of different metals and alloys, various methods employed and important findings are summarized in Table 1.

Influence of Fluoride ion on corrosion resistance of orthodontic wires

To strengthen the lifetime of teeth, fluoride is added in tooth pastes. This addition of fluoride may influence the strength of orthodontic wires. To know this influence several investigations have been undertaken. Corrosion resistance of metals and alloys in artificial saliva, in presence of fluoride has been investigated.^{31,38,43,45,51,71,73} It has been found that fluoride ion reduces the corrosion resistance of Titanium and Ti6AlV alloy. This has been proved by electrochemical studies.³¹ Similar observation is made with Ni-Cr-Ti alloy also.³⁸ Surprisingly the presence of fluoride ion increases the corrosion resistance of Ti-Cr alloy.⁴³ Robin and Meirelis observed that presence of fluoride in saliva enhanced porosity of the oxide film.⁴⁵ Mareci et al observed that fluoride increased the corrosion rate of Ti6Al7Nb and Ti30Ta alloys.⁵¹

Influence of extracts of natural of products on corrosion resistance of metals and alloys in artificial saliva

Extracts of natural products are added to the tooth paste. These extracts will definitely influence the corrosion resistance of orthodontic wires. Hence the corrosion resistance of extracts of plant materials on the corrosion resistance of orthodontic wires has to be studied thoroughly. But only a few studies have been made in this regard.^{29,73}

Presence of coriander in artificial saliva inhibited the pitting corrosion of AISI 304L orthodontic bands and stainless steel orthodontic bands.²⁹ Eugenol has protected Titanium from the attack of fluoride ions. Further, Eugenol has formed a protective film on titanium and prevented the dissolution of Titanium. This has been proved by electrochemical measurements and surface analysis techniques such as SEM.⁷³

Types of corrosion undergone by orthodontic wires.

There are several types of corrosion undergone by metals and alloys in the natural environment. Depending on the environment, they undergo general corrosion, galvanic corrosion, pitting corrosion etc. Similarly orthodontic wires also undergo several types of corrosion, depending on the natural of metals and alloys and the oral environment. Ti-6Al-4V undergoes fretting corrosion in presence of fluoride ion.² Ni-Cr and Co-Cr alloys undergo pitting corrosion in artificial saliva due to inhibition in artificial saliva for a long time.⁵ Hence the orthodontic wires have to be replaced every now and then. Vieira et al observed that Titanium undergoes fretting corrosion in artificial saliva.¹² This has been proved by electrochemical studies. Ludek Joska et al have noticed the non-uniform corrosion undergone by palladium-silver-copper alloy in model saliva.¹⁶ Orthodontic wires made of Ni-Ti alloy undergo pitting corrosion in artificial saliva. Similarly metals and alloys undergo non-uniform corrosion⁵⁸ and galvanic corrosion.⁶²

Influence of temperature on the corrosion resistance of orthodontic wires.

The average body temperature is 37°C . Hence the experiments are carried out at $37 \pm 0.1^\circ\text{C}$. However, when hot liquids such as hot water, hot coffee or tea, orally taken, they will affect the corrosion resistance of orthodontic wires in the oral environment. Hence researchers have carried out experiments at various temperatures also.^{8,19,46} It is observed⁸ that the corrosion rate of non precious dental alloys increases when the temperature is increased ($20, 37$ and 50°C). At low temperature, passive films are formed. At 25°C a passive film is formed on pure Titanium.⁴⁶

Influence of pH on the corrosion resistance of orthodontic wires.

Influence of pH on corrosion and passivity is a well established concept. At lower pH, because of acidic environment, many metals and alloys undergo corrosion. Same thing happens to metals and alloys of orthodontic wires in the oral environment.^{11,26,36,38,45,52,60,72} At pH 4 and 6, in presence of sodium fluoride, and artificial saliva, stainless steel and nickel-titanium alloy undergo pitting corrosion.³⁶ This has been proved by SEM. At low pH value of saliva, the oxide film formed on Ti-23T alloy was found that to be porous, which may enhance corrosion than at low pH = 2.5. The corrosion of Ti6AlNb and Ti30Ta alloys increased, in presence of fluoridated saliva.⁵¹ At low pH values, the bonding strength was reduced in Titanium-Porcelain.⁶⁰

Table 1. Corrosion resistance of different metals and alloys

No.	Metals	Medium	Methods	Findings	Ref.
1	Aluminum-bronze dental alloy	Artificial saliva (AS)	Polarization test, Polarization resistance measurements & weight loss method	Beverages are in contact with dental alloy in the oral environment.	1
2	Ti-6Al-4V	AS Containing 0, 190, 570, 1140 ppm of fluoride ions	Free corrosion potential measured as a function of time SEM & non – contact optical profile meter	Fretting corrosion behaviour dependence on the fluoride ion concentration.	2
3	Ti-Ag	AS	X - ray photoelectron spectroscopy (XPS) & X - ray diffraction (XRD) methods.	The addition of Ag to Ti is found to be effective in reducing corrosion current density and increasing OCP of Ti in AS environment.	3
4	Ti-15Mo alloy	0.15 M NaCl solution containing varying concentration fluoride ions (190, 570, 1140, 9500, ppm)	Potentiodynamic polarization, electrochemical impedance, spectroscopy (EIS) & Chronoamperometric current time transient (ctf)	Passivity at anodic potentials at all concentration of fluoride ions.	4
5	Recasting Ni-Cr & Co-Cr Non precious dental alloy	AS	(Chemical & Electro chemical technique) induced coupled plasma mass spectrometry (ICP/MS), potentiodynamic & impedance measurement	Alloy surface forming definite patches which may be the nucleus of pitting corrosion due to immersion for long time. Non-precious alloy have high corrosion resistance.	5
6	Non- precious dental alloy	Artificial saliva containing different concentration of hydrogen peroxide, carbamide peroxide & fluoride ions.	Potentiodynamic studies were conducted by (ACM) auto tafel potentiostat	Alloys suffer less corrosion rates in presence of carbamide peroxide than hydrogen peroxide.	6
7	Fe Pt – based alloy	AS at 37 °C	Electrochemical polarization measurements & SEM	Wiron99 > wironloy > wironit Highly stable also during long-term exposure	7
8	Non precious dent alloy	Aerated AS (20 °C, 37 °C, 50 °C)	Linear polarization method	Corrosion rate increased with increasing temperature.	8
9	Nickel-Based dental casting alloy	AS at different values of pH in the presence of crevice	Energy Dispersive X-ray analysis (EDX), SEM	Importance of the level of Cr in Ni-based alloy. Higher Cr (25wt%) led to a superior corrosion resistance	9
10	Ni-Credental casting alloy	De-aerated & aerated artificial saliva	Polarization studies	Alloys with low Cr content and without Mo always corrode.	10
11	i) Composition of the high noble metal, ii) Composition of noble metals, iii) Composition of base metals alloy	Acidified artificial saliva (pH=2.3)	ICP-AES, F-test	Corrosion resistance results obtained from the two methods were ranked and compared	11
12	Titanium	AS	Electrochemical measurements	Higher corrosion rate during fretting corrosion.	12
13	Nickel-Titanium	Fluoridated AS at 37 °C	TLA, Voltammetry	Corrosion behavior of Ni-Ti alloy is highly affected by the fluoride content.	13
14	Cobalt-Chromium dental alloy doped with precious metals	AS	Coulometric analysis, metallography & EDX	Gold doping produces heterogeneous microstructures that are vulnerable to corrosive attack	14
15	Palladium-Silver binary alloy	AS	Polarization resistance, potentiodynamic measurements, thermodynamic calculation	Commercial dental alloys containing Ag and Pd as major compounds.	15
16	Palladium-Silver-Copper alloy in model saliva	Model saliva	XPS, thermodynamic analysis	The alloying of the palladium silver binary system with copper leads to change in the corrosion behavior of the alloy	16
17	Au-Pd-In alloy	Physiological solutions i) 0.9N NaCl, ii) 0.1N NaCl, iii) +0.1N Lactic acid & AS	XPS, X-ray diffraction, Impedance spectroscopy and DC Voltammetry	In ₂ O ₃ main corrosion product on the surface. Same corrosion rate assuming different oxides on the surface	17
18	Ni-Ti Orthodontic wires	AS at 40 °C	ASTM F746, Potentiodynamic test	Ni-Ti wires have sufficient resistance against pitting corrosion in AS.	18
19	TiNi shape memory alloy (SMA) & Stainless steel (SS)	AS at 37 °C	Potentiodynamic polarization test	Lower the corrosion potential & the higher the current density.	19
20	TiO ₂ nanotubes	AS	Open circuit potential (OCP), Electrochemical impedance spectroscopy (EIS) & Potentiodynamic polarization test	Diameter that too large leads to decreased corrosion resistance.	20

Table 1. (cont.)

No.	Metals	Medium	Methods	Findings	Ref.
21	Dental alloys containing palladium	AS	Open-circuit potential (OCP) Potentiodynamic polarization, SEM	Optimal corrosion resistance values were obtained	21
22	Austenitic & duplex stainless steels	AS with addition of fluoride	Open-circuit potential (OCP), Electrochemical impedance spectroscopy(EIS) and Potentiodynamic measurements	The passive films on both materials predominantly contained Cr oxides.	22
23	i) SS316 ii) MS iii) MS-Zn	AS in the absence & presence of spirulina	Potentiodynamic polarization study, AC impedance spectra	Order of corrosion resistance SS316 > MS > MS-Zn	23
24	i) SS316 ii) MS iii) MS-Zn	AS in presence of electoral	Potentiodynamic polarization study, AC impedance spectra	Order of corrosion resistance SS316 > MS-Zn > MS	24
25	Austenitic 316L duplex 2205 stainless steel	AS and Hank's solution (PS)	Cyclic voltammetry, Electrochemical atomic force microscopy (EC-AFM) and XPS	Corrosion products formed during the oxidation process was observed.	25
26	Metal-ceramic dental casting alloy	AS (pH=2.3, 6.5); 0.9% saline solution of pH=7.3	Atomic absorption spectroscopy(AAS), SEM	Wirecer plus alloy presents a better electrochemical behavior & biocompatibility than Vera soft alloy	26
27	Nickel-titanium orthodontic arch wires	AS	Continuous bending stress throughout the 14 days experimental process	Bending stress, loading condition with respect to corrosion behavior	27
28	Titanium alloy	AS at 37 °C	Electron beam melting (EBM), Dynamic potentiostatic polarization	All the mechanical properties & corrosion character were tested	28
29	AlSi304L Orthodontic bands (or) Stainless steel orthodontic bands	AS containing spice extract	Electrochemical experiments were using analysed corrosion parameters	Coriander was found to inhibit pitting.	29
30	SUS304 stainless steel	AS	Polarization resistance measurements	Nano crystalline 304SS is more corrosion resistant than the microcrystalline 304SS	30
31	Ti & Ti6Al4V	AS	Electrochemical methods	Fluoride concentration increases corrosion resistance is decreased	31
32	Titanium Nitride (TiN) plating	AS with 1.23% acidulated phosphate fluoride (APF)	EZ test	TiN plating is a method to prevent metal corrosion and can increase the surface smoothness.	32
33	Nickel-titanium orthodontic wires	Solution containing streptococcus mutans oral bacteria & i) Ringer sterile AS ii) AS enriched with a sterile iii) addition of bacteria	Free corrosion potential, potentiodynamic curves & impedance spectroscopy	Ti coated metal a bracket with corrosion or without corrosion can't reduce the frictional force.	33
34	Titanium nitride plating metal brackets i) Blank control group ii) DLC coated group iii) TiN-coated gp	AS and mouthwash	Energy Dispersive spectroscopy, EZ- test.	The DLC coated groups exhibited lower static and kinetic than TiN-coated bracket	34
35	Dental metal-ceramic	Acidic AS	SEM-EDS	Decrease of mechanical strength of conventional metal-ceramic interface after immersion.	35
36	i)Stainless steel ii)nickel -titanium	Acidulated sodium fluoride (NaF) & AS pH=4 & 6	SEM	Pitting corrosion occurred on the surfaces of the brackets & wires	36
37	TiMo alloy	AS and commercial mouth wash solution with 450 ppm at 25 °C	Open-circuit potential (OCP), Electrochemical impedance spectroscopy (EIS) and potentiodynamic measurements	Superior corrosion resistance	37
38	Ti & Ni-Cr-Ti	AS contains 0.2 % NAF	Electrochemical technique, electric potential of corrosion (Ecorr), current density of corrosion (Icorr), polarization resistance(Rp)	AS containing fluoride ions decreases of the corrosion resistance of pure titanium	38
39	Ag20Pd5Au1.5Ti alloy	Carter-Bruguard AS un-doped & doped with 0.05M NaF different pH values Ringer brown solution	Potentiodynamic and linear polarization, EIS	High corrosion resistant.	39
40	Ni50.2Ti49.8	Hank's solution & AS	High pressure torsion (HPT) technique.	Nano crystalline higher pitting corrosion potential & than that of microcrystalline	40

Table 1. (cont.)

No.	Metals	Medium	Methods	Findings	Ref.
41	Type III gold alloy Group I (100% as received metal); Group II (50%wt new metal 50%wt once recast metal) Group III (100% once recast metal)	AS at 37 °C	SEM, X-ray energy-dispersive spectroscopy	Recasting protocol should produce acceptable corrosion resistance	41
42	i)SS316 ii)MS iii)MS-ZN Ti-Cr	AS in the absence & presence of D-Glucose	Potentiodynamic polarization study, AC impedance spectra	Order of corrosion resistant SS 316L > MS-Zn > MS.	42
43	Ti-Cr	AS containing fluoride	Potentiodynamic polarization study, (ESCA) Electron spectroscopy for chemical analysis.	Greater resistance to corrosion in the fluoride containing AS	43
44	i) Nickel alloy ii) Co-Cr alloy iii) AuAgPd	Fusayama-Meyer AS addition of Yeast extract	Open-circuit potential (OCP).	Ni Co-Cr alloy are passivity character AuAgPd alloy higher corrosion current	44
45	Ti-23Ta alloy	AS with different pH fluoride concentration	Electrochemical Impedance spectroscopy (EIS)	The presence of fluoride and low pH of saliva enhance porosity of the oxide film.	45
46	Pure titanium	Naturally aerated AS solution at 25 °C	Open-circuit potential (OCP), Potentiodynamic polarization.	Protective passive film is formed.	46
47	Casting alloy Ni-Cr(M1); Co-Cr(M2), Palladium based (M3) Gold based (M4)	AS at 37 °C	Potentiodynamic polarization test, Inductively coupled plasma mass spectrometry	Au and Pd based noble alloys dissolved less than Ni-Cr and Co-Cr based alloy	47
48	Y-TZP dental ceramic	AS	Static loading & Cyclic loading	Corrosion Plays an important role in the fatigue behaviour of dental zirconia	48
49	Dental implant system (in vivo & invitro)	AS at 37 °C	Potentiostat FE-SEM & EDS	Rp for clinically non-used implant system increases compared with clinically used implant system	49
50	Ag-20Pd-5Au-1.5Ti alloy	Carter-Brugard AS undoped and doped with 0.05MNaF different pH values & Ringer- brown solution	Potentiodynamic & linear polarization, EIS, OCP	Corrosion resistance is high	50
51	Ti6Al7Nb&Ti30Ta	i) AS pH=8.0 ii) 9.8g/l lactic acid pH=2.5 iii) Fluoridated saliva 1.0g/IF pH=8 iv) Fluoridated acidified saliva 9.8g/l lactic acid, 1.0 g/IF pH=2.5	OCP linear sweep voltametric analysis were used	The Corrosion of Ti6Al7Nb&Ti30Ta alloys is enhanced in fluoridated acidified saliva	51
52	Titanium alloy	AS & simulated body fluid (SBF) solution at 25 °C pH=2.5	Potentiodynamic polarization test	Hydroxyapatite layer has influence on corrosion resistant properties	52
53	Cobalt-chromium	Saliva & bacteria	Voltamperometric study	acidity of the salivary solution has a negative effect on the alloy Co-Cr	53
54	Ni-Cr-Mo dental alloy	AS	Electrochemical character	Friction & wear of dental alloy does not change their corrosion resistance	54
55	Ti50Ni47.2Co2.8	Deaerated AS	OCP, Potentiodynamic and potentiostatic technique and XPS	The addition of Co had little effect on the corrosion behaviour of NiTi as well as the formation of passive film	55
56	i) Ni-Cr ii) Co-Cr iii) c-p-Ti & one ceramic (three dental casting alloy)	AS brushed without or with one of four tooth pastes of different relative dentine abrasivity (RDA 50, 52, 80 & 114)	Non-parametric test	Variations in micro hardness & surface roughness were not clinically relevant	56
57	i) Ni-Cr ii) Co-Cr iii) c-p-Ti & one ceramic (three dental casting alloy)	AS brushed without or with one of four tooth pastes of different relative dentine abrasivity (RDA 50, 52, 80 & 114)	Inductively coupled plasma mass spectrometry, ANOVA and non-parametric test	Increase of the micro hardness, decrease of the corrosion resistance & an increase of the ion release	57

Table 1. (cont.)

No.	Metals	Medium	Methods	Findings	Ref.
58	Palladium-Silver-copper alloy	Model saliva	XPS, thermodynamic analysis	Non-uniform corrosion	58
59	Cast high noble alloy (72.7%-75.7% Au; 4.5 to 7 Pd; 10.7 to 11.1 Ag; 7.8-8.4% Cu & 1.0-1.4% Zn)	Fusayama AS(n=3) at 37°C	Potentiodynamic polarization, SEM, X-ray Energy dispersive.	Retained passivity under electrochemical conditions similar to the oral environment	59
60	i) Titanium – Porcelain ii) Interface between porcelain & Titanium	AS with addition of fluoride pH (2.7, 5.4, 7.0) F ⁻ (pH=7.0, 100 ppm) AS pH = (2.7, 5.4, 7.0) AS pH = (2.7, 5.4, 7.0)	Three - point flexure test.	i) Reduction of bonding strength ii) No decreasing of the bonding strength of Ti- Porcelain occurred	60
61	Dental cobalt – chromium alloy dental amalgam	AS	Potentiodynamics & potentiostatic polarization	Alloys could be reused by adding 50 % of new alloy pellets	61
62	Non – precious dental alloy & pure titanium (Co-Cr – Mo & Ni – Cr-Mo) & dental amalgam	AS	Cyclic polarization in each medium.	Galvanic corrosion does not pose a greater threat to the alloys than ordinary corrosion	62
63	Cobalt-Chromium dental alloy joints	AS	Potentiodynamic polarization & EIS	Corrosion resistance of the laser-welded joints was better than that of the brazed	63
64	Nickel-titanium orthodontic brackets	AS	EIS	Greater free corrosion potential, much lower passive current density and no breakdown upto 1.5v	64
65	Chromium based alloy(galvanic coupling between amalgam)	AS	Potentiodynamics and potentiostatic polarization	Correct design and use of dental alloy are important when determining the appropriate treatment for a specific patient	65
66	Ti-6Al-7Nb alloy brazed with bulk metallic glasses	AS	X-ray tomography	Pd40Cu30Ni10P20 promising brazing filler for dental (or) biomaterial devices	66
67	Titanium containing orthodontic wires	Acidic AS and different NaF concentration. (0%, 0.2%, 0.5%)	Potentiodynamic polarization, photoelectron spectrometry	Decreasing the corrosion rate & anodic current density.	67
68	Ti-5Ag	With and without thermal oxidation in AS solution	XRD, X-ray photoelectron spectroscopy, SEM	Thermal oxidation was an effective way to improve the corrosion resistance	68
69	Metallic orthodontic wires (Cr, Ni, NiTi & CuNiTi)	AS	Potentiodynamic method	NiTi material is most resistant	69
70	Ag-Pd & Co-Cr	AS	Polarization resistance, EIS, coulometric analysis	Co-Cr alloy excellent corrosion resistance	70
71	Ti-Nb & TMA	AS with and without the addition of lactic acid sodium fluoride	X-ray diffraction, EIS, Potentiodynamic polarization, SEM & X-ray photoelectron	Ti-Nb β alloy when fluoride is necessarily needed during dental procedures	71
72	Three CP Titanium (A, B, C)	AS (saliva with pH=5.5)	Open-circuit potential measurements, EIS & potentiodynamic polarization	Corrosion resistance & stability of their passive oxide films are quite different	72
73	Titanium	AS containing Fluoride enriched with eugenol at different concentration	Electrochemical measurements & SEM	The effects of eugenol are not only the protection of titanium from fluoride attack but also the suppression of dissolution of titanium ions via formation of eugenol films	73
74	Dental Silver amalgam	AS	Physical and Chemical properties	Practical problems are discussed	74
75	Ti	AS with citric acid, sodium nitrite, calcium carbonate(or) benzotriazole	Electrochemical Noise technique (TEN), SEM, EDX & Electrochemical Emission Spectroscopy	Fretting corrosion behavior of the material, resulting in a surface that is electrochemical more active with respect to the non-worn surface	75

Conclusion

One of the primary requisites of any metal or alloy that is to be used in the mouth is that it must not produce corrosion products that could be harmful to the body. Some metallic elements that are completely safe in the elemental state can form hazardous or even toxic ions or compounds. Besides, the degradation of the alloy should be limited in order to guarantee its service life. Several metals and alloy have been in dentistry as bracket, band, orthodontic wires it is essential to know the corrosion resistance of this materials in the presence of saliva. The corrosion resistances of these materials have been evaluated by electrochemical studies such as polarization study and AC impedance spectra. The film formed on the metal surface has been analysed by surface analysis techniques such as SEM, EDX, X-ray and AFM.

Acknowledgement

The authors are thankful to their Managements and St. Joseph's Research and Community Development Trust, Dindigul, India for their help and encouragement.

References

- ¹Gustavo, S., Duffo, Silvia B. Farina, *Mater. Chem. Phys.*, **2009**, **115**, 235.
- ²Sivakumar, B., Satendra Kumar, Sankara Narayanan, T. S. N., *Wear*, **2011**, **270**, 317.
- ³Zhang, B. B., Zheng Y. E., Liu, Y., *Dental Mater.*, **2009**, **25**, 672.
- ⁴Satendra, K., Sankara Narayanan, T. S. N., *J. Dentistry*, **2008**, **36**, 500.
- ⁵Ameer, M. A., Khamis, E., Ai-Motlaq, M., *Corros. Sci.*, **2004**, **46**, 2825.
- ⁶Ameer, M. A., Hamis, E., Ai-Motlaq, M., *Electrochim. Acta*, **2004**, **50**, 141.
- ⁷Gebert, A., Roth, S., Gopalan, R., Kundig, A. A., Schultz, L., *J. Alloys Compds.*, **2007**, **436**, 309.
- ⁸Weigman, H. O., Land Ketelaar, J. A. A., *J. Dent.*, **1987**, **15**, 166.
- ⁹Wilye, C. M., Shelton, R. M., Fleming, G. J. P., Davenport, A. J., *Dental Materials*, **2007**, **23**, 714.
- ¹⁰Meyer, J.-M., *Corros. Sci.*, **1977**, **17**, 971.
- ¹¹Al-Hity, R. R., Kappert, H. F., Viennot, S., Dalard, F., Grosgeat, B., *Dental Materials*, **2007**, **23**, 679.
- ¹²Vieira, A. C., Ribeiro, A. R., Rocha, L. A., Celis, J. P., *Wear*, **2006**, **261**, 994.
- ¹³Cioffi, M., Gilliland, D., Ceccone, G., Chiesa, R., Cigada, A., *Acta Biomater.*, **2005**, **1**, 717.
- ¹⁴Reclaru, L., Luthy, H., Eschler, P. Y., Blatter, A., Susz, C., *Biomaterials*, **2005**, **26**, 4358.
- ¹⁵Joska, L., Marek, M., Leitner, J., *Biomaterials*, **2005**, **26**, 1605.
- ¹⁶Joska, L., Poddana, M., Leitner, J., *Dental Mater.*, **2008**, **24**, 1009.
- ¹⁷Juzeliunas, E., Leinartas, K., Samuleviciene, M., Miecinskas, P., Juskenas, R., Sudavicius, A., *Corros. Sci.*, **2002**, **44**, 1541.
- ¹⁸Rondelli, G., Vicentini, B., *Biomater.*; **1999**, **20**, 785.
- ¹⁹Li, M. G., Sun, D. Q., Qiu, X. M., Yin, S. Q., *Mater. Sci. Eng.*, **2006**, **441**, 271.
- ²⁰Chenglong Liu, Yueji Wang, Meng Wang, Weijiu Huang, Paulchu K., *Surf. Coatings Technol.*, **2011**, **206**, 63.
- ²¹Viennot, S., Lissac, M., Malquarti, G., Dalard, F., Grosgeat, B., *Acta Biomater.*, **2006**, **2**, 321.
- ²²Kocijan, A., Kek Merl, D., Jenko, M., *Corros. Sci.*, **2011**, **53**, 776.
- ²³Rajendran, S., Paulraj, J., Rengan, P., Jeyasundari, J., Manivannan, M., *J. Dentistry Oral Hyg.*, **2009**, **1**, 1.
- ²⁴Rajendran, S., Chitra Devi, P., John, M. S., Krishnaveni, A., Kanchana, S., Lydia Christy, J., Nagalakshmi R., Narayanasamy, B., *Zastita Mater.*, **2010**, **51**, 149.
- ²⁵Conradi, M., Schon, P. M., Kocijan, A., Jenko, M., Vancso, G. J., *Mater. Chem. Phys.*, **2011**, **130**, 708.
- ²⁶Mutlu-Sagesen L., Ergun, G., Karabulut, E., *Dental Mater.*, **2011**, **30**, 598.
- ²⁷Liu, J. K., Lee, T. M., Liu, I. H., *Am. J. Orthodont. Dent. Facial Orthoped.*, **2011**, **140**, 166.
- ²⁸Koike, M., Martinez, K., Guok, L., Chahine, G., Kovacevic, R., Okabe, T., *Mater. Process. Technol.*, **2011**, **211**, 1400.
- ²⁹Mahoto, N., Sharma, M. R., Chaturvedi, T. P., Singh, M. M., *Mater. Lett.*, **2011**, **65**, 2241.
- ³⁰Nie, F. L., Wang, S. G., Wang, Y. B., Wei, S. C., Zheng, Y. F., *Dental Mater.*, **2011**, **27**, 677.
- ³¹Anwar, E. M., Kheiralla, L. S., Tammam, R. H., *Oral Implant.*, **2011**, **37**, 309.
- ³²Kao, C. T., Guo, J. U., Huang, T. H., *Orthodontics Dentofac. Orthoped.*, **2011**, **139**, 594.
- ³³Bahije, L., Benyahia, H., El Hamzaoui, S., Ebn Touhami, M., Bengueddour, R., Rerhrhaye Abdallaoui, F., Zaoui, F., *Int. Orthodont.*, **2011**, **9**, 110.
- ³⁴Huang, T. H., Guo, J. U., Kao, C. T., *Surf. Coat. Technol.*, **2010**, **205**, 1917.
- ³⁵Souza, J. C. M., Nascimento, R. M., Martinelli, A. E., *Surf. Coat. Technol.*, **2010**, **205**, 787.
- ³⁶Kao, C. T., Huang, T. H., *J. Orthodont.*, **2010**, **32**, 555.
- ³⁷Mareci D, Chelariu R, Gordin D M, Romas M, Sutiman D, Gloriant T, *Materials and Corrosion.*, **2010**, **61**, 829.
- ³⁸Liang, B. G., Shen, X. T., Liu, L., Lu, Y. X., Yu, Z. D., Yang, C. X., Zhang, Y. Z., *Med. Sci.*, **2010**, **39**, 399.
- ³⁹Vasilescu, E., Drob, P., Vasilescu, C., Mareci, D., Mirza-Rosca, T. C., *Revista chim.*, **2010**, **61**, 660.
- ⁴⁰Nie, F. L., Zheng, Y. F., Cheng, Y., Wei, S. C., Valier, R. Z., *Mater. Lett.*, **2010**, **64**, 983.
- ⁴¹Ayad, M. F., Ayad, G. M., *Prosthodontics*, **2010**, **19**, 194.
- ⁴²Rajendran, S., Uma, V., Krishnaveni, A., Jeyasundari, J., Shyamaladevi, B., Manivannan, M., *Sci. Eng.*, **2009**, **34**, 147.
- ⁴³Hsu, H. C., Wu, S. C., Wang, C. F., Ho, W. F., *J. Alloys Compds.*, **2009**, **487**, 439.
- ⁴⁴Gatin, E., Berlic, C., Iordache, B., Prioteasa, P., *Optoelectr. Adv. Mater.*, **2009**, **11**, 1870.
- ⁴⁵Robin, A., Meirelis, J. P., *Corros. Eng. Sci. Technol.*, **2009**, **44**, 352.
- ⁴⁶Mariano, N. A., Oliveira, R. G., *Revista Mater.*, **2009**, **14**, 878.
- ⁴⁷Tune, S. H., Pekmez, N. O., Keyf, F., Canli, F., *Dental Mater.*, **2009**, **25**, 1029.
- ⁴⁸Kosmac, T., Obla, K. C., *Key Eng. Mater.*, **2009**, **409**, 161.

- ⁴⁹Chung, C. H., Kim, H. J., Jeong, Y. T., Son, M. K., Jeong, Y. H., Choe, H. C., *Trans. Nonferrous Metals Soc. China.*, **2009**, *19*, 846.
- ⁵⁰Zhang, Y. M., Chai, F., Hornez, J. C., *Biomed. Mater.*, **2009**, *4*, 126.
- ⁵¹Mareci, D., Chelariu, R., Gordin, D. M., Gloriant, T., Carcea, I., *Metalurgia Int.*, **2009**, *14*, 10.
- ⁵²Mariano, N. A., Oliveiva, R. G., Braga, E. I., Rigo, E. C. S., *Key Eng. Mater.*, **2009**, *315*, 396
- ⁵³Zeroual, R., Adiou, S., Kaoun, K., Bellem Khannate, S., *Dakar Med.*, **2008**, *530*, 183.
- ⁵⁴Banu, A., Marcu, M., Radovici, O., *Rev. Roum. Chim.*, **2008**, *53*, 1007.
- ⁵⁵Wang, Q. Y., Zheng, Y. F., *Dental Mater.*, **2008**, *24*, 1207.
- ⁵⁶Nogues, L. I., Martinez Gomis, J., Molina, C., Peraire, M., Salsench, J., Sevilla, P., Gil, F. J., *Mater. Sci. Mater. Med.*, **2008**, *19*, 3041.
- ⁵⁷Molina C., Nogues, L. I., Martinez Gomis, J., Peraire, M., Salsench, J., Sevilla, P., Gil, F. J., *Mater. Sci. Mater. Med.*, **2008**, *19*, 3015.
- ⁵⁸Joska, L., Poddana, M., Leitner, J., *Dental Mater.*, **2008**, *24*, 1009.
- ⁵⁹Ayad, M. F., Vermilyea, S. G., Rosenstiel, S. F., *Prosthetic Dent.*, **2008**, *100*, 34.
- ⁶⁰Guo, L., Liu, X., He, Z., Gao, J., Yangm J., Guo, T., *Mater. Lett.*, **2008**, *62*, 2204.
- ⁶¹Van Vuuren, L. J., Odendaal, J. S., Pistorios, P. C., *Dental Assoc. Tydskrif Suid – Afr. Tandheel Kundige Vereing.*, **2008**, *63*, 34.
- ⁶²Bilhan, H., Bilgin, T., Cakir, A. F., Yuksel, B., Von Fraunhofer, J. A., *Biomater. Appl.*, **2007**, *22*, 197.
- ⁶³Zupancic, R., Legat, A., Funduk, N., *Mater. Technol.*, **2007**, *41*, 295.
- ⁶⁴Liu, C., Chu, P. K., Lin, G., Yangm D., *Corros. Sci.*, **2007**, *49*, 3783.
- ⁶⁵Ciszewski, A., Baraniak, M., Urbanek Brychczynska, M., *Dental Mater.*, **2007**, *23*, 1256.
- ⁶⁶Miura, E., Kato, H., Ogata, T., Nishiyama, N., Specht, E. D., *Mater. Trans.*, **2007**, *48*, 2235.
- ⁶⁷Her Hsiung Huang, Chia Ching Wang, Son Mou Chiu, Jen Feng Wang, Yu Cheng Liaw, Jen Feng Wang, Yu Cheng Liaw, Tzu Hsin Lee, Fang Lung Chen, *Chin Dent J.*, **2005**, *24*, 134.
- ⁶⁸Zhang, B. B., Wang, B. L., Li, L., Zheng, Y. F., *Dental Mater.*, **2011**, *27*, 214.
- ⁶⁹Ziebawicz, A., Walk, W., Barucha Kepka, A., Kiel, M., *Achiev. Mater. Manuf. Eng.* **2008**, *27*, 151.
- ⁷⁰Mareci, D., Sutiman, D., Cailean, A., Bolat, G., *Mater. Sci.*, **2012**, *33*, 491.
- ⁷¹Bai, Y. J., Wang, Y. B., Cheng, Y., Deng, F., Zheng, Y. F., Wei, S. C., *Mater. Sci. Eng.*, **2011**, *31*, 702.
- ⁷²Kadowaki, N. T., Martinez, G. S. S., Robin, A., *Mater. Res.*, **2009**, *12*, 363.
- ⁷³Kinani, L., Najih, L., Chtaini, A., *Leonardo J. Sci.*, **2008**, *19*, 243.
- ⁷⁴Darvell, B. W., *J. Oral Rehabil.*, **1978**, *5*, 41.
- ⁷⁵Vieira, A. C., Ribeiro, A. R., Rocha, L. A., Celis, J. P., *Mater. Sci.*, **2004**, *42*, 112.

Received: 22.11.2012.

Accepted: 04.01.2013.



CORROSION BEHAVIOUR OF BIOMATERIALS IN SYNTHETIC BIOLOGICAL SOLUTIONS – AN OVERVIEW

R. Nagalakshmi^[a], S. Rajendran^[b,c], J. Sathiyabama^[b], M. Pandiarajan^{[b]*},
and J. Lydia Christy^[d]

Keywords: Ringer solution, Hank solution, simulated body fluids, artificial urine, blood and serum.

Various biomaterials are implanted in the human body. Sometimes artificial organs are also implanted in the body. For this purpose various metals and alloys such as Ni-Al-Fe intermetallic alloys, titanium alloy, NiTi alloy, CoCrMo alloys, magnesium alloy, Cr- Ni stainless steel, Cr-Ni-Mo stainless steel, 316L stainless steel have been employed. The corrosion resistance of these biomaterials in various synthetic body fluids such as Ringer's solution, Hank's solution, simulated body fluids, artificial urine, blood, and serum have been investigated. Usually the corrosion resistance of these materials is investigated by electrochemical studies such as polarization, AC impedance and cyclic voltammetry study. The nature of the film formed on the metal surface has been analysed by surface analysis techniques such as SEM, AFM, etc. Study of this review paper will be very useful and time saving to researchers who would like to investigate the corrosion resistance of biomaterials in synthetic body fluids. The research findings will be very useful to the medical field.

* Corresponding Author

pandiarajan777@gmail.com

- [a] Department of chemistry, Aarupadai Veedu Institute of Technology, Chennai-603110, Tamilnadu, India.
E-mail: nagalakshmirajan@gmail.com .
- [b] PG and Research Department of Chemistry, GTN Arts College, Dindigul-624 005, Tamilnadu, India.
E-mail: pandiarajan777@gmail.com .
- [c] Research Centre RVS School of Engineering and Technology, Dindigul-624 005, Tamilnadu, India. Email: srmjoany@sify.com
- [d] Department of Chemistry, VSB Engineering College, Karur-639 111, Tamilnadu, India.

Metals and Alloys

Various metals and alloys have been used as biomaterials (see Table 1) whose corrosion resistance has been investigated in artificial body fluids; various metals and alloys such as Ni-Al-Fe intermetallic alloys,¹ titanium alloy,^{2,3,5,6,9,18,40,41,46,50,59,66,77} NiTi alloy,^{7,36,44,45,62,74} CoCrMo alloys,^{10,13,22,23,58,69} magnesium alloy,^{8,24,27,29,30,33,38,42,43,65,70} Cr-Ni stainless steel,⁵⁵ Cr-Ni-Mo stainless steel,⁵⁴ 316L stainless steel.^{15,31,49,53,61,76}

Methods

Usually to measure corrosion resistance of biomaterials, electro-chemical studies such as potentiodynamic polarization,^{1,3,7,14-16,18,22,23,27,32,40,46,55,58,59,67,73,74} electro

chemical impedance spectra,^{1,4,7,9,11,15,18,19,20,26,35,36-38,41,42,44,46,50,53,59,62,67,69,73} and electro-chemical noise measurement,^{1,13} have been employed (see Table 1). From these studies, corrosion parameters such as corrosion potential, corrosion current, Linear polarisation resistance, Tafel slopes, double layer capacitance, charge transfer resistance, phase angle value have been calculated and compared. When corrosion resistance increases, LPR value increases; corrosion current decreases; charge transfer resistance increases and double layer capacitance decreases.^{80,81}

Introduction

Corrosion resistance of metals and alloys in various body fluids has attracted the attention of many researchers.¹⁻⁸³ Corrosion resistance of biomaterials in synthetic body fluids such as blood plasma, urine, Hank solution, Ringer solution and artificial saliva has been extensively studied. The corrosion resistance of metals and alloys in artificial saliva has been reviewed recently.⁸²

Synthetic body fluids

Corrosion resistance of various metals have been investigated in various synthetic (simulated) body fluids (see Table 1) such as Ringer's solution,^{3,21,40,41} simulated body fluids,^{1,2,5,8,10,13-17,23-28,30,43,48,63,65-67,71-74,77} Hank solution,^{9,11,24,31,38,39,42,45,46,49,69,70,76} blood plasma,^{45,59,61} urine,^{55-57,59,61} bovine serum,³⁷ and artificial saliva.^{20,22,33,51,79,80}

Surface analysis

To understand surface morphology of the protective film formed on the metal surface, surface analysis techniques such as SEM,^{2,9,12,22,26,27,31,33,36,38,48,64,66,68,72,74,75} EDAX,^{9,31} FT-IR,^{9,33,34} X-ray analysis,^{9,12,23,26,34,36,48,56,71,72} have been employed (see Table 1).

Table 1. Corrosion behaviours of metals and alloys in biological solutions

No.	Metals	Medium	Methods	Findings	Ref.
1	Ni-Al-Fe intermetallic alloys	simulated human body fluid	potentiodynamic polarization curves, electrochemical impedance spectroscopy, and electrochemical noise measurements	These alloys showed a similar or higher corrosion resistance than conventional AISI 316L type stainless steel, and this corrosion resistance decreased as the Al content in the alloy increased.	1
2	titanium alloy TC4 (Ti-6Al-4V)	0.9% NaCl and simulated body fluid	translational pin-on-disc friction tester, SEM	The micro-arc oxidation coating treated for 20 minutes showed a better corrosion resistance and frictional performance. By comparing the SEM surface morphologies of the worn test pieces, the reasons for high friction of micro-arc oxidation films were analyzed, which was related to the large micro-hole diameter and surface roughness of micro-arc oxidation coating.	2
3	Ti-13Nb-13Zr and Ti-6Al-4V alloys	Ringer's solution	open circuit potential-time measurements and potentiodynamic polarization	Martensitic Ti-6Al-4V ELI alloy possesses the best combination of both corrosion and wear resistance, although its corrosion resistance is found to be slightly higher than that of the Ti-13Nb-13Zr alloy.	3
4	commercially pure magnesium (CP-Mg), and ZM21 Mg alloy	Ringer's solution	electrochemical impedance spectroscopy (EIS)	The formation of a mud-crack pattern and a large number of clusters of needle-like crystals offers a relatively lower corrosion resistance for CP-Mg, ZM21 Mg alloy is a promising candidate material for the development of degradable implants.	4
5	micro-arc oxidation (MAO) on the surface of TC4 titanium alloys	simulated body fluid (SBF)	Friction experiments	MAO TiO ₂ coatings presented good tribological properties with lower friction coefficient in SBF.	5
6	Ti-10Zr-5Ta-5Nb alloy	physiological fluids of different pH values	cytocompatibility, cell morphology and cell adhesion	Ti-10Zr-5Ta-5Nb alloy presented self-passivation, with a large passive potential range and low passive current densities, namely, a very good anticorrosive resistance in Ringer solution of acid, neutral and alkaline pH values.	6
7	Ni-Ti alloy	simulated human body fluid	potentiodynamic polarization curves and electrochemical impedance spectroscopy	Addition of either 200 or 500 ppm B decreased the corrosion rate, but with the addition of 1000 ppm B or thermal annealing the alloy increased it.	7
8	AZ91D magnesium alloy	simulated body fluid	immersion and electrochemical testing	β -Mg ₁₇ Al ₁₂ precipitates in T6 microstructure facilitated intergranular corrosion and pitting, but the rate of corrosion was less than those of as-cast and T4 microstructures.	8
9	Ti-6Al-4V ELI (Extra Low Interstitial) alloy	Hanks solution	scanning electron microscopy (SEM), electron dispersive X-ray analysis (EDAX), and Fourier Transformation Infra Red (FT-IR) analysis, polarization and impedance spectroscopy (EIS)	to investigate the nucleation and growth of apatite on the chemically and thermally treated Ti-6Al-4V ELI alloy	9
10	CoCrMo alloys	simulated body fluids	electrochemical and mechanical processes for different abrasion-corrosion test conditions	The finding of this study implies that the smaller/softer third body particles generated in vivo could also result in significant wear-induced corrosion and therefore potential metal ion release, which could be potentially detrimental to both the patient health and the life span of the implants.	10
11	Nickel-free Fe-based bulk metallic glass (BMG), Fe ₄₁ Co ₇ Cr ₁₅ Mo ₁₄ C ₁₂ B ₆ Y ₂ alloy	Hank's solution with pH value 7.4 and artificial saliva solution with pH value 6.3	EIS analysis and cyclic polarization measurements	Pitting corrosion potential, polarisation resistance value are higher than that of 316L SS resulting in very few ions releasing into the SBFs while a significant amount of Ni and Fe ions release was found for 316L SS under the same condition.	11
12	nickel-free austenitic stainless steel	artificial body solution and distilled water	scanning electron microscopy (SEM), X-ray photoelectron spectroscopy (XPS)	The lubricative surface film formed on the wear scars in the artificial body solution could reduce the friction coefficient, and result in a lower wear loss in the artificial body solution than that in the distilled water.	12
13	east CoCrMo alloy	0.9% NaCl, phosphate buffered saline solution, 25% and 50% bovine serum solutions with 0 or 1 g cm ⁻³ SiC at 37 °C	electrochemical noise measurements	A severely deformed nano crystalline layer was identified immediately below the worn surface for both proteinaceous and inorganic solutions.	13

Table 1. (cont.)

No.	Metals	Medium	Methods	Findings	Ref.
14	macro-arc oxidation (MAO) coating on Mg alloy AZ91	simulated body fluids	potentiodynamic electrochemical technique and micro-abrasion tribometer	HCO ₃ ⁻ ions enhance the corrosion rates of the AZ91 alloys more significantly than the alloys with MAO coating. MgCO ₃ film formed in HCO ₃ ⁻ containing solutions leads to an enhancement in micro-wear resistance. MAO coating deteriorates the erosion corrosion resistance of AZ91 alloy due to the formation of oxidation debris resulted from the broken MAO coating.	14
15	AISI 316L stainless steel	Aerated simulated body fluid (SBF)	electrochemical impedance spectroscopy (EIS) and anodic polarization curves	study these materials as well as the characteristics of the superficial film formed in physiologic media in infection conditions in order to control their potential toxicity due to the release of metallic ions in the human body	15
16	plastic deformation of diamond-like carbon (DLC) coated and uncoated stainless steel	simulated body fluid environment	radio frequency plasma assisted chemical vapor deposition (R.F.-PACVD) method, potentiodynamic polarization test	increasing the thickness of the Si interlayer of film improved the corrosion resistance with reduction of spallations and cracks	16
17	Ti-Ca-P biocomposite	dry and simulated body fluid	Tribological experiments	to reporting the measured tribological data, a major focus of the work was in understanding dominant wear mechanisms under dry ambient and physiological environment	17
18	oxygen and albumin on the electrochemical behavior of a Ti-6Al-4V alloy	simulated inorganic plasma (SIP) solution	Potentiokinetic scans and electrochemical impedance spectroscopy	The hydrated porous oxide film results from the porous rutile layer reacting with H ₂ O ₂ formed as an intermediary component of oxygen reduction at the Ti-6Al-4V surface. The passive film-albumin interaction would affect the processing of titanium alloys in their surface preparation for biocompatibility, as well as determining the reactivity of titanium alloys to proteins	18
19	boronized tantalum	dry and simulated body fluid (SBF) conditions	Electrochemical methods	Fatigue cracks formed under dry conditions and tribochemical wear cracks formed under SBF conditions.	19
20	Zr-based bulk metallic glasses	artificial saliva solution (ASS), phosphate buffered solution (PBS) and artificial blood plasma solution (ABP)	electrochemical polarization and galvanostatic-step measurements	Compared with Zr ₆₅ Cu _{17.5} Ni ₁₀ Al _{7.5} base system, the BMGs containing Nb, or Nb and Pd, exhibited superior corrosion resistance against pitting, indicating that the addition of Nb enhanced the corrosion resistance	20
21	Laser surface melting (LSM) of Ti-6Al-4V	simulated body fluid (Ringer's solution)	electrochemical polarization experiments	The wear resistance of laser-treated Ti-6Al-4V in simulated body fluid is enhanced compared to that of the untreated one. Fragmentation of wear debris assisted by microcracking was responsible for mass loss during the wear of untreated Ti-6Al-4V in Ringer's solution	21
22	Co-Cr-Mo	artificial saliva, artificial saliva with modified temperature (7°C-47°C) and pH (1.4-13.4), and containing fluoride (1500 ppm)	electrochemical (Open Circuit Potential (OCP) and potentiodynamic polarization) and surface analysis techniques (Scanning Electron Microscopy (SEM) and Energy Dispersive Spectroscopy (EDS))	The electrochemical processes were markedly influenced by solution temperature and pH, whereas the presence of fluoride did not produce changes in the system.	22
23	CoCrMo alloy	simulated body conditions	Electrochemical techniques such as potentiodynamic and potentiostatic polarisation, cyclic voltammetry, rotating disc electrode and electrochemical impedance spectroscopy were employed. Further, ex situ X-ray photoelectron spectroscopy	The passive and transpassive behaviour of the alloy is hence dominated by the alloying element Cr, during activation/passivation cycles, cobalt dissolution is greater than expected from the composition of the alloy. Therefore, active dissolution behaviour is mainly dominated by the alloying element Co	23
24	nitrogen(N)ion implantation on the corrosion behavior of surgical materials, such as SUS316L stainless steel, Co-Cr alloy, commercially pure titanium and Ti-6Al-4V alloy	Hank's simulated body fluid	electrochemical technology, AES	After nitriding the corrosion resistance of the Co-Cr alloy is better than that of SUS316L due to the appearance of cobalt and chromium nitrides on the surface that protect the matrix and reduce the corrosion rate. As for SUS316L stainless steel, the surface was coated with iron and chromium nitrides which could prevent the Cr ³⁺ from hydrolyzing and increases the formation of Fe ₃ O ₄ , which plays an important role in protecting the matrix.	24
25	Mg alloys - AZ91D and WE43	simulated body fluid (SBF)	cyclic loading	The overload zone of the extruded WE43 alloy exhibited a ductile fracture mode with deep dimples, in comparison to a brittle fracture mode for the die-cast AZ91D. The corrosion rate of the two experimental alloys increased under cyclic loading compared to that in the static immersion test.	25

Table 1. (cont.)

No.	Metals	Medium	Methods	Findings	Ref.
26	TiO ₂ nanotubes	simulated body fluid (SBF)	anodization method	The nanotube length dependence of apatite formation can be ascribed to the different dissolution rate of nanotubes during the deposition of calcium phosphate (Ca-P) coatings, as well as the different penetration rate of Ca and P ions toward nanotube layer.	26
27	biocorrosion studies of TiO ₂ nanoparticle-coated Ti-6Al-4V implant	simulated biofluids (SBF), namely, (1) NaCl solution, (2) Hank's solution, and (3) Cigadasolution	micro-Raman spectroscopy, electrochemical techniques, and scanning electron microscopy (SEM) with energy dispersive X-ray spectroscopy (EDS)	TiO ₂ nanoparticle coatings increased the thickness of the pre-existing oxide layer on the Ti-6Al-4V surface, serving to improve the bioimplant corrosion resistance.	27
28	AZ31 magnesium alloy	in simulated body fluids was compared in chloride solution (8 g l ⁻¹) and in phosphate-buffer solution (PBS)	electrochemical techniques such as open circuit potential, polarization curves, transient currents and electrochemical impedance spectroscopy, complemented with scanning electron microscopy and energy dispersive spectroscopy	The best corrosion behaviour of the AZ31 alloy was obtained for the finest grain alloy associated with the highest transfer resistance value, after long periods of immersion in PBS.	28
29	bare and TiO ₂ nanoparticles coated Ti-6Al-4V bioimplants	simulated biofluid solutions: 1) NaCl solution; 2) Hank's solution; and 3) Cigada solution.	signal analysis techniques in both the time and frequency domains	FOSP may provide a better signal analysis tool to evaluate the ECN signals than the conventional fast Fourier transforms (FFT) processing method.	29
30	pure magnesium (Mg) and three Mg alloys with different Al contents	modified simulated body fluid (m-SBF)	immersion tests, Tafel experiments, and electrochemical impedance spectroscopic (EIS)	The microstructure and the Al content in the α-Mg (Al) matrix significantly affected the corrosion properties of the alloys in the m-SBF. With the increase in Al content, the corrosion resistances of the samples were improved.	30
31	magnesium alloy	Hank's solution and simulated blood plasma (SBP) solution	electrochemical and weight loss testing	The SV/SA ratio significantly affected the corrosion rate of magnesium alloy. By changing the ratio, the bio-corrosion behaviour of magnesium implant in different implantation sites can be simulated, for example, low ratio for the case of in muscle and high ratio for the case of in marrow cavity.	31
32	metal release and formation of surface precipitate at stainless steel grade 316	Hanks solution with or without H ₂ O ₂	SEM EDXS, XPS and Kelvin Probe measurements	In the absence of H ₂ O ₂ , formation of a surface layer consisting mainly of Ca ₃ (PO ₄) ₂ was observed, most likely it was responsible for the observed decrease of the release rates.	32
33	op Ti, without and with coating of the hydroxyapatite	artificial saliva and simulated body fluid (SBF) solution	potentiodynamic polarization curves	It was observed that hydroxyapatite layer has influence on corrosion resistance properties.	33
34	the composition of corrosion product layers on a magnesium rare-earth alloy	simulated body fluid (m-SBF) containing albumin in physiological concentration	energy dispersive X-ray analysis, grazing incidence X-ray diffraction, and FT-IR spectroscopy, scanning electron microscopy and light microscopy	Nature of surface layers on Mg rare-earth alloys formed in complex SBFs, with the aim to elucidate the influence of specific electrolyte components on the morphology, structure, and composition of corrosion layers on Mg alloys.	34
35	cobalt (Co) and chromium (Cr) ions	simulated biological fluids	Energy-dispersive X-ray analysis, elemental analysis, and Fourier Transform Infrared (FT-IR) spectroscopy	Understanding the relationship between toxicity and the chelating capabilities of various metal ions in vitro and in vivo	35
36	single layered titanium oxycarbide, TiC _x O _y	bio-fluid (an artificial perspiration solution) at room temperature	Electrochemical Impedance Spectroscopy (EIS)	the change in mechanisms of the tribological and corrosion parameters for such coatings, as a function of load and applied potential	36
37	NiTi alloy	fetal bovine serum (FBS)	open circuit potential (OCP), electrochemical impedance spectroscopy (EIS), scanning electron microscopy (SEM), X-ray photoelectron spectroscopy (XPS), and inductively coupled plasma mass spectrometry (ICP-MS)	Pits form on the NiTi alloy after immersion in FBS for 200 h but they are not observed on the sample immersed in PBS. XPS shows that the composition of the oxide film formed in FBS is similar to that formed in PBS and it is composed of mainly Ti oxides with a small amount of Ti hydroxide. The presence of FBS can accelerate leaching of Ni ions.	37
38	Stearic acid coating on magnesium for enhancing corrosion resistance	Hanks' solution (a simulated body fluid)	electrochemical methods	The corrosion resistance of the coated samples was much higher than that of bare magnesium. Degradation of the coating occurred due to cracking in long-term immersion, with the formation of magnesium hydroxide and apatite.	38
39	Mg-Ca, AZ31 and AZ91	Hank's solution, Dulbecco's Modified Eagle's Medium (DMEM) and serum-containing medium (DMEM adding 10% fetal bovine serum (DMEM+FBS))	linear polarization and electrochemical impedance spectroscopy (EIS); after 7 day immersion, potentiodynamic polarization tests, scanning electron microscopy (SEM) observation complemented by energy-disperse spectrometer (EDS) analysis	A Mg-Ca alloy exhibited an increased corrosion rate in the presence of serum protein. An AZ31 alloy showed an increased corrosion rate in DMEM+PBS in the initial 3 day immersion and the corrosion rate decreased thereafter. An AZ91 alloy, with high Al content, showed a reduced corrosion rate with the addition of FBS into DMEM.	39

Table 1. (cont.)

No.	Metals	Medium	Methods	Findings	Ref.
40	Ti base bio-alloy	Ringer solutions of different pH values (from 2.33 to 9.12)	electrochemical parameters and anticorrosive properties	New ternary Ti-6Al-4Zr alloy has higher corrosion resistance than Ti-6Al-4V alloy, improved as result of the beneficial, favourable effects of the replacement of vanadium with zirconium.	40
41	Ti6Al4V-ELI alloy	Ringer solutions of different pH values	electrochemical cyclic potentiodynamic polarization, electrochemical impedance spectroscopy and scanning electron microscopy	All alloys exhibited high corrosion resistance in Ringer solutions for 2000 exposure hours. SEM observations indicated the formation of calcium phosphate on the alloy surface.	41
42	Ti6Al7Nb alloy	Hank's Balanced Salt Solution (HBSS)	electrochemical polarization and electrochemical impedance spectroscopy techniques.	The presence of albumin proteins in HBSS improved the corrosion resistance of Ti6Al7Nb alloy.	42
43	AZ31 magnesium alloy	simulated body fluid (SBF)	electrochemical polarization and electrochemical impedance spectroscopy (EIS) tests and scanning electron microscope (SEM) observation	Protective film layer was formed on the surface of AZ31 in SBF. With increasing of immersion time, the film layer became more compact. The hydroxyapatite is the essential component of human bone, which indicates the perfect biocompatibility of AZ31 magnesium alloy.	43
44	magnesium alloy AX53	Hank's solutions, 0.9 wt% NaCl + 0.7 g/L NaHCO ₃ solutions and 0.9 wt% NaCl solutions at room temperature	scanning electron microscope, and the chemical compositions were examined through x-ray diffraction	Corrosion rates in Hank's solutions were lower than in the other solutions. Intergranular corrosion occurred in these solutions.	44
45	NiTi alloys	0.9% NaCl solution, Hank's simulated body solution and Tyrodé's simulated blood solution	electro chemical methods	The corrosive behaviour of NiTi alloy in physiological environments containing Cl ⁻ ion is Ni selective corrosion, and is pitting corrosion.	45
46	NiTi	Hank's solution	potentiostatically controlled stimulation-repassivation scheme in the presence of a crevice former, EDS analysis	The results of the stimulation-repassivation tests, the susceptibility of various samples to crevice corrosion in Hank's solution at 37 °C and pH 7.4 may be ranked in ascending order as: $cp \text{ Ti} \approx \text{Ti6Al4V} < 316L < \text{NiTiCu} < \text{NiTi}$. The beneficial effect of Cu could be attributed to the redeposition of Cu inside the crevice.	46
47	Ti-6Al-4V alloy	simulated inorganic plasma (SIP) solution	potentiokinetic scans and electrochemical impedance spectroscopy	The hydrated porous oxide film results from the porous rutile layer reacting with H ₂ O ₂ formed as an intermediary component of oxygen reduction at the Ti-6Al-4V surface. The passive film-albumin interaction would affect the processing of titanium alloys in their surface preparation for biocompatibility, as well as determining the reactivity of titanium alloys to proteins.	47
48	boronized tantalum	dry and simulated body fluid (SBF) conditions	electrochemical methods	Fatigue cracks formed under dry conditions and tribochemical wear cracks formed under SBF conditions.	48
49	nickel-free austenitic stainless steel	Hank's solution	SEM and XRD	The friction coefficient is reduced due to the formation of soft surface film on the steel surface.	49
50	seven grades of stainless steels	two synthetic body fluids, Gamble's solution, artificial lysosomal fluid (ALF)	macrophages	The more acidic environment of ALF resulted in significantly higher total metal release rates (0.3–4.6 $\mu\text{g cm}^{-2} \text{ week}^{-1}$) compared to Gamble's solution (<0.1 $\mu\text{g cm}^{-2} \text{ week}^{-1}$).	50
51	Titanium and its Ti-45.5Ni alloy	Tani & Zucchi (pH = 2.5 and 7) and Fusayama (pH = 5.5) artificial saliva.	electrochemical methods	Corrosion potentials for Ti-45.5Ni alloy in Carter-Brugiard saliva presented more electronegative values than titanium, but no form of local corrosion was registered during 4000 exposure hours. Cell proliferation is considerable in the first 48 hours of culture. Slight cytotoxic effects specially developed after 72 incubation hours.	51
52	ZrAlCuNi bulk metallic glasses	artificial body fluid	electrochemical measurements, XPS analysis, inductively coupled plasma mass spectrometry (ICP-MS)	The addition of Nb considerably reduced the ion release of all kinds of metals of the base system. This is probably attributed to the promoting effect of Nb on a rapid formation of highly protective film.	52
53	Metals	saliva and the second to plasmatic serum	open circuit potential, polarisation curves and electrochemical impedance on high speed steel	The organic components in the fluids partially block the metal surface and reduce the corrosion rate. From the results obtained, an approximate order of corrosion rate was established as: Artificial saliva ~ Glandosane ~ Krebs-Ringer solution < Artificial saliva without lactic acid ~ PBS.	53

Table 1. (cont.)

No.	Metals	Medium	Methods	Findings	Ref.
54	316L stainless steel	natural plasma and plasma modified with different artificial media (Physiological serum, Glucose, Dextran 70, Aminoseryl, Yamin, Inralipid and Kabiven)	electrochemical methods	of the formation of passive film for which the stability strongly depends on the corrosive activity of the physiological media	54
55	Cr-Ni-Mo stainless steel	simulated urine	applied technique of stent implantation	The deformability tests of the passive layer were carried out with the use of a bend test followed by a corrosion test.	55
56	Cr-Ni stainless steel	artificial urine solution	potentiodynamic method	The analysis of the results of electrochemical corrosion resistance tests showed positive impact of wire surface treatment by means of electrolytic polishing and chemical passivation method on improvement of its corrosive properties.	56
57	X2CrNiMo 17-12-2 stainless steel surface	artificial urine	potentiodynamic method, using X-ray photoelectron spectroscopy (XPS)	To determine suitability of X2CrNiMo 17-12-2 steel with modified surface and diversified strain hardening for production of wire used in urology.	57
58	CoCr alloy, Ti, and the experimental alloy MA956 coated with α -alumina	kidneys, livers, lungs and spleens	Inductively Coupled Plasma (ICP) with Mass Spectrometry (MS)	The organs of rats implanted with the α -alumina coated experimental MA956 did not present any variation in Al content after 12 months, which means there was no degradation of the alumina layer surface.	58
59	Co-Cr-Mo implant alloys	urine, serum and joint fluid	potentiodynamic scan method, cyclic voltammetry (CV), and ac impedance spectroscopy	Based on the result of CV, the Co-Cr-Mo implant alloy only exhibits small passive region in joint fluid and serum, but a much large region for urine. However, the corrosion resistance of Co-Cr-Mo implant alloys in urine ($5128 \Omega \text{ cm}^2$) was slightly lower than that in joint fluid ($6513 \Omega \text{ cm}^2$) and serum ($6691 \Omega \text{ cm}^2$) at E_{cor} and 37°C based on the result of ac analyses, the experimental results of Tafel plot analyses were found in good agreement with that of ac impedance analyses.	59
60	Ti-6Al-4V implant alloy	urine, serum and joint fluid	potentiodynamic method, cyclic voltammetry, electrochemical impedance spectroscopy (EIS)	The Ti-6Al-4V implant alloy in three biological solutions showed a characteristic of a capacitive behaviour. The experimental results of Tafel plot analyses were found in good agreement with that of EIS analyses.	60
61	Ti-6Al-4V implant alloy	three biological fluid solutions, i.e. urine, serum and joint fluid, in phosphate buffered saline (PBS) solutions at different pH values	that the corrosion current densities of Ti-6Al-4V implant alloy in PBS solutions of different pH values were about the same order of magnitude, which was at a level of $1-2 \mu\text{Acm}^{-2}$ at 37°C . In contrast, the corrosion current densities in biological fluids were lower at an order of $0.1-0.3 \mu\text{Acm}^{-2}$ at 37°C	The Ti-6Al-4V implant alloy in three biological body fluid solutions showed a characteristic of one capacitive behaviour.	61
62	medical grade AISI Type 316L (UNS S31603) stainless steel	pure distilled water, the Ringer's body fluid, and 3% sodium chloride (NaCl) aqueous solution (the most aggressive environment)	open-circuit potential and polarization curve	The proposed MEP process shifts the corrosion potentials into the direction of greater corrosion resistance.	62
63	NiTi-based alloy (Nitinol)	simulated body fluids (-0.313 ± 0.003 V/SCE in AFNOR S90-701 artificial saliva; -0.334 ± 0.001 V/SCE in artificial urine; -0.239 ± 0.007 V/SCE in Ringer's solution)	electrochemical methods	The importance of evaluating the corrosion resistance of Nitinol under realistic conditions (mechanical loads, wear and fatigue) in order to establish multifaceted mechanisms that might lead to accelerated dissolution and failure of implanted stents.	63
64	Nitinol	simulated body fluids	surface treatment	Preconditioning of samples alters surface properties and modulates the cell response regardless of the initial surface treatment and its properties.	64
65	Ni-free Zn-based bulk metallic glasses	simulated body fluid	SEM and EDS	Compared with the Ti alloy, the BMG exhibits much less volume loss in the PBS solution, demonstrating that the BMG has a better wear resistance than the Ti alloy, though he former has a larger friction coefficient. The wear mechanism of the BMG is dominated by the corrosion wear with oxidation of the surface and fatigue flake mechanism.	65
66	AZ91D magnesium alloy	simulated body fluid	immersion and electrochemical testing	Fine $\beta\text{-Mg}_{17}\text{Al}_{12}$ precipitates in T6 microstructure facilitated intergranular corrosion and pitting, but the rate of corrosion was less than those of as-cast and T4 microstructures.	66

Table 1. (cont.)

No.	Metals	Medium	Methods	Findings	Ref.
67	CoCrMo alloy	simulated body environments	Nano-indentation and nano-scratch tests	The abrasive wear rate and wear mechanisms of the CoCrMo are dependent on the nature of the third body abrasives, their entrainment into the contact and the presence of the proteins.	67
68	CP Titanium, Ti-6Al-4V and Ti-based intermetallic Ti-13.4Al-29Nb	simulated body condition (Hank's solution)	potentiodynamic polarization and electrochemical impedance spectroscopy techniques	The resistance of the passive film increased with duration of immersion for CP Titanium and Ti-13.4Al-29Nb. Therefore, the order of corrosion resistance under simulated human body conditions is Ti-Nb > Ti > Ti-V.	68
69	Mg-Ca, AZ31 and AZ91 alloys	Hank's solution	potentiodynamic polarization tests, scanning electron microscopy (SEM), energy-disperse spectrometer (EDS) analysis energy-disperse spectrometer (EDS) analysis	A Mg-Ca alloy exhibited an increased corrosion rate in the presence of serum protein. An AZ31 alloy showed an increased corrosion rate in DMEM+PBS in the initial 3 day immersion and the corrosion rate decreased thereafter. An AZ91 alloy, with high Al content, showed a reduced corrosion rate with the addition of PBS into DMEM.	69
70	CoCrMo alloy	simulated body fluids	electrochemical impedance spectroscopy (EIS)	Wear of CoCrMo alloy is negligible under cathodic and in the cathodic-anodic transition and considerably increases in the passive domain.	70
71	Mg-Y-RE alloy (WE43)	simulated body fluid	thermo gravimetric analysis (TGA), X-ray diffraction spectra, Auger electron spectroscopy	Oxidized samples exhibit a slow initial degradation rate which increases when the protection of the oxide layer is reduced.	71
72	TiO coatings on Ti-6Al-4V	simulated body fluid	X-ray diffraction and X-ray fluorescence, ellipsometry, electrochemical polarization and AC impedance studies	The coating produced by 10-h electrolysis from bath of Ca/P ratio 1.5 showed low corrosion current and high impedance to the week-long attack of SBF.	72
73	metallic copper and a novel composite	simulated body fluid	scanning electron microscopy, X-ray energy dispersive spectroscopy, X-ray diffraction, and atomic absorption spectrophotometer	No significant change on time-dependence was found for the release rates of cupric ions in the composite compared with that of metallic copper.	73
74	CP Titanium, Ti-6Al-4V and Ti-based intermetallic Ti-13.4Al-29Nb	simulated body condition (Hank's solution)	potentiodynamic polarization and electrochemical impedance spectroscopy techniques	The resistance of the passive film increased with duration of immersion for CP Titanium and Ti-13.4Al-29Nb. Therefore, the order of corrosion resistance under simulated human body conditions is Ti-Nb > Ti > Ti-V.	74
75	NiTi alloy wires	Hank's solution at different PH values and the pH 7.4 NaCl solution for different CP concentrations	potentiodynamic tests, Scanning electron microscope, electron probe microanalyzer	Corrosion resistances of a laser spot-welded joint and base metal decreased with increasing of the Cl ⁻ concentration and PH value.	75
76	thin calcium phosphate (CaP) films were electrochemically deposited on titanium substrates	modified simulated body fluid at 37 °C	scanning electron microscopy, X-ray diffractometry, X-ray photoelectron spectroscopy, Cell culture experiments	The coatings possessed a similar surface chemistry to that of natural bone minerals, which yielded a Ca:P ratio of 1.65, close to that of hydroxyapatite. the CaP surfaces are nontoxic to MG63 osteoblastic cells in vitro and were able to support cell growth for up to 4 days, outperforming the untreated titanium surface in a direct comparison.	76
77	SS 316L, mild steel (MS) and mild steel coated with zinc (MS-Zn)	artificial saliva	Potentiodynamic polarization study and AC impedance spectra	The order of corrosion resistance of metals in artificial saliva, in the absence and also in the presence of spirulina was SS 316L > MS > MS-Zn.	77
78	Titanium and Titanium Alloy	Artificial Saliva	potentiodynamic anodic Polarisation and open circuit potential tests	The passive range was higher for the Nb-alloy compared to the potentiodynamic test for commercially pure titanium.	78
79	Titanium and Titanium Alloy metals	different artificial body fluids	open circuit potential, polarisation curves and electrochemical impedance	It was found that the organic components in the fluids partially block the metal surface and reduce the corrosion rate. From the results obtained, an approximate order of corrosion rate was established as: Artificial saliva ~ Glandosane ~ Krebs Ringer solution < Artificial saliva without lactic acid ~ PBS.	79
80	SS 316L, mild steel (MS) and mild steel coated with zinc (MS-Zn)	artificial saliva	Potentiodynamic polarization study and AC impedance spectra	The order of corrosion resistance of metals in artificial saliva, in the absence and also in the presence of D-Glucose was SS 316L > MS-Zn > MS.	80
81	SS 316L, mild steel (MS) and mild steel coated with zinc (MS-Zn)	artificial saliva	Potentiodynamic polarization study and AC impedance spectra	The order of corrosion resistance of metals in artificial saliva, in the absence and also in the presence of electoral was SS 316L > MS > MS-Zn.	81

Findings

The micro-arc oxidation coating treated for 20 minutes showed a better corrosion resistance and frictional performance. By comparing the SEM surface morphologies of the worn test pieces, the reasons for high friction of micro-arc oxidation films were analyzed, which was related to the large micro-hole diameter and surface roughness of micro-arc oxidation coating.² MAO TiO₂ coatings presented good tribological properties with lower friction coefficient in SBF.⁵ The overload zone of the extruded WE43 alloy exhibited a ductile fracture mode with deep dimples, in comparison to a brittle fracture mode for the die-cast AZ91D. The corrosion rate of the two experimental alloys increased under cyclic loading compared to that in the static immersion test.²⁵ The analysis of the results of electrochemical corrosion resistance tests showed positive impact of wire surface treatment by means of electrolytic polishing and chemical passivation method on improvement of its corrosive properties.⁵⁶ Based on the result of CV, the Co-Cr-Mo implant alloy only exhibits small passive region in joint fluid and serum, but a much large region for urine. However, the corrosion resistance of Co-Cr-Mo implant alloys in urine (5128 Ω cm²) was slightly lower than that in joint fluid (6513 Ω cm²) and serum (6691 Ω cm²) at E_{corr} and 37°C based on the result ac analyses, the experimental results of Tafel plot analyses were found in good agreement with that of ac impedance analyses.⁵⁹

Acknowledgement

The authors are thankful to their Managements and St. Joseph's Research and Community Development Trust, Dindigul, India for their help and encouragement.

References

- Castaneda, I. E., Gonzalez-Rodriguez, J. G., Colin, J., Neri-Flores, M. A., *J. Solid State Electrochem*, **2010**, 14(7), 1145.
- Zhai, W.-J., Zhu, B.-Q., Liu, L.-F., *Mocaxue Xuebao/Tribology*, **2009**, 29(5), 425.
- Cvijovic-Alagic, I., Cvijovic, Z., Mitrovic, S., Panic, V., Rakin, M. Ye., *Corros. Sci.*, **2011**, 53(2), 796.
- Jamesh, M., Kumar, S., Sankara Narayanan, T. S. N., *Corros. Sci.*, **2011**, 53(2), 645.
- Zhou, G., Ding, H., Zhang, Y., Liu, A., Lin, Y., Zhu, Y., *Tribology Letters*, **2010**, 40(3), 319.
- Vasilescu, E., Drob, P., Raducanu, D., Cojocar, V.D., Cinca, I., Iordachescu, D., Ion, R., Popa, M., Vasilescu, C., *J. Mater. Sci-Mater. Med*, **2010**, 21(6), 1959.
- Ruiz, J. A., Rosales, I., Gonzalez-Rodriguez, J. G., Uruchurtu, J., *Int. J. Electrochem. Sci.*, **2010**, 5(4), 593.
- Zhou, W., Shen, T., Aung, N. N., *Corros. Sci.*, **2010**, 52(3), 1035.
- Tamilselvi, S., Raman, V., Rajendran, N., *J. Appl. Electrochem*, **2010**, 40(2), 285.
- Sun, D., Wharton, J. A., Wood, R. J. K., *Tribology Int.*, **2009**, 42(11), 1595.
- Wang, Y.B., Li, H.F., Cheng, Y., Wei, S.C., Zheng, Y.F., *Electrochem. Commun*, **2009**, 11(11), 2187.
- Zhou, G., Zhang, Y., Ding, H., *Mater.Sci. Forum*, **2009**, 610, 1183.
- Sun, D., Wharton, J. A., Wood, R. J. K., Ma, L., Rainforth, W. M., *Tribology Int.*, **2009**, 42(1), 99.
- Chen, J., Zeng, R.-C., Huang, W.-J., Zheng, Z.-Q., Wang, Z.-L., Wang, J., *Trans. Nonferr. Metal. Soc.*, **2008**, 18(1), 361.
- Loez, D. A., Durán, A., Cere, S. M., *J.Mater. Sci-Mater. Med*, **2008**, 19(5), 2137.
- Choi, H. W., Lee, K.-R., Park, S. J., Wang, R., Kim, J.-G., Oh, K.H., *Surf. Coat. Techn.*, **2008**, 202(12), 2632.
- Karanjai, M., Kumar, B. V. M., Sundaresan, R., Basu, B., Rama Mohan, T. R., Kashyap, B. P., *Mater. Sci. Eng A*, **2008**, 475(1), 299.
- Padilla, N., Branson, A., *J. Biomed. Mater. Res - Part A*, **2007**, 81(3), 531.
- Ribeiro, R., Ingole, S., Usta, M., Bindal, C., Ucisik, A. H., Liang, H., *Wear*, **2007**, 262(11), 1380.
- Liu, L., Qiu, C. L., Chen, Q., Zhang, S. M., *J. Alloys Compd.*, **2006**, 425(1), 268.
- Singh, R., Kurella, A., Dahotre, N. B., *J. Biomater.Appl*, **2006**, 21(1), 49.
- Giacomelli, F. C., Giacomelli, C., Spinelli, A., *J. Braz. Chem. Soc.*, **2004**, 15(4), 541.
- Hodgson, A. W. E., Kurz, S., Virtanen, S., Fervel, V., Olsson, C.-O. A., Mischler, S., *Electrochim. Acta*, **2004**, 49(13), 2167.
- Chenghao, L., Liang, G., Wan, C., *XiyouJinshuCailiao Yu Gongcheng*, **2002**, 31(4), 277.
- Gu, X.N., Zhou, W.R., Zheng, Y.F., Cheng, Y., Wei, S.C., Zhong, S.P., Xi, T.F., Chen, L.J., *Acta Biomater*, **2010**, 6(12), 4605.
- Liang, Y., Yang, X., Cui, Z., Zhu, S., *Curr. Nanosci*, **2010**, 6(3), 256.
- Zaveri, N., McEwen, G.D., Karpagavalli, R., Zhou, A., *J. Nano part. Res*, **2010**, 12(5), 1609.
- Alvarez-Lopez, M., Pereda, M. D., del Valle, J. A., Fernandez-Lorenzo, M., Garcia-Alonso, M. C., Ruano, O. A., Escudero, M. L., *Acta Biomater*, **2010**, 6(5), 1763.
- Sheng, H., Zaveri, N., Chen, Y., Zhou, A., *Proc. ASME Int. Design Eng. Techn. Conf. Comput. Inform. Eng. Conf.* **2009**, **2010**, 1157.
- Wen, Z., Wu, C., Dai, C., Yang, F., *J. Alloys Compd*, **2009**, 488(1), 392.
- Yang, L., Zhang, E., *Mater. Sci Eng C*, **2009**, 29(5), 1691.
- Cieslik, M., Reczyński, W., Janus, A. M., Engvall, K., Socha, R. P., Kotarba, A., *Corros. Sci.*, **2009**, 51(5), 1157.
- Mariano, N. A., Oliveira, R. G., Braga, E. I., Rigo, E. C. S., *Key Eng. Mater*, **2009**, 396, 315.
- Rettig, R., Virtanen, S., *J. Biomed. Mater. Res - Part A*, **2009**, 88(2), 359.
- Tkaczyk, C., Huk, O. L., Mwale, F., Antoniou, J., Zukor, D. J., Petit, A., Tabrizian, M., *Biomaterials*, **2009**, 30(4), 460.
- Mathew, M. T., Ariza, E., Rocha, L. A., Vaz, F., Fernandes A. C., Stack, M. M., *Electrochim. Acta*, **2010**, 56(2), 929.
- Hang, R., Ma, S., Ji, V., Chu, P. K., **2010**, 55(20), 5551.
- Ng, W. F., Wong, M. H., Cheng, F. T., *Surf. Coat. Tech*, **2010**, 204(11), 1823.
- Gu, X. N., Zheng, Y. F., Chen, L. J., *Biomed. Mater*, **2009**, 4(6), Art. no. 065011,
- Popa, M. V., Vasilescu, E., Drob, P., Vasilescu, C., *IFMBE Pro.*, **2009**, 25(10), 24.

- ⁴¹ Vasilescu, E., Drob, P., Raducanu, D., Cinca, I., Mareci, D., Calderon Moreno, J. M., Popa, M., Mirza Rosca, J. C., *Corros. Sci.* **2009**, *51*(12), 2885.
- ⁴² Daniel, M., Cailean, A., Bolat, G., Cretescu, I., Sutiman, D. *Stud. Univ. Babeş-Bolyai. Chem.* , **2009**, *1*, 93.
- ⁴³ Song, Y., Shan, D., Chen, R., Zhang, F., Han, E.-H., *Mater. Sci. Eng C*, **2009**, *29*(3), 1039.
- ⁴⁴ Wang, J., Zeng, R., Chen, J., Chen, R., *Mater. Sci. Forum* , **2009**, *610*, 1174.
- ⁴⁵ Su, X., Hao, W., Wang, T., Han, F., Zhang, B., He, L., *Cailiao Yanjiu Xuebao*, **2007**, *21*(5), 454.
- ⁴⁶ Cheng, F. T., Lo, K. H., Man, H. C., *J. Alloys Compd.*, **2007**, *437*(1), 322.
- ⁴⁷ Padilla, N., Branson, A., *J. Biomed. Mater. Res - Part A*, **2007**, *81*(3), 531.
- ⁴⁸ Ribeiro, R., Ingole, S., Usta, M., Bindal, C., Ucisik, A. H., Liang, H., *Wear*, **2007**, *262*(11), 1380.
- ⁴⁹ Zhou, G.-H., Ding, H.-Y., Dai, Q.-X., *Cailiao Rechuli Xuebao*, **2007**, *28*(1), 62.
- ⁵⁰ Herting, G., Odneval Wallinder, I., Leygraf, C., *Corros. Sci.*, **2007**, *49*(1), 103.
- ⁵¹ Popa, M. V., Vasilescu, E., Drob, P., Iordachescu, D., Cimpean, A., Ionita, D., Vasilescu, C., *Proc. 2006 Int. Conf. Microtechnol. Med. Biol.* **2006**, 81, Art. no. 4281314.
- ⁵² Qiu, C. L., Liu, L., Sun, M., Zhang, S. M., *J. Biomed. Mater. Res - Part A*, **2005**, *75*(4), 950.
- ⁵³ Brett, C. M. A., Muresan, I., *Key Eng. Mater.*, **2002**, *230*, 459.
- ⁵⁴ Tutunaru, B., Samide, A. P., Preda, M., *Rev. Chim.* **2007**, *58*(10), 923.
- ⁵⁵ Kajzer, W., Chrzanowski, W., Marciniak, J., *Int. J. Microstruct. Mater. Prop.*, **2007**, *2*(2), 188.
- ⁵⁶ Przondziona, J., Walke, W., *Arch. Mater. Sci. Eng.* **2009**, *35*(1), 21.
- ⁵⁷ Walke, W., Przondziona, J., *Solid State Phenomena*, **2010**, *165*, 404.
- ⁵⁸ Rubio, J. C., Garcia-Alonso, M. C., Alonso, C., Alobera, M. A., Clemente, C., Munuera, L., Escudero, M. L., *J. Mater. Sci- Mater. Med.* **2008**, *19*(1), 369.
- ⁵⁹ Hsu, R. W.-W., Yang, C.-C., Huang, C.-A., Chen, Y.-S., *Mater. Chem. Phys.* **2009**, *93*, 531.
- ⁶⁰ Hsu, R. W.-W., Yang, C.-C., Huang, C.-A., Chen, Y.-S., *Mater. Sci. Eng. A*, **2004**, *380*(1), 100.
- ⁶¹ Hsu, R. W.-W., Yang, C.-C., Huang, C.-A., Chen, Y.-S., *Mater. Chem. Phys.* **2004**, *86*(2), 269.
- ⁶² Hryniewicz, T., Rokicki, R., Rokosz, K., *Corros*, **2008**, *64*(8), 660.
- ⁶³ Pertile, L. B., Silva, P. M. S., Peccin, V. B., Peres, R., Silveira, P. G., Giacomelli, C., Giacomelli, F. C., Spinelli, A., *J. Biomed. Mater. Res - Part A*, **2009**, *89*(4), 1072.
- ⁶⁴ Chrzanowski, W., Abou Neel, E. A., Armitage, D. A., Zhao, X., Knowles, J. C., Salih, V., *J. Biomed. Mater. Res - Part A*, **2010**, *93*(4), 1596 .
- ⁶⁵ Huang, C., Chen, Q., Liu, L., *Jinshu Xuebao*, **2010**, *46*(6), 681.
- ⁶⁶ Zhou, W., Shen, T., Aung, N. N., *Corros. Sci.*, **2010**, *52*(3), 1035.
- ⁶⁷ Sun, D., Wharton, J. A., Wood, R. J. K., *Wear*, **2009**, *267*(11), 1845.
- ⁶⁸ Shukla, A. K., Balasubramaniam, R., Bhargava, S., *Intermet.*, **2005**, *13*(6), 631.
- ⁶⁹ Ghoneim, A. A., Fekry, A. M., Ameer, M. A., *Electrochim. Acta* , **2010**, *55*(20), 6028.
- ⁷⁰ Igal Munoz, A., Casabán, J. L., *Electrochim. Acta*, **2010**, *55*(19), 5428.
- ⁷¹ Hännzi, A. C., Gunde, P., Schinhammer, M., Uggowitz, P. J., *Acta Biomater*, **2009**, *5*(1), 162.
- ⁷² Narayanan, R., Seshadri, S. K., Kwon, T.-Y., Kim, K.-H., *J. Biomed. Mater. Res - Part A*, **2008**, *86*(2), 502.
- ⁷³ Li, J., Suo, J., Huang, X., Ye, C., Wu, X., *J. Biomed. Mater. Res. - Part B Appl. Biomater*, **2008**, *85*(1), 172.
- ⁷⁴ Shukla, A. K., Balasubramaniam, R., *Corros. Sci.* **2006**, *48*(7), 1696.
- ⁷⁵ Yan, X.-J., Yang, D.-Z., *J. Biomed. Mater. Res - Part A*, **2006**, *77*(1), 97.
- ⁷⁶ Peng, P., Kumar, S., Voelcker, N. H., Szili, E., Smart, R. St. C., Griesser, H. J., *J. Biomed. Mater. Res - Part A*, **2006**, *76*(2), 347.
- ⁷⁷ Rajendran, S., Paulraj, J., Rengan, P., Jeyasundari, J., and Manivannan, M *J. Dent. Oral Hyg.*, **2009**, *1*(1), 1.
- ⁷⁸ Raman, V., Tamilselvi, S., Nanjundan, S., and Rajendran, N., *Trends Biomater. Artif. Organs*, **2005**, *18*(2), 137.
- ⁷⁹ Christopher, M. A., Brett and Ioana Muresan, *Key Eng. Mater.* **2002**, *230*, 459.
- ⁸⁰ Rajendran, S., Uma, V., Krishnaveni, A., Jeyasundari, J., Shyamala Devi, B., and Manivannan, M., *Arab. J. Sci. Eng.* **2009**, *34*(2c), 149.
- ⁸¹ Rajendran, S., Johnmary, S., Krishnaveni, A., Kanchana, S., Lydia Christy, J., Nagalagshmi, R., Narayana Samy, B., *Zastit. Mater.* **2010**, *51*(3), 149.
- ⁸² Saranya, R., Rajendran, S., Krishnaveni, A., Pandiarajan, M., Nagalakshmi, R., *Eur. Chem. Bull.*, **2013**, *2*(4), 163-170.
- ⁸³ Nagalakshmi, R., Rajendran, S., Sathiyabama, J., Pandiarajan, M., and Lydia Christy, J., *Eur. Chem. Bull.* **2013**, *2*(4), 150.

Received: 29.11.2012.

Accepted: 05.01.2013.



AN OVERVIEW ON SYNTHETIC METHODS OF ALKYL CINNAMATES

Gao Wenyi^{[a]*}, Liu Shu^[a] and You Hongjun^[b]

Keywords: overview; synthetic methods; catalysts; alkyl cinnamates

Some industrial synthetic methods for an analogous series of C₁₋₅ alkyl cinnamates using different catalysts such as sulfonic acids (*p*-toluene-sulfonic acid), inorganic salts (NH₄Fe(SO₄)₂·12H₂O) and solid superacids (SO₄²⁻/La₂O₃-ZrO₂-HZSM-5) are reviewed. Yields of an analogous series of C₁₋₅ alkyl cinnamates are improved by the addition of the above mentioned catalysts. The main advantages of these methods are the simple process operation and low investment costs.

* Corresponding Author

Fax: 86-24-56860869

E-Mail: youhongjun@hotmail.com

[a] Liaoning Shihua University, Fushun, Liaoning, P.R. China.

[b] SAIT Polytechnic, Calgary AB, Canada.

(methanol, ethanol, *n*-propyl, *n*-butanol, isobutanol, *n*-amyl and isoamyl alcohol) produced an analogous series of alkyl cinnamates.

Introduction

Alkyl cinnamates are important organic intermediates and are widely used in perfume, soap and flavouring essences due to pronounced fruit or flower aromas.¹ Cinnamic acid in presence of a catalyst reacts with alcohol to produce alkyl cinnamates. An analogous series of alkyl cinnamates consists of methyl, ethyl, *n*-propyl, *n*-butyl, isobutyl, *n*-pentyl and isopentyl cinnamate etc.² Two methods (the classical method and the microwave heating method) are used to synthesize alkyl cinnamates in the industry. In the classical method cinnamic acid in presence of a catalyst reacts with methanol or ethanol to produce corresponding cinnamate. The disadvantage of this method is that it takes a long time to finish the reaction, benzene or toluene has to be used as dehydrating agent, requires a large amount of catalyst and gives low yield of alkyl cinnamates. The microwave heating method, though decreases the reaction time and increases the yield of alkyl cinnamates, the unit is very complicated and it is difficult to increase output of alkyl cinnamates.³

The present paper discusses new catalysts such as *p*-toluene-sulfonic acid, NH₄Fe(SO₄)₂·12H₂O and solid superacids (SO₄²⁻/La₂O₃-ZrO₂-HZSM-5).

Results and Discussion

p-Toulene sulphonic acid as a catalyst

Xu Tongtao² discussed different reaction conditions on yields of alkyl cinnamates such as methyl, ethyl, *n*-propyl, *n*-butyl, isobutyl, *n*-pentyl and isopentyl cinnamate. Using *p*-toluene-sulfonic acid as a catalyst and cinnamic acid and alcohols

Table 1 shows optimal reaction conditions for the synthesis of C₁₋₅ alkyl cinnamates. The experimental results showed that different yields of alkyl cinnamates were obtained. Methyl cinnamate had the highest yields and that of isobutyl cinnamate was the lowest. This may be related to their molecular structure. On the other hand, although *n*-butyl and isobutyl cinnamate or *n*-pentyl and isopentyl cinnamate have similar molecular weights, the yields of *n*-butyl and *n*-pentyl cinnamate were more than that of isobutyl and isopentyl cinnamate respectively. This may be related with steric hindrance of larger alkyl groups.

NH₄Fe(SO₄)₂·12H₂O as a catalyst

Wen Ruiming⁴ described the use of NH₄Fe(SO₄)₂·12H₂O as a catalyst for the synthesis of alkyl cinnamates. The effect of different reaction conditions such as the reaction time, the molar ratio of cinnamic acid to alcohol, the amount of NH₄Fe(SO₄)₂·12H₂O on yields of alkyl cinnamates were discussed. Table 2 presents the relationship between different reaction conditions and yields of alkyl cinnamates. The experimental results show that the yield of ethyl cinnamate was the highest and that of isobutyl cinnamate was the lowest.

SO₄²⁻/La₂O₃-ZrO₂-HZSM-5 as a catalyst

Chen Shufen⁵ described the use of SO₄²⁻/La₂O₃-ZrO₂-HZSM-5 as the catalyst and discussed the effect of different reaction conditions such as the amount of SO₄²⁻/La₂O₃-ZrO₂-HZSM-5 and the molar ratio of cinnamic acid to *n*-butyl alcohol on yields of alkyl cinnamates. Table 3 shows the effect of different reaction conditions on yields of alkyl cinnamates. It is noted that the yield of *n*-pentyl cinnamate was the highest and that of ethyl cinnamate was the lowest.

Table 1. Optimal reaction conditions for the synthesis of C₁₋₅ alkyl cinnamates

Alkyl cinnamates	Amount of catalyst, g	Amount of alcohol, mol	Molar ratio of cinnamic acid to alcohol	Reaction time, h	Yield, %
methyl cinnamate	6.41% of total reactant weight	0.15	0.02:0.15	5.0	90.2
ethyl cinnamate	5.32% of total reactant weight	0.18	0.02:0.18	5.0	80.4
<i>n</i> -propyl cinnamate	4.00% of total reactant weight	0.20	0.02:0.20	5.0	81.6
<i>n</i> -butyl cinnamate	3.97% of total reactant weight	0.30	0.02:0.30	3.5	80.0
isobutyl cinnamate	3.97% of total reactant weight	0.30	0.02:0.30	3.5	75.0
<i>n</i> -pentyl cinnamate	4.85% of total reactant weight	0.20	0.02:0.20	3.5	80.3
isopentyl cinnamate	4.85% of total reactant weight	0.20	0.02:0.20	3.5	78.0

Table 2. The relationships between different reaction conditions and yields of C₁₋₅ alkyl cinnamates

Alkyl cinnamates	Amount of a catalyst, g	Amount of alcohol, mol	Molar ratio of cinnamic acid to alcohol	Reaction time, h	Yield, %
methyl cinnamate	53.19% of total reactant weight	0.20	1.0:10.0	7.0	87.5
ethyl cinnamate	40.98% of total reactant weight	0.20	1.0:10.0	7.0	94.3
<i>n</i> -propyl cinnamate	33.33% of total reactant weight	0.20	1.0:10.0	7.0	89.5
<i>n</i> -butyl cinnamate	15.34% of total reactant weight	0.40	1.0:20.0	2.0	80.0
isobutyl cinnamate	15.34% of total reactant weight	0.40	1.0:20.0	2.0	75.0
<i>n</i> -pentyl cinnamate	24.27% of total reactant weight	0.20	1.0:10.0	2.0	84.9
isopentyl cinnamate	24.27% of total reactant weight	0.20	1.0:10.0	2.0	75.7

Table 3. The effect of different reaction conditions on yields of an analogous series of C₁₋₅ alkyl cinnamates

Alkyl cinnamates	Amount of a catalyst, g	Molar ratio of cinnamic acid to alcohol	Reaction time, h	Yield, %
methyl cinnamate	1.8% of total reactant weight	1.0:5.0	2.0	92.7
ethyl cinnamate	1.8% of total reactant weight	1.0:6.0	2.5	86.5
<i>n</i> -propyl cinnamate	1.8% of total reactant weight	1.0:6.0	2.5	89.8
<i>n</i> -butyl cinnamate	1.8% of total reactant weight	1.0:5.0	2.0	92.7
isobutyl cinnamate	1.8% of total reactant weight	1.0:5.0	2.0	91.3
<i>n</i> -pentyl cinnamate	1.8% of total reactant weight	1.0:5.0	2.0	93.6

Conclusion

Based on the above results it is noted that the yield of ethyl cinnamate in the presence of *p*-toluene sulfonic acid was the highest and that of isobutyl cinnamate was the lowest. On the other hand, although *n*-butyl and isobutyl cinnamate or *n*-pentyl and isopentyl cinnamate have similar molecular weights, yet the yields of *n*-butyl- and *n*-pentyl cinnamate were more than that of isobutyl and isopentyl cinnamate respectively.

The yield of ethyl cinnamate was the highest using NH₄Fe(SO₄)₂·12H₂O as the catalyst whereas the yield of isobutyl cinnamate was the lowest.

Using SO₄²⁻/La₂O₃-ZrO₂-HZSM-5 as the catalyst, the yield of *n*-pentyl cinnamate was the highest and that of ethyl cinnamate was the lowest.

References

- ¹Guan, S. B., Wen, R. M., Yu, S. X. and Zhang, L. X., *Guangzhou Chem.*, **2004**, 29(3), 24.
- ²Xu, T. T., *Jiangsu Province Salt Sci. Technol.*, **2003**, 2, 11.
- ³Wang, M. and Xu, F., *Guangdong Chem. Ind.*, **2009**, 36(4), 37.
- ⁴Wen, R. M., Luo, X. X., Yu, S. X. and Zhang, L. X., *Chin. J. Synth. Chem.*, **2001**, 9(3), 269.
- ⁵Chen, S. F., Gan, L. M., Shi, W. Q., Ma, L. H., Suo, L. N. and Yang, X. K., *J. Lanzhou Petrochem. College Technol.*, **2010**, 10(3), 9.

Received: 25.11.2012.

Accepted: 05.01.2013.



ASSESSMENT OF SYNTHETIC PYRETHROIDS RESIDUES IN THE WATERS AND SEDIMENTS FROM THE WEIJA LAKE IN GHANA

Samuel Afful^{[a],*}, Johannes A. M. Awudza^[b], Shiloh Osae^[a]
and Stevester K. Twumasi^[b]

Keywords: synthetic pyrethroid residues; Weija lake, sediment, lake water

The spectrum and levels of synthetic pyrethroids in the Weija Lake waters and sediments have been investigated as a case study. Sampling was done at eight sampling locations along the Lake. Liquid-liquid extraction using 3:1 acetone/hexane mixture and soxhlet extraction were used for extraction of the pyrethroid from the water and sediment samples respectively. Analysis of the pyrethroids extracts was done with gas chromatography equipped with electron capture detector. In all, seven synthetic pyrethroids namely, fenpropathrin, cyfluthrin, cypermethrin, fenvalerate, deltamethrin, allethrin, and permethrin were detected in the Lake waters. In addition to the above pyrethroids, bifenthrin and lambda cyhalothrin were detected in the sediments. Cyfluthrin was the most ubiquitous pyrethroid in the Weija water with 100 percent occurrence, while, cyfluthrin, fenvalerate were the most ubiquitous pyrethroids. Both were detected with 87.5 percent occurrence. The concentrations of the detected pyrethroids ranged from 0.10 – 3.50 ng L⁻¹ and 0.15 – 6.60 ng g⁻¹ for the water and sediment samples respectively. The concentrations of detected pyrethroids in the Weija waters were far below maximum residue limits set by European Union (EU) and the Japanese Government. The results therefore suggest that pyrethroids residue concentration in the Weija waters may not pose health hazard in terms of synthetic pyrethroid pollution.

*Corresponding Authors

E-Mail: affulsammy@yahoo.com

Mobile: +233275809933

Fax: +233400807

- [a] Nuclear Chemistry Environmental Research Center, Ghana Atomic Energy Commission, Box LG. 80, Legon, Accra, Ghana
- [b] Chemistry Department, Kwame Nkrumah University of Science & Technology, Kumasi, Ghana

Introduction

Synthetic pyrethroids are organic compounds similar to the natural pyrethrins which are synthesized derivatives of naturally occurring pyrethrins. They are produced from pyrethrum, the oleoresin extract of dried chrysanthemum flower. The insecticidal properties of pyrethrins are derived from ketoalcoholic esters of chrysanthemic and pyrethronic acids.¹ Pyrethroids now constitute the majority of commercial household insecticides.² Natural pyrethrins and synthetic pyrethroids though chemically and toxicologically similar, pyrethrins are extremely sensitive to light, heat and moisture. In direct sunlight, half-lives can be measured in hours. However, synthetic pyrethroids were developed to capture the effective insecticidal activity of botanical insecticide, with increased stability in light, yielding longer residence time.³ In the concentrations used in such products, they may also have insect repellent properties and are generally harmless to human beings in low doses but can harm sensitive individuals. They are usually broken apart by sunlight and the atmosphere in one or two days, and do not significantly affect groundwater quality.⁴ Pyrethroids are however toxic to aquatic organism.

Synthetic pyrethroids were introduced in the late 1900 by a team of Rothamsted Research scientists following the elucidation of the structures of pyrethrin by Hermann Staudinger and Leopold Ružička in the 1920.⁵ Synthetic

pyrethroids therefore represent a major advancement in the chemistry that synthesized the analog of the natural version found in pyrethrum. Their development coincided with the identification of problems with DDT use. Their work involved identifying the most active components of pyrethrum, extracted from East African chrysanthemum⁵. The first generation pyrethroids, developed in the 1960s, include bioallethrin, tetramethrin, resmethrin and bioresmethrin. These are more active than the natural pyrethrum but are unstable in sunlight. Activity of pyrethrum and the first generation pyrethroids is often enhanced by addition of the synergist such as piperonyl butoxide

By 1974, the Rothamsted team had discovered a second generation of more persistent pyrethroids notably permethrin, cypermethrin and deltamethrin.⁵ They are substantially more resistant to degradation by light and air, thus making them suitable for use in agriculture, but they have significantly higher mammalian toxicities. One of the less desirable characteristics, especially of second generation pyrethroids is that they can be an irritant to the skin and eyes. The latest groups of synthetic pyrethroids are photo-stable, as well as extremely toxic to insects. Their efficacy is also good that a dose of only 10 - 40 g active ingredient per hectare is just required. These new pyrethroids are not mixed with synergists. They include bifenthrin, cyfluthrin, cyhalothrin, cypermethrin, fenpropathrin, flucythrinate, fluvalinate and tralomethrin. In Ghana, after the ban of organochlorine pesticides, synthetic pyrethroids are the most preferred pesticides on the market for agricultural and household purposes. Most of their formulations exist in combination with other pesticides, such as organophosphorous or nitroguanidine compound. Some of these synthetic pyrethroids are registered in Ghana for production of vegetables and other cash crops such as cocoa. This includes deltamethrin cypermethrin, deltamethrin, Lambda cyhalothrin and pyrethrums.⁶

Many pyrethroids have been linked to disruption of the endocrine system, which can adversely affect reproduction and sexual development, interfere with immune system and increase chances of breast cancer. Pyrethroids contain xenoestrogens which can increase the amount of estrogen in the body.⁷ When tested, certain pyrethroids demonstrate significant estrogenicity and increase the levels of estrogen in breast cancer cell.⁸ Synthetic pyrethroids interfere with ionic conductance of nerve membranes by prolonging the sodium current. This stimulates the nerves to discharge repeatedly causing hyper-excitability in poisoned animals. The WHO explain that synthetic pyrethroids are neuropoisons acting on the axons in the peripheral and central nervous systems by interacting with sodium channels in mammals.⁹

In Ghana, the Weija Lake is among the important water resources that the nation can boast of. The Weija Lake was created by damming the Densu river to provide potable water for the residents of western Accra, for irrigation and also to increase the fishery potential of the river system. As a result of availability of water for irrigation, vegetables cultivation at the catchment of the lake has become lucrative. Thus, communities dotted around the Lake are engaged in vegetable crop cultivation. In their effort to fight the menace of insects, synthetic pyrethroids and related pesticides are used by the farmers to spray their crops. Residues of these pesticides are therefore likely to be washed into the lake through run-off from the farm lands. There is therefore the need to assess the burden of pyrethroid residues in the Lake to establish the water quality and health status of the lake in terms synthetic pyrethroid pollution.

The study area

Weija Lake lies 17 km west of Accra between 5° 33' to 5° 40' N and 0° 20' to 0° 24' W in the coastal savannah thicket and grassland vegetation zone in southern Ghana. The lake is shallow with a maximum water level of 15.3 m Ordinary Datum (OD) during the peak of the rainy season and covers an area of about 33.6 km². Area of water shed is 2264 km² with mean surface water level of 14.3 m. Principally, the vegetation consists of dense thickets interspersed with patches of grass. The nature of the soils in the catchments have been reported to be well drained, friable, porous loam savannah ochrosols which are low in nutrients especially phosphorus and nitrogen.¹⁰⁻¹¹ Also, the soils in the catchment are sodium uleisols and lithosols.¹²⁻¹³ In the Lake District rainfall is low, averaging 840 mm a year, erratic and two-packed occurring mainly from May to June and in October. The catchment area for the Weija Lake, however, extends into much higher rainfall areas of the country¹⁴. The hottest months are in February to April with the highest mean monthly temperature of 32°C occurring in March, whilst the lowest mean monthly temperature of 21.7°C occurs in August. The occupation of the people in the catchment of the lake includes fishing, animal rearing and crops farming. The main economic activities of the people in the catchment of the lake includes fishing (small-scale canoe fishing), animal rearing, stone quarrying and crops farming. Major crops include maize, cassava, sugarcane and vegetables. The normal surface elevation is estimated at 14.37 km with maximum of 15.24 km.¹⁵ To protect the Lake, the dam and the buffer zone and to minimize the effects of

possible flooding, the government in 1977, under the State Lands Act, 1962 (Act 125), acquired a total area of 13,580 acres around the site, for which compensation was duly paid.

Materials and Methods

Sampling and sample treatment

Sampling were done in eight sampling locations, namely Weija water works, Weija village, Machigen, Amanfro, Domeabra, Soga kope, Jomo and Afuaman of the Lake. Fishman fishing canoe was used to reach the sampling points. Surface water samples were collected by using 500 ml plastic bottles. At sampling point the sampling bottle with the lid on was lowered into the water and then opened while under the water to fill the bottle after which it was covered with the lid immediately. Sediment samples were collected at various points in the neighborhood of the place where the water samples were collected using Eckman grab while sitting in the fisherman canoe. Sediment samples were taken from a depth of about 20 cm. The samples were wrapped in aluminium foil and then bagged in polyethylene bags. At each sampling point, three samples were collected. In the laboratory the water samples were kept in fridge and the sediment samples were dried at room temperature. The sediments were then milled with pestle and mortar and sieved with 500 µm mesh size sieve to remove stones and other debris. The sieved samples were then wrapped in aluminium foil and kept at room temperature in a clean cupboard.

Chemicals and Reagents

All chemicals and reagents used in this study were of high purity and were of analytical grade. Hexane (95+ %), acetone (99.8 %) were from Sigma –Aldrich, Germany. Florisil adsorbent was from Hopkin and Williams, England. The reference pesticide standards (allethrin, bifenthrin, fenprothrin, lambda-cyhalothrin, permethrin, cyfluthrin, cypermethrin, fenvalerate, deltamethrin), were from Dr. Ehrenstorfer GmbH of Augsburg in Germany.

Extraction for synthetic pyrethroids

Liquid-liquid extraction with hexane was used for the extraction of the extractable pyrethroids from the water samples. Twenty ml portion of the water sample was shaken with 20 ml of hexane as extraction solvent in 100 ml separating funnel. The hexane extract (organic layer) was separated from the aqueous layer. Extraction was repeated three times and the organic layers were put together and dried over anhydrous sodium sulphate.

Soxhlet extraction method using 180 ml of 3:1 hexane/acetone mixture as extraction solvent was used for the sediment samples. Twenty gramme of the sediment was used in each case. The extracts from water and sediment samples were then concentrated on rotary evaporator to about 5 ml and subjected to clean up.

Table 1. Concentrations (ng mL⁻¹) of synthetic pyrethroids in the sediments from the Weija Lake

Sampling locations	Compounds								
	Bifen-thrin	Fenpro-pathrin	λ-cyhalo-thrin	Cyflu-thrin	Cypermethrin	Fenvalerate	Delta-methrin	Allethrin	Permethrin
water works	<LOD	<LOD	<LOD	<LOD	0.05±0.01	<LOD	<LOD	<LOD	<LOD
Machigeni	<LOD	1.65±0.24	<LOD	0.65±0.20	0.35±0.22	<LOD	<LOD	0.60±0.08	<LOD
Amanfro	<LOD	3.50±0.72	<LOD	3.00±0.40	0.25±0.02	<LOD	0.20±0.03	0.40±0.03	<LOD
Weija village	<LOD	3.50±0.61	<LOD	2.30±0.12	0.10±0.02	<LOD	<LOD	1.50±0.24	<LOD
Domeabra	<LOD	<LOD	<LOD	0.25±0.32	0.55±0.07	3.10±0.12	0.70±0.11	0.25±0.04	0.20±0.01
Afuaman	<LOD	<LOD	<LOD	0.55±0.10	0.30±0.06	0.10±0.02	<LOD	<LOD	0.45±0.06
Agbozume	<LOD	<LOD	<LOD	0.20±0.05	0.15±0.03	0.15±0.01	0.30±0.01	<LOD	<LOD
Jomo	<LOD	<LOD	<LOD	0.20±0.04	<LOD	0.10±0.02	<LOD	<LOD	<LOD

Table 2. Concentrations (ng g⁻¹) of synthetic pyrethroids in the sediments from the Weija Lake

Sampling location	Synthetic pyrethroids								
	Bifen-thrin	Fenpropa-thrin	λ-cyhalo-thrin	Cyflu-thrin	Cypermethrin	Fenvalerate	Deltamethrin	Allethrin	Permethrin
water works	<LOD	3.55±0.24	1.85±0.66	0.45±0.03	1.40±0.07	<LOD	<LOD	0.35±0.04	0.23±0.02
Machigeni	<LOD	1.15±0.92	0.35±0.01	1.25±0.07	1.45±0.05	0.80±0.13	0.30±0.05	0.25±0.02	6.60±0.79
Amanfro	<LOD	<LOD	<LOD	2.80±0.05	3.20±0.03	0.19±0.02	2.15±0.02	1.05±0.01	<LOD
Weija village	<LOD	2.88±0.25	<LOD	1.25±0.05	2.45±0.08	<LOD	2.40±0.21	<LOD	<LOD
Domeabra	<LOD	2.25±0.88	0.55±0.04	0.20±0.01	1.05±0.09	0.65±0.06	1.20±0.07	1.35±0.08	2.55±0.22
Afuaman	0.10±0.02	2.25±0.65	2.30±0.12	0.15±0.02	0.60±0.07	0.25±0.04	<LOD	0.55±0.11	3.00±0.23
Agbozume	0.05±0.03	0.60±0.04	1.85±0.22	<LOD	0.70±0.13	<LOD	<LOD	1.60±0.12	3.80±0.30
Jomo	0.75±0.12	<LOD	0.36±0.03	0.80±0.11	<LOD	2.10±0.82	0.25±0.01	0.30±0.02	0.40±0.02

Florisil clean up of extracts

Clean-up analysis was carried out according to the procedure of Afful et al with slight modifications¹⁶. Florisil solid phase extraction columns were prepared by packing 6 ml extraction column with 1 g pre-activated florisil adsorbent with 0.5 g anhydrous sodium sulphate packed on top of the florisil. The columns were each conditioned with 10 ml hexane. The extracts from the samples, blanks and spiked samples were eluted through the column and the eluate collected into 50 ml flask. The column was further eluted with 10 ml hexane. The eluate was concentrated on rotary evaporator to almost dryness and extracted in 1.5 ml ethyl acetate for GC analysis.

Gas chromatography analysis

A Varian CP-3800 Gas Chromatograph equipped with electron capture detector was used for analysis. A volume of 1 µl aliquots of extract was injected. The operation conditions were capillary column: VF – 5mS, 40m x 0.25mm x 0.25 µm, temperature programme: 70 °C (2min) to 180 °C (1min) 25 °C min⁻¹ to 300 °C at 5 °C min⁻¹, injector temperature: 270 °C, detector temperature: 300 °C, carrier gas: N₂ at 1.0ml min⁻¹, make up: nitrogen at 29ml min⁻¹.

The pesticide residues were identified based on comparison of relative retention times to those of known standards and quantified by external standard method using peak area. The limit of quantification (LOD) was estimated as ten times the signal to noise ratio of the blank.

Results and Discussion

Tables 1 and 2 show the levels of synthetic pyrethroid detected in the study area. Margins of errors of the concentrations measured are standard deviation based on triplicate determination. In all, seven synthetic pyrethroids

namely, fenpropathrin, cyfluthrin, cypermethrin, fenvalerate, deltamethrin, allethrin, and permethrin were detected in the Lake waters. In addition to the above mentioned pyrethroids, bifenthrin and λ-cyhalothrin were detected in the sediments as well. Indeed the levels of bifenthrin and lambda cyhalothrin in the water samples were below the detection limit.

The detection of these compounds shows wide use of pyrethroids in the catchment of the Weija Lake. Frimpong¹⁷ similarly detected these nine pyrethroids in cocoa beans from Ghana. This is not surprising at all since the use of pyrethroids has now become phenomenal in Ghana for vegetable and other cash cultivation after the ban on organochlorine pesticides.¹⁷

In general, the concentrations of the compounds in the sediments were more prominent compared to the water samples. Thus the trends of the pyrethroids distribution in the Lake water and sediments indicate higher pyrethroid concentration in sediments than in water. In an aquatic medium, pesticides residues tend to settle more in sediments than remain in the overlying water. Sediments therefore serve as sink for pesticide residue. The concentration of the detected pyrethroids ranged from 0.10 – 3.50 ng L⁻¹ for the water samples. The highest concentration of 3.50 ng L⁻¹ was detected for fenpropathrin at Amanfro and Weija village while the lowest concentration of 0.01 ngL⁻¹ was also recorded for fenvalerate sampled at Afuaman. In the case of the sediment mean pyrethroid concentrations range from 0.15 – 6.6 ng g⁻¹ with the highest concentration of 6.60 ng g⁻¹ recorded for permethrin sampled from Machigeni.

Frimpong et al reported a higher concentration range of 11.9 – 29.4 ng g⁻¹ for synthetic pyrethroid residues in cocoa beans.¹⁶

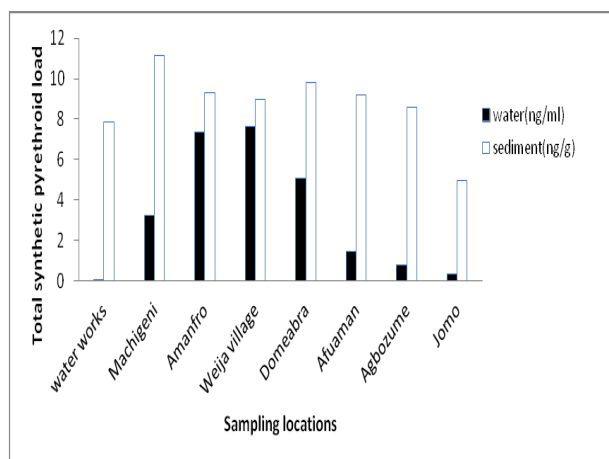


Figure 1. Total synthetic pyrethroid load at the various sampling locations along the Weija Lake.

Figure 1 shows the total pyrethroid load (sum of the levels of all the individual pyrethroids) at the eight sampling locations on the Weija Lake. The highest total pyrethroid load recorded for the sediments was 11.15 ng g^{-1} at Machigeni. This came as no surprise as the inhabitants at Machigeni are engaged mainly in vegetable growing. Residue of these chemicals left on the field after use are likely to be washed into the Lake by surface run-off. The lowest pyrethroid load in the sediments was recorded at Jomo, a predominant fishing community, with a pyrethroid load of 4.96 ng g^{-1} . In the case of the water samples the highest pyrethroid load of 7.65 ng ml^{-1} obtained at Weija village.

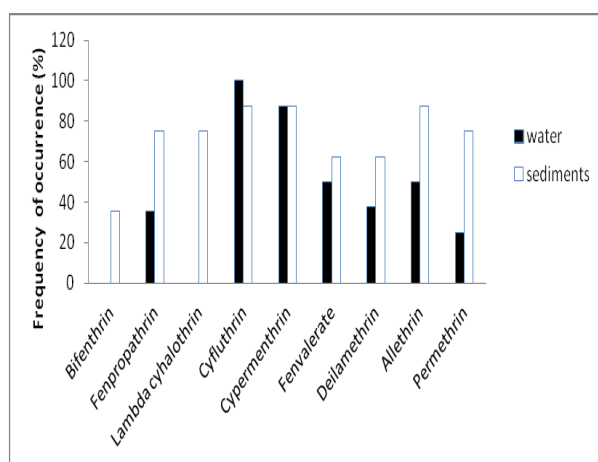


Figure 2. Percentage occurrence of the pyrethroids in the waters and sediments from the Weija Lake

Figure 2 presents percentage occurrence of the compounds in the Lake water and sediments. Cyfluthrin was the most ubiquitous pyrethroid in the Weija water with 100 percent occurrence, while permethrin was found to be the least ubiquitous with percentage occurrence of 25.0 %. In the case of the sediments, cyfluthrin, fenvalerate were the most ubiquitous pyrethroids. Both were detected with 87.5 % occurrence. Bifenthrin was the least ubiquitous pyrethroid in the sediments with 37.5 % occurrence.

Table 3. Comparison of concentrations (ppb) synthetic pyrethroids in the Weija Lake waters to maximum residue limits (MRL) stipulated by EU and Japan.¹⁷

Synthetic pyrethroid	This work (ppb)	EU MRL (ppb)	Japanese MRL (ppb)
Bifenthrin	<LOD	100	100
Fenpropathrin	8.65	20	10
λ -Cyhalothrin	<LOD	50	10
Cyfluthrin	6.90	100	20
Cypermethrin	1.75	100	30
Fenvalerate	3.45	50	10
Deilamethrin	1.20	50	50
Allethrin	2.75	10	10
Permethrin	0.65	100	50

Comparison of Pyrethroid residue levels to International standards

Table 3 compares mean pyrethroid concentration of the compounds in the present study to European Union (EU) and Japanese maximum residue limit (MRL)¹⁷. Residue levels reported in the present study represent the sum of individual pyrethroid in all the eight sampling locations. Generally, the levels of the pyrethroids in the Weija waters were far below maximum residue limits set by European Union (EU) and the Japanese Government. The results are therefore a suggestive that pyrethroids residue concentration in the Weija waters may not pose health hazard in the waters of the Lake in terms of synthetic pyrethroid pollution.

References

- Reigart, J. M. D., *Recognition and management of pesticides poisonings*, USEPA, **1999**
- Metcalf R. L., *Encyclopedia of Industrial Chemistry*, Wiley- VCH, Weinheim, **2002**.
- Gosselin, R. E., *Clinical Toxicology of commercial products*. Williams and Wilkin, Baltmores, **1984**.
- USEPA, "Permethrin, resmethrin, sumithrin, synthetic pyrethroids for mosquito control". <http://www.epa.gov/pesticides/health/mosquitoes/pyrethroids4mosquitoes.htm>. **2002**, Retrieved 2008-04-04.
- Pyrethroids – Wikipedia*. C:\Document and Setting\DIGIT\Desktop\pyrethroids-the free encyclo-pedia
- EPA Ghana. Register of pesticides as at 31st December 2009 under Part 11 of the environmental protection agency act, (Act 490), **2009**.
- Garey, J. and Wolff, M., *Biochem Biophys Res Commun*. **1998**, 251(3), 859.
- Go, V., *Env. Health Perspect*. **1999**, 107, 3.
- World Health Organization (WHO). D-Phenothrin, *Environ. Health Criteria*, Geneva, **1990**.
- Boateng, E. A., *A Geography of Ghana, 2nd Edition*, Cambridge University Press, London, **1970**.
- Dickson, K. B., Benneh, G., *A new Geography of Ghana, 1st Edition*, Longman, **1970**
- Ameka, G. K., G. K., De Graft-Johnson, K. A. A., Akuamoah, R. K., *J.of the Ghana Sci. Assoc.*. **2000**, 2(2), 147.
- Ayibotele, N. B., Tuffour-Darko, T., *Sediment load in southern rivers*, Publication of Water Resources Research, Accra, **1979**.

- ¹⁴Hall, J. B., Swaine, M. D. *Forest and vegetation in Ghana, Dr. W. Junk Publication, 1981*
- ¹⁵Nukunya, G.K., Boateng, E. A., *A report submitted to the Canadian International Development Agency, I.S.S.E.R. 1979.*
- ¹⁶Afful, S., Anim, A.K., Serfor - Armah, Y., *J. Env. Earth Sci.* **2010**, 2(3), 133.
- ¹⁷Frimpong, S. K., Yeboah, P. O., Fletcher, J. J., Pwamang, J. and Adomako, D., *Elix. Food Sci*, **2012**, 49, 9875.

Received: 12.12.2012.

Accepted: 06.01.2013.



CHARACTERISATION OF POLYCYCLIC AROMATIC HYDROCARBONS (PAHs) IN ROAD PAVING ASPHALT

Ilechukwu Ifenna^{[a]*} and Leo C. Osuji^[a]

Keywords: asphalt, polycyclic aromatic hydrocarbons (PAHs), diagnostic isomer ratios

This study characterised the polycyclic aromatic hydrocarbons (PAHs) in five road paving asphalt samples randomly collected from two hot mix asphalt (HMA) plants in Port Harcourt, Nigeria. The $\Sigma 16$ PAHs of the samples ranged from 103.79 mg kg⁻¹ - 190.93 mg kg⁻¹. Naphthalene, acenaphthylene, fluorene and benzo[g,h,i]perylene were not detected in any of the samples. The characteristic isomer ratios of the asphalt samples were also calculated to serve as a reference for road runoffs and leachates studies.

*Corresponding Authors

E-mail: ifennai@yahoo.com

Mobile phone No: +2348030933408

[a] Department of Pure and Industrial Chemistry, University of Port Harcourt, P.M.B 5323, Choba, Port Harcourt, Nigeria

(PAHs) in road paving asphalt. The results obtained from this study will give an overview of the potential risk of contamination in case of improper use and undue exposure to both humans and the environment.

Introduction

The growing demand for road expansion in Nigeria has led to a huge increase in asphalt production. Asphalt is a primary road paving material that consists of a mixture of mineral aggregates (inert mineral materials such as sand, gravel, crushed stones, slag, rock dust or powder) and bitumen. Bitumen, a product of non-destructive distillation of crude oil during petroleum refining consists of aliphatic and cyclic alkanes, aromatic hydrocarbons, heterocyclic compounds containing oxygen, nitrogen and sulphur as well as metals like nickel, vanadium and iron.¹ It is the cement that binds the aggregate materials together. The emissions generated during the production and application of asphalt contains a large number of substances, some of which are potentially harmful to health.² Exposure to compounds contained in asphalt can occur through inhalation or even absorption through the skin during application to streets and roads.³ Asphalt can also be released to the environment through the degradation of the road surface and this may contaminate surrounding water bodies.⁴ Polycyclic aromatic hydrocarbons (PAHs) which may be generated during asphalt operations are toxic to human health. They are a class of diverse organic compounds containing two or more fused aromatic rings of carbon and hydrogen atoms. They are ubiquitous environmental contaminants found in air, water, and soil and are always found as a mixture of individual compounds. They are mainly released during the combustion of petroleum products. PAHs comprise the largest class of chemical compounds known to be cancer-causing agents. Some (especially the 4-6 rings) are known carcinogens while the others (2-3 rings) may act as synergists.⁵ PAHs are difficult to degrade due to the complexity and stability of their molecular structures. Hence they are part of a group of adverse environmental contaminants known as persistent organic pollutants (POPs). This study, therefore, focuses on the characterisation of polycyclic aromatic hydrocarbons

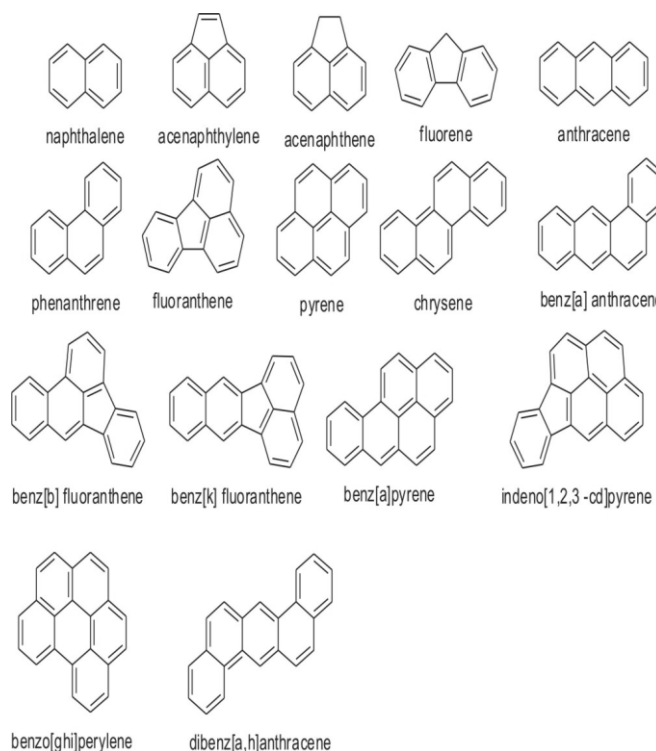


Figure 1. The chemical structure of sixteen priority PAHs

Materials and Methods

Sampling

Five asphalt samples were randomly collected from two asphalt production plants in Port Harcourt. The samples were collected immediately after production.

Extraction and Analysis by GC/FID

Extraction of hydrocarbons from the asphalt samples was done by mechanical shaking. 20 ml of dichloromethane was added to 5 g of the asphalt samples and shaken for 10 h using a bench shaker and this was repeated twice for each of the samples. The extracts were further purified in a silica gel (100 – 200 mesh) column (1 cm × 15 cm) and eluted with 30ml hexane/dichloromethane (1:1 v/v) to obtain the PAHs

Table 1. PAHs content of asphalt samples

PAHs/SAMPLES	A	B	C	D	E
Naphthalene	nd	nd	nd	nd	nd
Acenaphthylene	nd	nd	nd	nd	nd
Acenaphthene	nd	nd	nd	10.15	nd
Fluorene	nd	nd	nd	nd	nd
Phenanthrene	7.79	1.07	nd	11.67	nd
Anthracene	9.54	nd	nd	3.98	nd
Fluoranthene	5.37	2.49	5.87	14.30	3.74
Pyrene	6.46	2.38	7.68	14.55	2.35
Benz[a]anthracene	5.31	27.41	53.36	58.26	40.30
Chrysene	12.20	10.43	15.01	19.57	10.56
Benzo[b]fluoranthene	12.66	23.39	2.99	12.87	13.55
Benzo[k]fluoranthene	1.56	4.57	nd	2.79	1.20
Benzo[a]pyrene	8.05	11.98	7.74	8.06	5.11
Benzo[g,h,i]perylene	nd	nd	nd	nd	nd
Dibenz[a,h]anthracene	25.75	24.11	4.45	10.72	5.06
Indeno[1,2,3-cd]pyrene	75.98	56.74	22.21	24.01	21.92
∑16PAHs (mg kg⁻¹)	170.67	164.57	119.31	190.93	103.79
Fluoranthene/pyrene	0.83	1.05	0.76	0.98	1.59
Benz[a]anthracene/chrysene	0.44	2.63	3.55	2.98	4.61
Benzo[k]fluoranthene/benzo[b]fluoranthene	8.12	5.12	-	4.61	11.29

nd: not detected.

Results and Discussions

The result of the polyaromatic hydrocarbons (PAHs) in the asphalt samples is shown in table 1 while the chromatograms are shown in Supplementary Materials, Fig 2a-2e). The concentration of the PAHs in the samples ranges from 103.79 mg kg⁻¹ - 190.93 mg kg⁻¹ with sample D having the highest value and followed by samples A, B, C and E respectively (Table 1).

The results showed clear dominance of high molecular weight PAHs (4-6 rings PAHs). The domination of PAHs in asphalt binder by high molecular weight PAHs (4-6 rings PAHs) has been reported.² Most of the low molecular weight PAHs were not detected in the samples except for acenaphthene in sample D, phenanthrene in samples A, B, C and anthracene in samples A and D respectively. This may be attributed to the loss of low molecular weight PAHs during the refining of the parent crude oil and the combustion process that accompanies asphalt production since they are more susceptible to heat deformation than the higher molecular weight PAHs. Indeno[1,2,3-cd]pyrene was found to have the highest concentration in samples A and B while benz[a]anthracene dominated in samples C,D and E respectively. Benzo[g,h,i]perylene was not detected in any of the asphalt samples. This may be attributed to the

fractions. The fractions were concentrated to 1 ml using a rotary evaporator and 1 µl of each of the fractions was analysed with Agilent 6890 gas chromatography equipped with flame ionization detector (FID) with the following operational conditions; flow rate (H₂, 40 ml/min, air; 450 ml/min, N₂, 30 ml/min); injection temperature (initial 60 °C, final 325 °C); detector temperature (350 °C). The chromatograms were quantified with respect to internal standards.

characteristic parent crude and an indication that the hot mix asphalt (HMA) plants might have obtained their bitumen from the same source.

Characteristic isomer ratios have been reported for PAHs from various pollution sources in road runoffs and leachate studies.^{6,9} The characteristic isomer ratios of the asphalt samples were calculated to serve as a reference point in petroleum hydrocarbon pollution studies especially in the Niger Delta area of Nigeria where such study is routine due to the vibrant oil and gas industry in the region. Flu/pyr ratio ranged from 0.76-1.59 while B[a]anth/chry ratio ranged from 0.44-3.82. B[b]fl/B[k]fl was between 4.61-11.29 (Table 1). Wang et al⁷ have reported B[b]fl/B[k]fl ratio between 1.07-1.95 for emission from vehicular exhaust.

Conclusion

This study showed the dominance of high molecular weight PAHs (4-6 rings) over the low molecular weight PAHs (2-3 rings) in the asphalt samples. Naphthalene, Acenaphthylene and fluorene were not detected in any of the samples. Asphalt exposure to both workers and the environment should be minimised to prevent the health risks and adverse environmental effects associated with polycyclic aromatic hydrocarbons.

References

- ¹National Institute for Occupational Safety and Health (NIOSH), *Hazard Review; Health Effects of Occupational Exposure to Asphalt.*, NIOSH Publication No. 2001-110. **2001**
- ²Fernandes R.N.P, Soares S. A, Nascimento R.F, Soares B. J, Cavalcante M.R., *J. Chromatogr. Sci.*, **2009**(47), 789-793.
- ³Binet S, Pfohl-Leszkiwicz, A., Brandt, H., Lafontaine, M., Castegnaro, M., *Sci. Total Environ*, **2002**, 300. 37-49.
- ⁴Sadler, R., Delamont, C., White, P., Connel, D., *Toxicol Environ. Chem.*, **1999**(68), 71-81
- ⁵Anyakora, C., Arbabi, M. and Coker, H., *Am. J. Env. Sci.*, **2008**, 4(2), 145-150.
- ⁶Xinag, L., Yingxia, L., Yang, Z., Shi, J., *J. Env. Sci. Health Part A*, **2010**, 45, 339-347.
- ⁷Wang, G., Zhang, Q., Peng, M. A., Rowden, J., Mielke, H. W., Gonzales, C., Powell, E., *Soil Sediment Contam.*, **2008**, 17, 1-17.
- ⁸Kose, T., Yamamoto, T., Aneqawa, A., Mohri, S., Ono, Y., *Desalination*, **2008**, 226, 151-159.
- ⁹Brandt, H. C. A. and De Groot, P. C., *Aq. Wat. Res.*, **2001**, 35(17), 4200-4207.

Received: 31.12.2012.

Accepted: 08.01.2013.



SAFFRON EXTRACTS AS ENVIRONMENTALLY SAFE CORROSION INHIBITORS FOR ALUMINIUM DISSOLUTION IN 2M HCl SOLUTION

T. Y. Soror^{[a]*}

Keywords: saffron; HCl corrosion inhibitor; aluminium; Tafel; LP and SEM

The inhibitive effect of aqueous extract of *Saffron* leaves toward the corrosion of aluminium in 2 M HCl solution has been investigated by weight loss and electrochemical polarization study. The extract functions as a good inhibitor. The inhibition efficiency increased with extract concentrations. The plant extract behaves as cathodic-type inhibitor. Surface morphology has been analysed using SEM. The adsorption of the extract components on the aluminium surface follows Temkin adsorption isotherm.

* Corresponding Author:

E-mail: tamers21us@yahoo.com

[a] Chemistry Department, Faculty of Science, Qassim University, KSA

Introduction

Pure aluminium and its alloys find a tremendous spectrum of technological and industrial applications, especially in aerospace and household industries, owing to the combination of their characteristics of low density (consequently light weight), low cost, mechanical strength, good appearance and corrosion resistance. Therefore, the economic importance of such materials has attracted many researchers to spot light on their corrosion behaviour in different corrosive environments.¹⁻⁸

Usually, a thin, compact, passive, invisible, non-porous, adherent, and instantly self-renewing film is formed on aluminium surface upon exposure to ambient atmosphere or aqueous solutions.⁹ In spite of such great walls of aluminium citadel, corrosion is the silent enemy of such metals, attacks. It is uncontested that the corrosion of aluminium is due to dissolution of such film mainly when exposed to high concentration of acids, bases, or neutral solutions containing pitting agents such as chloride ions. However, improvements in such materials, particularly in the development of suitable methods for the protection was achieved by using inhibitors.

Inorganic inhibitors, which are mainly oxidizing agents, such as chromates, iodates, and tungstates, act as anodic inhibitors and their metallic atoms are enclosed in the film improving its corrosion resistance.¹⁰⁻¹² Lanthanide salts, which have a low toxicity, were used in the inhibition of aluminium corrosion.^{13, 14} Unfortunately, these compounds are very expensive. Although many of these tested compounds have high inhibition efficiencies, the usage of them still undesired due to their adverse effects on human beings, environment, as well as their high costs.

In the recent years, there is an increasing awareness of environment and green chemistry. Therefore, many experiments were conducted to use the eco-friendly

substances as corrosion inhibitors, instead of the harmful synthetic chemicals.¹⁵⁻¹⁹ Some investigation have in recent times been made into the corrosion inhibiting properties of natural products of plant origin and have been found to generally exhibit good inhibition efficiencies.²⁰⁻⁴⁰ The significance of this area of research is primarily due to the fact that natural products are environmentally friendly and ecologically acceptable. Nevertheless, the known hazardous effects of most synthetic organic inhibitors and the need to develop cheap, non-toxic, and environmentally benign processes have now made researchers to focus on the use of natural products.

In fact, the first patented corrosion inhibitors used were either natural products, such as flour, yeast, etc.⁴¹ or by-products of food industries for restraining iron corrosion in acid media.⁴² El-Etre⁴³ studied the application of natural honey as corrosion inhibitor for copper in aqueous solution. Kliskic et al. analyzed aqueous extract of *Rosmarinus Officinalis*⁴⁴ as corrosion inhibitor for aluminium alloy corrosion in chloride solution. El-Hosary et al.¹⁹ studied the corrosion inhibition of aluminium and zinc in HCl solution using *Hibiscus Subdariffa* extract. Muller⁴⁵ investigated the effect of saccharides (reducing sugars, fructose and mannose) on the corrosion of aluminium and zinc in alkaline media. A series of reports have been highlighted on studies of natural products (exudates gums) as corrosion inhibitors of mild steel and aluminium in acidic and basic media.^{17,18,24, 46}

Available, inexpensive, non-toxic, environmentally safe and relatively high inhibition efficiency are conditions that must be satisfied by a good inhibitor. This paper will study the inhibitive effect of aqueous extract of *Saffron* plant leaves on the aluminium corrosion in 2 M HCl solution using weight loss, open circuit potential (OCP), and electrochemical polarization (Tafel, Linear polarization) measurements.

SEM investigations were used to explore the morphological behaviour of aluminium in the presence of *Saffron* extract. In addition, the adsorption mode of components extract will be studied.

Experimental section

Plant classification and composition

The binomial name of *Saffron* is *Crocus Sativus* L. Its scientific classification is shown in Table 1. On the other hand, the proximate analysis of *Saffron* is presented in Table 2. In addition, chemical structures of some *Saffron* extract components are found in Table 3.

Table 1. Scientific classification of *Saffron*.

Kingdom	Plantae
(unranked)	Angiosperms
(unranked)	Monocots
Order:	Asparagales
Family:	Iridaceae
Subfamily:	Crocoideae
Genus:	<i>Crocus</i>
Species:	<i>C. sativus</i>

Table 2. Proximate analysis of *Saffron*.

Components	Mass %
Water-soluble components	53.0
(i) Gums	10.0
(ii) Pentosans	8.0
(iii) Pectins	6.0
(iv) Starch	6.0
(v) α -Crocin	2.0
Other carotenoids	1.0
Lipids	12.0
(i) Non-volatile oils	6.0
(ii) Volatile oils	1.0
Inorganic matter ("ash")	6.0
(i) HCl-soluble ash	0.5
Protein	12.0
Water	10.0
Fiber(crude)	5.0

Preparation of plant extract

A sample from crude *Saffron* leaves was soaked in triply distilled water and the plant extract was concentrated in 1 L, and found to contain 1 mg ml⁻¹ of the plant compounds (1000 ppm).

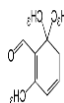
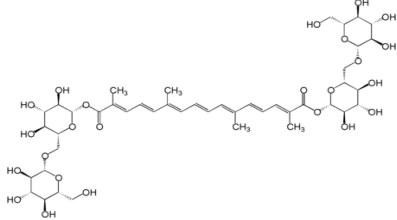
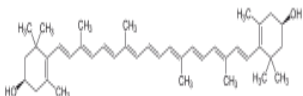
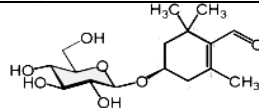
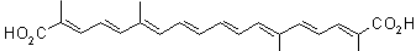
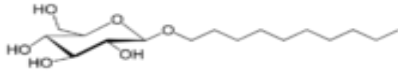
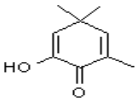

Preparation of specimens

Measurements were made on ultrapure aluminium (99.99%). The samples were polished successively using 1/0 to 6/0 emery papers, degreased with acetone and washed by distilled water before use.

Electrolyte

The solutions used were made of AR grade hydrochloric acid. Appropriate concentrations of acids were prepared by using triple distilled water.

Table 3. Chemical structures of some *Saffron* extract components.

Name	Structure
Safranal	
Crocin	
Zeaxanthin	
Picrocrocin	
Crocetin	
Decyl glucoside	
2-Hydroxy-4,4,6-trimethyl-2,5-cyclohexadien-1-one	
Lycopene	

The concentration range of the inhibitor (plant extract) employed was varied from 200 to 800 ppm and the electrolyte volume used was 100 ml, at 25 ± 1 °C.

Weight loss method

Weight loss of rectangular aluminium specimens of size (5 cm x 3 cm x 0.1 cm) in duplicate immersed in 100 ml of electrolyte with and without addition of different concentrations of plant extract was determined after 30 min at room temperature (25 ± 1 °C). The percentage inhibition efficiency (IE) was calculated from,

$$IE(\%) = \frac{W_{un} - W_{inh}}{W_{un}} 100 \quad (1)$$

where W_{un} is the weight loss of the sample in the blank solution and W_{inh} the weight loss of the sample in presence of the additive.

Table 4. Variation of polarization parameters for aluminium in 2 M HCl solution at (25 ± 1 °C) with extract addition.

Technique	Inhibitor dose, ppm	E_{corr} , mV	B_a , V/d	B_c , V/d	I_{corr} , $\mu\text{A cm}^{-2}$	R_p , Ω	CR, mpy	IE, %
Tafel	Blank	-847	0,3879	0,2573	1114	—	1.433 x 103	—
	600	-793.6	0,3628	0,3159	171.2	—	220.3	84.6
LP	Blank	-856	0,100	0,100	740.5	14.66	952.9	—
	600	-805.2	0,100	0,100	158.8	68.37	204.4	78.5

Electrochemical measurements

A three electrode cell assembly consisting of aluminium coupon of the size (1.0 cm x 1.0 cm x 0.1 cm) embedded in specimen holder as working electrode (WE), a platinum sheet as counter electrode (CE) and saturated calomel electrode (SCE) as reference electrode (RE) containing 100 ml of electrolyte was used for electrochemical measurements at 25 ± 1 °C.

Open circuit potential (OCP) measurements

The OCP of aluminium electrode/2 M HCl and its potential in inhibited solution was followed as a function of immersion time till steady state values were reached. All potentials were measured referred to saturated calomel electrode (SCE) using EG & G (Princeton Applied Research) Model 352/352 potentiostat/galvanostat interfaced to an IBM ps/3 computer, the software is V, -5.36.

Polarization measurements

(i) Tafel

Tafel polarization curves were recorded by using computer controlled electrochemical system mentioned before. The potential increased with the speed of 5 mV s⁻¹. Experiments were carried out from -1150 to -450 mV potential ranges. Before recording the polarization curves, the (WE) was maintained at its corrosion potential for 10 min until a steady state was reached.

(ii) Linear polarization (LP)

Polarization resistance (R_p) was measured using the linear polarization method by potential scanning over the range of $E_{\text{corr}} \pm 20$ mV at 1 mV/s. The R_p values were obtained from the current-potential plot, for aluminium in 2 M HCl in the absence and presence of 600 ppm concentrations of the inhibitor at room temperature.

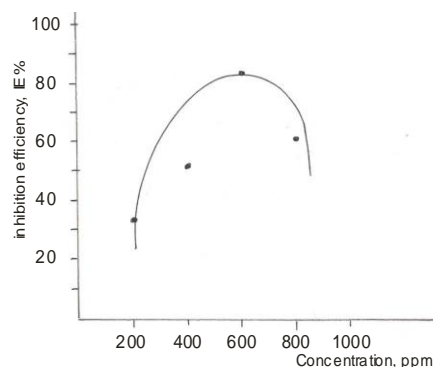
Surface analysis

The test coupons of the size 1 x 1 cm² were exposed to 100 ml of 2 M HCl having 600 ppm plant extract for 1 h at 25 ± 1 °C and washed with distilled water. After washing, specimens were dried, and examined for their topographical features using scanning electron microscope (SEM).

Results and Discussion

Weight loss measurements

The weight losses (gravimetric measurements) for aluminium in 2 M HCl containing different concentrations of the leaves of *Saffron* extract ranging from 200-800 ppm indicate that the inhibition efficiency increases as the concentration of the added extract is increased up to 600 ppm that gave 84% efficiency and then decreases after that, Fig. 1. The observed inhibition action of the *Saffron* extract could be attributed to the adsorption of its components on aluminium surface. The formed layer, of the adsorbed molecules, isolates the aluminium surface from the aggressive Cl⁻ ions medium leading to decrease in weight loss. Fig. 2 represents the variation in inhibition efficiency IE% with immersion time 30-90 min using the optimum dose (600 ppm) of *saffron* extract. Good performance behaviour of our inhibitor over 11/2 h (90 min) processing.

**Figure 1.** Variation of inhibition efficiency IE% with inhibitor concentration

To study the adsorption behaviour of *Saffron* extract on aluminium surface in 2 M HCl medium, the adsorption isotherm must be defined. The nature of corrosion inhibition has been deduced in terms of the adsorption characteristics of the inhibitor.⁴⁷ The metal surface in aqueous solution is always covered with adsorbed water dipoles. Therefore, the adsorption of the inhibitor molecules from aqueous solution is a quasi substitution process.^{48,49} Therefore, the relation between the concentration of the extract (c) and the fraction of aluminium surface covered by adsorbed components (θ) was obtained. Because the inhibition action is postulated as a result of the adsorption, (θ) is directly related with the inhibition efficiency (IE) and was calculated using the equation: (θ) = IE/100.

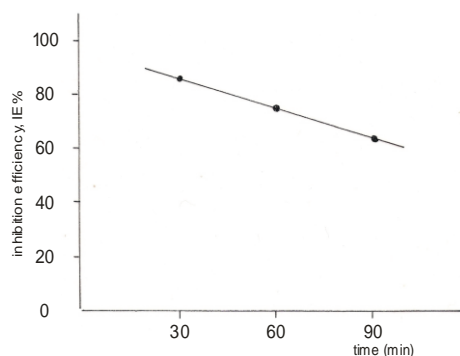


Figure 2. Effect of exposure time

Adsorption isotherm analysis

A graphic representation of the relationship between logarithm (extract concentration) and surface coverage (θ) is given in Fig. 3. Inspection of Fig. 3 reveals that a straight line was obtained fitting Temkin adsorption isotherm.

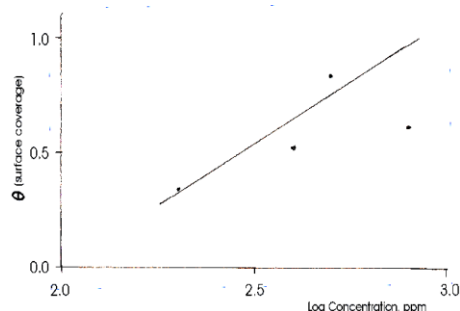


Figure 3. Temkin adsorption isotherm (θ) vs. $\log C$.

Open circuit potential studies

Potential Vs time plots for aluminium in 2 M HCl in absence and presence of (600 ppm) *Saffron* extract at room temperature (25 ± 1 °C) are shown in Fig. 4, curves (a) and (b) respectively. The curves indicated that in the presence of 600 ppm inhibitor, curve (b), the potential was shifted to less negative values. Whereas, the potential of a blank solution curve (a) was noticed to have more negative magnitudes.

Polarization measurements

Fig. 5 represents the anodic and cathodic Tafel polarization curves of aluminium electrode in solution of 2 M HCl alone and in the presence of 600 ppm inhibitor extracts concentration. Inspection of Fig. 5 reveals that the polarization curves are shifted towards less negative potentials and less current densities with inhibitor addition, curve (b). This behaviour indicates the inhibitive action of the added extract on aluminium corrosion in the acid solution. Various kinetic parameters, such as corrosion current (I_{corr}), corrosion potential (E_{corr}), cathodic Tafel slope (β_c), anodic Tafel slope (β_a) and inhibition efficiency (IE %) are given in Table 4.

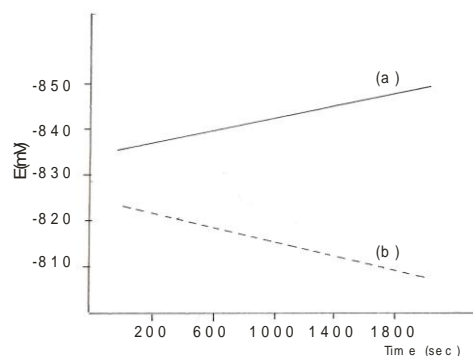


Figure 4. Potential vs. time plots for aluminum in 2 M HCl solution at (25 ± 1 °C): (a) blank, (b) 600 ppm inhibitor

The addition of plant extract does not change the value of anodic Tafel slope (β_a) significantly. Corrosion current of aluminium decreases much in the presence of 600 ppm inhibitor addition. Increase in cathodic Tafel slope (β_c) with plant extract dose applied indicates that *Saffron* inhibitor inhibits corrosion by inhibiting cathodic reaction by simply blocking the available surface area. The inhibitor molecules decrease the surface area of corrosion and cause only inactivation of the part of the surface with respect to the corrosion medium.

The corrosion rate (CR) is directly related to the R_p and can be calculated from it.⁵⁰ The R_p value can help us to assess the relative ability of a material to resist corrosion. Since R_p is inversely proportional to I_{corr} , so the materials with highest R_p (and thus the lowest I_{corr}) have the highest corrosion resistance. From all these facts, we can discuss and correlate between the data obtained from R_p and those computed from Tafel plots. Polarization parameters for aluminium corrosion in 2 M HCl and the presence of 600 ppm *Saffron* extract are shown in Table 3. It is observed that, in the presence of inhibitor, E_{corr} shifts to more positive values. Furthermore, the value of R_p increases, while the value of I_{corr} decreases with additive. From the data depicted in Table 4, it has been found that the addition of *Saffron* to aluminium in 2 M HCl enhances the corrosion inhibition efficiency (IE %).

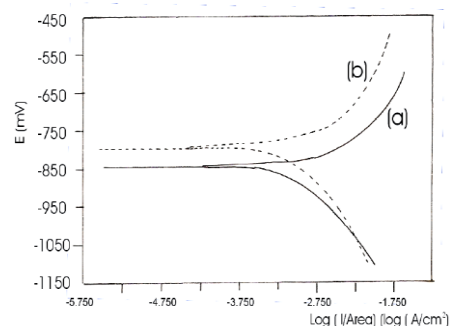


Figure 5. Polarization curves for aluminum in 2 M HCl solution: (a) blank, (b) 600 ppm inhibitor

SEM investigation

Scanning electron micrographs (SEM) of aluminium surface immersed in 2 M HCl (blank) and 2 M HCl containing 600 ppm plant extract are shown in Fig. 6.

A rough surface was noticed for aluminium immersed in 2 M HCl solution. In case of aluminium immersed in 2 M HCl with 600 ppm *Saffron* extract, a smooth surface was noticed and it is easily comparable with the polished surface. This shows that, this plant extract inhibits corrosion of aluminium in 2 M HCl solution.

Inhibition mechanism

The existing data show that most organic inhibitors get adsorbed on the metal surface by displacing water molecules and form compact barrier film.⁵¹ Availability of lone pairs and π (π) electrons in inhibitor molecules facilitate electron transfer from the inhibitor to the metal, forming a coordinative covalent bond.⁵² The strength of chemisorption bond depends on the electron density on the donor atom of the functional group and also the polarizability of the group. Observation of the chemical structures of *Saffron* reveals that these compounds can adsorb on aluminium surface via the lone pairs of electrons present on their oxygen atoms.



Figure 6 (a)

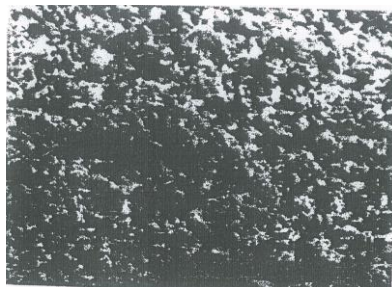


Figure 6 (b)

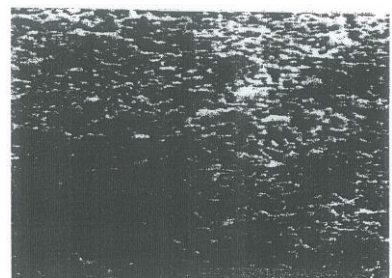


Figure 6 (c)

Figure 6. SEM graphs of aluminium (a) polished clean surface, (b) immersed in 2 M HCl solution, (c) immersed in 2 M HCl with 600 ppm of plant extract.

The adsorption of such compounds on the aluminium surface make a barrier for charge and mass transfer leading to decrease the interaction of the metal with the corrosive environment (2 M HCl). As a result, the corrosion rate of aluminium is decreased.

Conclusions

From the overall experimental results the following conclusions can be deduced:

The aqueous extract of *Saffron* (LV) acts as a good inhibitor for corrosion of aluminium in 2 M HCl solution.

The inhibition efficiency increases with increasing extract concentration and attain a maximum value of 84.6 % at 600 ppm.

Saffron acts as a cathodic inhibitor with modifying the hydrogen reduction mechanism.

The inhibitive action of extract was attributed to the adsorption of its components on aluminium surface.

The adsorption of extract components follows Temkin adsorption isotherm.

References

- Rozenfeld, I. L. , *Corrosion Inhibitors*, McGraw-Hill, New York, **1981**
- Tomcsanyi, L., Varga, K., Bartik, I., Horanyi G. and Maleczki, E., *Electrochim. Acta*, **1989**, *34*, 855.
- Stevanovic, R. M., Despic, A. R. and Drazic, D. M., *Electrochim. Acta*, **1988**, *33*, 397.
- Frers, S. E., Stefenel, M. M., Mayer, C. and Chierchie, T., *J. Appl. Electrochem.*, **1990**, *20*, 996.
- Maayta, A. K. and Al-Rawashdeh, N. A. F., *Corros. Sci.*, **2004**, *46*, 1129.
- Ovari, F., Tomcsanyi, L. and Turmezey, T., *Electrochim. Acta* **1988**, *33*, 323.
- Young, L., *Anodic Oxide Films*, Academic Press, New York, **1961**, p. 4-10.
- Saleh, M. R. and Shams El Din, A. M., *Corros. Sci.* **1981**, *12*, 688.
- Telegdi, J., Kalman, E. and H. Karman, H., *Corros. Sci.* **1992**, *33*, 199.
- Mahmoud, S. S., *Bull. Electrochem.* **1995**, *11*, 366.
- Hiuton, B. R.W., Arnott, D. R. and T. Ryan, *Mater. Forum* **1986**, *9*, 162 .
- Bazzi, L., Kertit, S. and Hamani, M., *Bull. Electrochem.* **1998**, *14*, 34
- Mansfeld, F., Lin, S., Kim, S. and Shih, H., *Corros. Sci.* **1987**, *27*, 997.
- Macdonald, D. D., *Electrochem. Soc.* **1993**, *138*, L 27.
- El-Etre, A.Y., *Corros. Sci.* **1998**, *40*, 1845.
- Bouyanzer, A., Hammouti, B. and Majidi, L., *Mater. Lett.* **2006**, *60*, 2840.
- El-Etre, A.Y., *Corros. Sci.* **2001**, *43*, 1031.
- El-Etre, A.Y., *Corros. Sci.* **2003**, *45*, 2485.
- El Hosary, A. A., Saleh, R. M. and Shams El-Din, A. M., *Corros. Sci.* **1972**, *12*, 897.

- ²⁰Ekpe, U. J., Ebenso, E. E., Ibok, U. J. and Afri, W., *Sci. Assoc.* **1994**, 37, 13.
- ²¹Ebenso, E. E., Ekpe, U. J. and Afri, W., *J. Bio. Appl. Chem.* **1996**, 41, 21.
- ²²Avwiri, G. O. and Igho, F. O., *Matter. Lett.* **2001**, 57, 3705.
- ²³Ebenso, E. E., Ibok, U. J., Ekpe, U. J., Umoren, S., Jackson, E., Abiola, O. A., Oporika, N. C. and Martinez, S., *Trans. SAEST* **2004**, 39, 117.
- ²⁴El-Etre, A. Y., Abdallah, M. and El-Tantawy, Z. E., *Corros. Sci.* **2005**, 47, 385.
- ²⁵El-Etre, A. Y. and El-Tantawy, Z. E., *Port. Electrochem. Acta* **2006**, 24, 347.
- ²⁶Umoren, S. A., Obot, I. B., Ebenso, E. E., Okafor, P. C., Ogbobe, O. and Oguzie, V., *Anti. Corros. Meth. Mater.* **2006**, 53, 277.
- ²⁷Oguzie, E. E., Onuchukwu, A. I., Okafor, P. C. and Ebenso, E. E., *Pigm. Res. Technol.* **2006**, 35, 63.
- ²⁸Oguzie, E. E., *Mater. Chem. Phys.* **2006**, 99, 441.
- ²⁹Oguzie, E. E., *Corros. Sci.* **2007**, 49, 1527.
- ³⁰Okafor, P. C., Ekpe, U. J., Ebenso, E. E., Umoren, E. M. and Leizou, K. E., *Bull. Electrochem.* **2005**, 21, 347.
- ³¹Okafor, P. C., Ekpe, U. J., Ebenso, E. E., Oguzie, E. E., Umo, N. S. and Etor, A. R., *Trans. SAEST* **2006**, 21, 82.
- ³²Okafor, P. C., Osabor, V. I. and Ebenso, E. E., *Pigm. Res. Technol.* **2007**, 35, 299.
- ³³Okafor, P. C. and Ebenso, E. E., *Pigm. Res. Technol.* **2007**, 36, 134.
- ³⁴Umoren, S. A., Obot, I. B., Ebenso, E. E., Okafor, P. C., Ogbobe, O., and Oguzie, E. E., *Anti. Corros. Methods Mater.* **2006**, 53, 277.
- ³⁵Khuzaeu, V. U. and Aripova, S. F., *Chem. Nat. Compound* **2000**, 36, 418.
- ³⁶Sangeetha, M., Rajendran, S., Sathiyabama, J., Krishnaveni A., Santhy, P., Manimaran, N., Shyamaladevi, B., *Port. Electrochim. Acta*, **2011**, 29, 429.
- ³⁷Sirbharathy, V., Rajendran, S., Sathiyabama, J., *Int. J. Chem. Sci. Technol.*, **2011**, 3, 108.
- ³⁸Syamala Devi, B., Rajendran, S., *Int. J. Chem. Sci. Technol.*, **2011**, 1, 79.
- ³⁹Sangeetha, M., Rajendran, S., Muthu Megala T. S., and Krishnaveni, K., *Zast. Mater.*, **2011**, 52, 35.
- ⁴⁰Antony, N., Benita Sherina, H., and Rajendran, S., *Int. J. Eng. Sci. Technol.*, **2010**, 2, 2774
- ⁴¹Bablwin, J., *British Patent* 2327, **1895**.
- ⁴²Putilova, N., Balezin, S. A. and Barannik, V. P., *Metallic Corrosion Inhibitors* **1960**, (Pergamon Press, Oxford, London).
- ⁴³El-Etre, A. Y. and Abdallah, M., *Corros. Sci.* **2000**, 42, 731.
- ⁴⁴Kliskic, M., Radosevic, J., Gudic, S. and Katolinic, V., *J. Appl. Electrochem.* **2000**, 30, 823.
- ⁴⁵Muller, B., *Corros. Sci.* **2002**, 44, 1583.
- ⁴⁶El-Etre, A. Y., *Appl. Surf. Sci.* **2005**, 252, 8521.
- ⁴⁷Bentiss, F., Lagrenee, M., Traisnel, M., Mernari, B. and El-Attari, H., *J. Appl. Electrochem.* **1999**, 29, 1073.
- ⁴⁸Rudresh, H. B. and Mayanna, S. M., *J. Electrochem. Soc.* **1977**, 124, 340.
- ⁴⁹Bockris, J. O., Devanathan, M. A. V. and Muller, K., *Proc. Roy. Soc. London A* **1963**, 274, 55.
- ⁵⁰Uhling, H. H. and Revie, R. W., *Corrosion and Corrosion control*, 3rd edition, Wiley, New York, **1985**.
- ⁵¹Muralidharan, S., Phani, K. L. N., Pitchumani, S., Ravichandran, S. and Iyer, S. V. K., *J. Electrochem. Soc.* **1995**, 142, 1478.
- ⁵²Hackerman, N. and Hard, R. M., *Proc. Int. Congress. of Metallic Corrosion*, Butterworth, London, **1962**.

Received: 28.11.2012.
Accepted: 09.01.2013.



AN ENCOUNTER WITH CORROSION INHIBITORS

C. Mary Anbarasi^[a,b], S. Rajendran^{[b,c]*}, M. Pandiarajan^{[b]*}, and
A. Krishnaveni^[d]

Keywords: corrosion, inhibitors, additives, methods, metals.

Corrosion is a natural process. It can be defined as the destructive attack of a metal through interaction with its environment. A corrosion inhibitor is a chemical compound that, when added to a liquid or gas in small amount decreases the corrosion rate of a metal or an alloy. Corrosion inhibitors are added to coolants, fuels, hydraulic fluids, boiler water, engine oil and many other fluids used in industry. The rate of various types of corrosion inhibitors which are used in different environment to reduce the corrosion of various metals and alloys are discussed in this paper.

* Corresponding Author
pandiarajan777@gmail.com

- [a] PG Department of Chemistry, Jayaraj Annapackiam College for Women, Periyakulam-625601, India.
E-mail: anbuc_m@yahoo.co.in
- [b] Corrosion Research Centre, PG and Research Department of Chemistry, GTN Arts College, Dindigul-624005, India.
E-mail: pandiarajan777@gmail.com
- [c] Department of Chemistry, RVS School of Engineering and Technology, Dindigul, India.
E-mail: srmjoany@sify.com
- [d] Department of Chemistry, Yadava College, Madurai, India.

Introduction

There are several methods to control corrosion. One method is modification of the environment. This can be achieved by addition of corrosion inhibitors. Corrosion inhibitors are commonly added to coolants, fuels, hydraulic fluids, boiler water, engine oil, and many other fluids used in industry. A corrosion inhibitor is a chemical compound, which when added to an environment (aqueous solution, oil, fuels and atmosphere) reduces the corrosion rate. The aim of the present paper is to provide a review on inhibitors used in various environments to reduce corrosion of various metals and alloys. Corrosion inhibition by amino acids¹ and phosphonic acids² has been reviewed by us recently.

Types of corrosion inhibitors

Inhibitors have been conveniently classified as Cathodic corrosion inhibitors, Anodic corrosion inhibitors, Adsorption corrosion inhibitors, Volatile corrosion inhibitors (VCI), and Mixed Inhibitors.

Cathodic corrosion inhibitors

Cathodic inhibitors reduce the corrosion rate due to retarding cathodic reactions. A cathodic inhibitor causes formation of insoluble compounds precipitating on the

cathodic sites in form of a barrier film. The effective cathode area is one of the factors of galvanic corrosion. Therefore its reduction results in decrease of corrosion rate.

The following compounds are used as cathodic inhibitors: zinc salts,³⁻⁹ calcium salts,¹⁰⁻¹³ magnesium salts,^{14,15} and polyphosphates.¹⁶⁻²²

Anodic corrosion inhibitors

Anodic inhibitors reduce the corrosion rate due to retarding anodic reactions. An anodic inhibitor shifts the equilibrium of the corrosion process to the passivation zone (Pourbaix diagrams) causing formation of a thin invisible passivation oxide film on the anodic sites, which increases the anode potential and depresses the oxidation process. Reduction of the effective anode area results in decrease of corrosion rate.

Anodic inhibitors have a serious disadvantage: at low concentrations, they cause increase of corrosion rate, therefore it is important to avoid decrease of the inhibitor content below the optimum level.

The following compounds are used as anodic inhibitors: chromate (CrO_4^{2-}),²³⁻³⁴ nitrite (NO_2^-),³⁵⁻³⁹ molybdate (MoO_4^{2-}),⁴⁰⁻⁴⁶ and orthophosphate (PO_4^{3-}).⁴⁷⁻⁵²

Adsorption corrosion inhibitors

Adsorption inhibitors reduce the corrosion rate due to Polarization of the metal by extremely thin layer of their molecules adsorbed on the surface. Decrease of the effective surface area results in reduction of the corrosion rate. Adsorption inhibitors are substances (mainly organic) capable to form chemisorbed bonds with surface metal atoms.

The following compounds are used as adsorption inhibitors: amines (R-NH_2),⁵³⁻⁵⁸ carboxyls (R-COOH),⁵⁹⁻⁶² thiourea (NH_2CSNH_2),⁶³⁻⁷⁰ phosphonates ($\text{R-PO}_3\text{H}_2$),⁷¹⁻⁷⁹ benzoate ($\text{C}_6\text{H}_5\text{COO}^-$),⁸⁰⁻⁸⁵ sulphonates.⁸⁶⁻⁹³

Table 1. Corrosion inhibitors

No.	Metal	Medium	Inhibitor	Additives	Methods	Findings	Ref
1	carbon steel	aqueous	sodium salt of diethyldithiocarbamate, 1-hydroxy ethylidene-1,1-diphosphonic acid	ZnSO ₄	weight loss, polarization, SEM and EDS studies	NaDEDTC, HEDDP and ZnSO ₄ ·7H ₂ O in 1.0:1.4:1.0 ratio can decrease corrosion. System functions as both cathodic and anodic inhibitor. Protective film containing of Fe ²⁺ -HEDDP, Zn ²⁺ -HEDDP, Zn ²⁺ -DEDTC complexes is formed on the metal surface.	3
2	carbon steel	low chloride environment	ascorbate	2-phosphonobutane-1, 2, 4- carboxylic acid and Zn ²⁺	polarisation, cathodic-impedance studies, XPS	Mixture functions as a mixed inhibitor. Immersion period of 24 h is necessary for the formation of the protective film, with a very high charge transfer resistance. The surface film consists of oxides/hydroxides of iron(III), Zn(OH) ₂ and [Zn(II)-PPTC-ascorbate] complex.	4
3	copper	0.5 M HCl	methionine	Zn ²⁺ ions	CV studies, EIS and polarization	The presence of Zn ²⁺ ions increases the inhibition efficiency to 92%. The adsorption of methionine on copper surface follows Langmuir isotherm. The adsorption free energy of methionine on copper (-26 kJ mol ⁻¹) reveals a strong physical adsorption of the inhibition on the copper surface.	5
4	mild steel	ground water	1-(2-pyrrole carbonyl) benzotriazole (PCBT) and 1-(2-thienylcarbonyl) benzotriazole (TCBT)	Zn ²⁺ and 3-PPA	polarization, EIS, FT-IR and XRD	Characterization studies confirm the adsorption of inhibitor and the formation of corrosion products on the mild steel surface. Combination of PCBT along with Zn ²⁺ and 3-PPA shows better corrosion inhibition efficiency than other inhibitor combinations and the individual inhibitors.	6
5	mild steel	sodium triphosphate sodium hexametaphosphate and adenosine triphosphate	1-(2-pyrrole carbonyl) benzotriazole and 1-(2-thienylcarbonyl) benzotriazole	zinc acetate	weight loss, polarisation and SEM	Inhibition efficiency increased with increase in concentration for STPP and SHMP whereas it decreased for ATP. However, inhibition efficiency decreased for all the three phosphates with increase in temperature. All the three phosphates acted as mixed inhibitors though anodic reactions are suppressed more in comparison to the cathodic reactions. STPP acted through chemisorption whereas SHMP and ATP are physically adsorbed over the surface of mild steel	7
6	epoxy-coated steel		zinc phosphate	-	EIS, electrochemical noise measurement and SEM	Zinc phosphate exhibited inhibition effect on the corrosion of the scratched epoxy-coated steel. The SEM results implied that the scratched surface under zinc phosphate coating was re-healed by an insulating film.	8
7	Armco iron	3% chloride solution	piperidin-1-yl-phosphonic acid	Zn ²⁺	polarization, FTIR, weight loss method and surface analysis	Synergistic effect exists between Zn ²⁺ and PPA. The film formed on iron indicates phosphonates zinc salt formation. The surface film analysis showed that in the absence of Zn ²⁺ , the protective film consists of Fe ²⁺ -PPA complex formed on the anodic sites of the metal surface, whereas in the presence of Zn ²⁺ , the protective film consists of Fe ²⁺ -PPA complex and Zn(OH) ₂ .	9
8	steel	concrete	calcium nitrite	pulverised fuel, ground granulated blast furnace slag	electrochemical assessment	Calcium nitrite was significantly effective in increasing the resistance to corrosion risk. For OPC concretes, an increase in the calcium nitrite content resulted in an increase in the time to corrosion	10
9	steel	saturated Ca(OH) ₂	Ca(NO ₂) ₂	trisodium phosphate, calcium nitrite, 1,2,3-benzotriazole, calcium glycerolphosphate, sodium tetraborate	open-circuit potential mapping and EIS, XPS, AFM	The passive oxide film, which is formed on the metal surface in the presence of Ca(NO ₂) ₂ .	11
10	mild Steel	oxygen-containing solutions	zinc-1-hydroxyethylidene-1,1-diphosphonic acid (HEDDP)	calcium and zinc	electrochemical study	The zinc-HEDDP mixtures give effective inhibition at a zinc:HEDDP molar ratio of 2:1 and are attributed to anodic inhibition by the 2:1 complex anion.	12
11	mild Steel	tap water	calcium gluconate	1-hydroxyethane-1,1-diphosphonic acid	weight loss, polarization and AC impedance	At higher concentrations (>50ppm), HEDDP was found to be aggressive towards mild steel. But a formulation consisting of 25 ppm HEDDP and 200 ppm calcium gluconate was found to protect mild steel effectively.	13
12	aluminium	organosilane based sol-gels	magnesium(II) nitrate	-	EIS, PDS, AFM, SEM and EDS	Superior anticorrosion properties of the Mg ²⁺ -rich sol-gel are due to the pore blocking mechanism of insoluble magnesium precipitates formed during the hydrolysis process.	14

Table 1. (cont.)

No.	Metal	Medium	Inhibitor	Additives	Methods	Findings	Ref
13	mild steel (C1018)	aqueous	phosphates, phosphonates, zinc and magnesium salts	anti-scaling agents	weight loss, inhibitor index	Corrosion inhibitor with the highest I.I. = 9.1 was selected and recommended for use in the cooling water system of the Oil Refinery.	15
14	carbon steel	cooling water	trisodium phosphate	Zn ²⁺	weight loss and electrochemical polarization technique	The inhibitor provides good inhibition efficiency and acts as anodic inhibitor when present alone and mixed inhibitor with zinc ions.	16
15	copper	aqueous	Na ₃ PO ₄ , Na ₃ P ₃ O ₁₀	-	weight loss	The optimum experimental conditions maximum IE is Na ₃ P ₃ O ₁₀ , [Na ₃ P ₃ O ₁₀] = 0.017 mol/l and passivation time t _p = 2.17 h.	17
16	-	aqueous	polyaspartic acid	-	viscosimetry, static anti-scaling method and shaking-bottle incubating test	The PASP has the best scale inhibition performance when its viscosity-average molecular weight is 10000 g/mol, and its inhibiting efficiency reaches over 90% to the scale of CaCO ₃ , CaSO ₄ , and BaSO ₄ , biodegradation rate can reach over 70%.	18
17	mild steel and copper	aqueous	polyphosphates and organophosphonates	CTAB, CPB	polarization studies	The inhibition efficiency towards copper was observed to be more than mild steel due to the addition of CTAB and CPB with inhibitor. Polarization studies revealed that the presence of biocide CTAB with inhibitor gives the inhibition efficiency of about 80% for mild steel. CPB with inhibitor shows higher interference between biocide and inhibitor, whereas CPB alone is found to act as an inhibitor for copper (73%), which shows that the inhibitor might interfere in the biocidal action on copper.	19
18	carbon steel	aqueous	polyphosphate	sodium silicate	weight loss, EIS and polarization measurements	Silicates and polyphosphates can be useful as corrosion inhibitors for reducing the corrosion of carbon steel in potable water supply distribution systems. The optimal concentration for silicate alone was determined to be 11 ppm and for polyphosphate alone was 8 ppm. The optimum ratio of concentration for sodium silicate to sodium polyphosphate was 4:3.	20
19	steel	aqueous	condensed phosphates and polyphosphates	aluminium in a combination with zinc, strontium, calcium	weight loss	The high anticorrosion efficiency was found at a comparative pigment, represented by zinc phosphosilicate.	21
20	zinc	aqueous	zinc	polyphosphate	EIS, cyclic voltammetry	The effect of calcium to polyphosphate ratio on the corrosion rate of zinc was studied.	22
21	carbon steel	aqueous	monoethanolamine (MEA)-based compound absorbent for CO ₂	piperazine (PZ) or 2-amino-2-methyl-1-propanol (AMP)	weight loss, corrosion rate	When such corrosion inhibitors were added, corrosion by MEA solution was significantly inhibited and carbon steel materials were protected effectively against corrosion. The corrosion inhibition efficiency was in the order sodium metavanadate > potassium chromate > potassium dichromate > sodium nitrite > sodium nitrate > sodium phosphate > sodium sulfite.	23
22	zinc	0.1 M NaCl	zinc chromate and zinc phosphate	-	EIS, SVET	Zinc was protected from corrosion in both extracts. SVET detected the anodic and cathodic distribution along the scribes, EIS was able to distinguish processes occurring on the metal surface exposed by the scribe in different samples. For primers with anticorrosive pigment, a time constant at high frequencies was attributed to a layer of protective nature, probably formed by metal ions from the substrate and inhibitive ions leached from the anticorrosive pigments.	24
23	duralumin alloy	acid rain solution	strontium chromate	phosphate and calcium-containing pigments	-	Nonchromate composition decreases the efficiency of cathodic processes on the intermetallic part of the model better than the chromate inhibitor due to the formation of a stable adsorption film containing zinc and aluminium phosphates.	25
24	aluminium-copper	acid medium	strontium chromate	zinc phosphate/molybdate	surface analysis	Protective effect is caused by the deposition of a protective film on the aluminium matrix (anode) and intermetallic phase (cathode). Under the corrosion potential, a protective film, consisting of a mixture of zinc and calcium phosphates with admixture of zinc hydroxide, is formed on a specimen of the alloy.	26
25	duplex stainless steel (DSS)	LiBr media	chromate	bromide	anodic cyclic polarization curves and AC impedance measurements	The addition of halides strongly increased the inhibition efficiency of chromate. The passive film becomes more resistant when bromide concentration increases, although film thickness decreases.	27

Table 1. (cont.)

No.	Metal	Medium	Inhibitor	Additives	Methods	Findings	Ref
26	zinc	aqueous containing different amounts of chloride ions	chromate	-	FTIR, XANES and SIMS	A negative effect of the increasing chloride-to-chromate surface molar ratio on corrosion can be seen in the increasing ability to reduce oxygen on the zinc surface measured by the scanning Kelvin probe (SKP) technique. Inhibition of the cathodic reaction by chromate was less effective at higher ratios.	28
27	duplex stainless steel (DSS)	LiBr media	chromate	bromide	anodic cyclic polarization curves and AC impedance measurements.	Depending on the chromate/bromide ratio: pitting corrosion susceptibility highly decreased from a chromate/bromide ratio lower than 0.01. The comparative investigations carried out in LiBr and LiBr + 0.032 Li ₂ CrO ₄ verify the assumption that the halide ions facilitate inhibitor adsorption. The addition of halides increased inhibition efficiency to a considerable extent. Passive film becomes more resistant when bromide concentration increases, although film thickness decreases.	29
28	steel	aqueous	chromate	1-, 2-, 3-benzotriazole trimolybdate, tungstate	impedance tests, Frumkin-Temkin isotherm	According to the data of impedance tests and the results of evaluation of the degree of packing of these compounds on the steel surface, it is concluded that their inhibiting effect is caused by chemisorption satisfactorily described by the Frumkin-Temkin isotherm.	30
29	iron	0.1 M NaCl	zinc chromate	phosphate,	EIS, SVET and OCP measurements	Iron corroded uniformly in the phosphate extract, whereas in the chromate extract nucleation of metastable pits occurred. Evolution of the chromate layer with time was revealed, which was interpreted as being due to the formation of a porous healing layer formed on repassivated pits.	31
30	mild steel	cassava fluid	sodium chromate	diethylene amine	weight loss	The results of this study show that diethylene amine is a much better inhibitor than sodium chromate. The inhibition efficiencies by diethylene amine are higher than 85% for the 0.5, 1.0 and 1.5 M concentrations. For sodium chromate, inhibition efficiencies only become significant for 1.0 M and 1.5 M concentrations. Generally, the pH of all cassava fluid with and without inhibitors increased with duration of exposure and the corrosion rates of the mild steel decreased with increase in the pH of the cassava fluid.	32
31	mild steel	artificial acid rain solution (pH 4-5)	strontium chromate	-	polarisation, electrochemical impedance, XPS and solution analysis	The results show that, at low concentration, strontium chromate affects the cathodic reaction, with reduction of Cr ⁶⁺ to Cr ³⁺ , and the surface film was composed of magnetite and hydrated chromium hydroxide. The presence of strontium was not found significantly to affect the inhibitory performance.	33
32	hot-dip galvanized steels		zinc coating	chromate	SKP, XPS and AES surface analysis techniques	The paper focuses on the synergetic effect of three different constituents of the chromating product: phosphates, chromates and surfactants. For this purpose two types of products have been compared, an industrial formulation (PInd) which is currently applied in the industrial lines and a reference product which has been formulated in the laboratory (PLab) in order to sort out the effect of each constituent.	34
33	mild steel	aqueous 8.6 mM NaCl solutions (pH 8)	MoO ₄ ²⁻ or NO ₂ ⁻	-	XPS	For either anion these films are 0.5 nm deep, and the primary chemical state of iron is Fe ³⁺ . Following exposure to MoO ₄ ²⁻ , the film consists of a sub-layer (4.1 nm) composed largely of ferric oxide/hydroxide, overlaid by Fe ₂ (MoO ₄) ₃ (0.6 nm). As regards NO ₂ ⁻ , spectra are consistent with the film being closely related to γ-Fe ₂ O ₃ . A reduction product of NO ₂ ⁻ , potentially N ₂ is present, displaying a depth profile comparable to that of molybdate.	35
34	mild steel	near neutral 8.6·10 ⁻³ M (500 ppm) NaCl solution	nitrite	molybdate	polarization, weight loss, electrochemical and optical microscopy	Both nitrite and molybdate act as passivating anodic inhibitors, and they appear to have little effect on the cathodic kinetics. Various binary mixtures of these anions were also examined, and a number exhibited effective inhibition. Furthermore, two mixtures were concluded to exhibit synergistic behaviour, as regards corrosion inhibition.	36
35	steel	aqueous	nitrite	chloride	polarization method	From the results of the experiments, it was confirmed that the lithium, calcium nitrite corrosion inhibitor and new corrosion inhibitor over dosage 0.6 (NO ₂ ⁻ /Cl ⁻) molar ratio is very effective in protecting reinforcement from corrosion in mortar in which chloride ions have contained.	37
36	steel	cement mortar	nitrites of sodium, potassium and calcium	chloride	gravimetric measurements, potentiodynamic polarisation studies	Potentiodynamic polarisation studies for steel in binary and ternary cement environments showed the favourable influence of the presence of higher amounts of chlorides. Nitrites of sodium, potassium and calcium act as anodic inhibitors and they compete with chloride ions for the ferrous ions at the steel to form a film of ferric oxide.	38

Table 1. (cont.)

No.	Metal	Medium	Inhibitor	Additives	Methods	Findings	Ref
37	steel	neutral and acidic solutions	nitrite	ferrous chloride and sodium chloride	gravimetrically determined weight losses, EIS	It has not been observed a significant improvement in using nitrite as inhibiting agent in these systems. The corrosion seems to be related to the $[Cl^-]/[OH^-]$ ratio in three different regions of pH identified from acid to alkaline pH values.	39
38	steel	5% NaCl saturated $C_3(OH)_2$ solution	sodium molybdate	NaCl	polarization, EIS and Mott-Schottky analysis technique	The inhibition behavior of sodium molybdate is due to the stability of film on the metal surface through the competitive adsorption with Cl^- . Mott-Schottky (M-S) measurements confirmed the passive film formed on steel rebar surface was an n-type semi-conductor. Moreover, with increasing concentration of inhibitor, the passive film was more compact and stable than that in the absence of inhibitor.	40
39	hot-dip galvanized steels	aqueous	molybdate	silane	SEM, XPS, AES, and RAIR	The results showed that the molybdate/silane composite film formed in the single-step process had a similar double-layer structure as that obtained in the two-step process. For the film corrosion current was reduced, the impedance and the corrosion resistance were increased.	41
40	Q235 steel	5 g/L Cl^- solution	molybdate	silicate, phosphate and organic amine A	EIS, weight loss	Molybdate can reach better inhibition effect by compounding with silicate, phosphate and organic amine A. Corrosion inhibition efficiency of the compound inhibitors is near 84.4%, which is better than any individual inhibitor studied.	42
41	carbon steel	0.5 M NaCl solution	molybdate	chromate	AFM, polarization, EIS	Both CrO_4^{2-} and MoO_4^{2-} have inhibition effect on carbon steel corrosion, and the inhibition efficiency increases with increase in concentrations of CrO_4^{2-} and MoO_4^{2-} at the same concentration, the inhibition efficiency of CrO_4^{2-} is higher than that of MoO_4^{2-} . The increase in concentrations of CrO_4^{2-} and MoO_4^{2-} anions causes a shift of the breakdown potential (E_b) in the positive direction, indicating the inhibitive effect of the added anions on the pitting attack. AFM force-distance curves indicate that the passive film of CrO_4^{2-} is much stiffer than that of MoO_4^{2-} .	43
42	cold rolled steel (CRS)	peracetic acid (PAA) solution	sodium molybdate	-	gravimetric measurements, polarization curves, EIS	Na_2MoO_4 acts as a very good inhibitor in PAA solution. The inhibition efficiency increases with increasing concentration of Na_2MoO_4 and immersion time. The inhibition efficiencies, calculated from the three techniques are in reasonably good agreement and are very similar in the three cases. Na_2MoO_4 behaves as an anodic passive type inhibitor.	44
43	mild steel	LiBr-ethylene glycol soln.	lithium molybdate	-	rescale range analysis (R/S), EIS	The fractal analysis of electrochemical noise helps to evaluate the inhibitor protection performance under the tested corrosion conditions.	45
44	bronze	0.5 mol/L NaCl solution	sodium molybdate	benzotriazole (BTA)	polarization, EIS, XPS	The results show that combined action of BTA and sodium molybdate had a good synergistic effect of corrosion inhibition. They increased the resistance of anodic polarization of bronze. A polymer protective layer is formed on the bronze surface. The surface layer was consisted of [Cu (I) BTA] polymer film with deposit of SnO_2 , PbO , MoO_3 . It shows a good compactness and a good protection from chloride ion.	46
45	lead	chlorinated water	orthophosphate	-	SEM, TEM, XRD, and XANES analysis	In the absence of orthophosphate (DIC = 10 mg C/L, 24 °C, pH 7.75-8.1, 3 mg Cl_2/L goal), $Pb(IV)$ oxides formed with time following a transformation from the $Pb(II)$ mineral hydrocerussite. Orthophosphate dosing inhibited the formation of $Pb(IV)$ oxides. The $Pb(II)$ mineral hydroxypyromorphite, $Pb_5(PO_4)_3OH$, was the only mineral phase identified during the entire study of over 600 days, although the presence of some chloropyromorphite, $Pb_5(PO_4)_3Cl$, could not be ruled out. The findings provide an important explanation for the absence of $Pb(IV)$ oxides in some water systems that have used, or currently use.	47
46	copper	aqueous	phosphate	-	using standardised on-site corrosion tests	Phosphate dosing decreased the copper oxidation and resulted in lower copper concentration in water. Likewise phosphate hindered the precipitation of cupric ions, which prolonged the existence of copper in water and resulted in a higher copper concentration.	48
47	copper	aqueous	orthophosphate	sodium alginate and fulvic acid	weight loss	Effect of stagnation time on soluble copper release from different aged copper pipe in soft water was highly variable. Compared to the system of no organic matters, organic matters markedly decreased the efficiency of orthophosphate corrosion inhibition for copper pipe in soft water.	49
48	mild steel	phosphoric acid	phosphate of aluminum	-	weight-loss, potentiodynamic polarisation and EIS measurements	Polarization studies show that PA is a mixed-type inhibitor and acts both on the cathodic and anodic reactions without changing the mechanism of the hydrogen evolution reaction. PA adsorbs on the steel surface according to a Langmuir isotherm adsorption model.	50

Table 1. (cont.)

No.	Metal	Medium	Inhibitor	Additives	Methods	Findings	Ref
49	copper	aqueous	polyphosphate	-		Moderate doses of polyphosphate or orthophosphate generally decreased copper release whereas higher doses of orthophosphate tend to decrease copper solubility.	51
50	copper	aqueous	orthophosphate	hydroxyl binder groups		The highest anticorrosion efficiency is reached with pigments which are modified by organic corrosion inhibitors. The highly water soluble phosphate pigments reduce the anticorrosion coating properties. The effect of cation in phosphate pigments on the corrosion inhibition was confirmed.	52
51	silver	dilute nitric acid (0.01M)	methylamine, ethylamine, n-propylamine, and n-butylamine	-	electrochemical polarization technique, Tafel plots	Inhibition efficiency obtained from Tafel plots improved when the inhibitor concentration and the length of the alkyl chain.	53
52	steel	saturated NaCl solution	amine-alcohol	-	EIS, polarisation	The surface of the electrode changes from passive state to active state. The best inhibition was obtained in the presence of the Cl ⁻ inhibitor.	54
53	aluminium	1.0 M HNO ₃	thiosemicarbazone derivatives	-	polarization curves, EIS with quantum chemical calculations and molecular dynamics simulations	he thiosemicarbazone derivatives were of mixed-type inhibitors. EIS plots indicated that the addition of thiosemicarbazone derivatives increases the charge-transfer resistance of the corrosion process, and hence the inhibition performance. The molecular dynamics simulation results show that the three thiosemicarbazone derivatives can adsorb on the A ₂ O ₃ (111) surface through the sulphur and nitrogen atoms as well as π-electrons in the pyridyl structure.	55
54	copper	acid	methyl amine, dimethyl amine, diethyl amine, triethyl amine, diethanol amine, and triethanol amine	-	anode limiting current, Langmuir, Flory-Huggins, and kinetic adsorption isotherms	It is suggested that the decrease in the rate of corrosion is attributed to the increase in interfacial viscosity of the solution and decrease the diffusion coefficient of the copper ion. It has been found that the rate of inhibition is increases in order: methyl amine, dimethyl amine, diethyl amine, triethyl amine, diethanol amine, and triethanol amine.	56
55	mild steel	1M HCl	N, N'-dibenzylideneethane-1,2-diamine (baen)	chloro, methyl, and hydroxyl substituents	polarisation method	The presence of chloro, methyl and hydroxyl substituents enhance the inhibitive properties of N, N'-dibenzylideneethane-1, 2-diamine. Cbaen achieved the highest inhibition efficiency of 80.76% at 1·10 ⁻³ M.	57
56	iron	1M HCl	poly(p-phenylene diamine)	-	polarization techniques and electrochemical impedance spectroscopy	Poly(p-phenylene diamine) was a more efficient corrosion inhibitor than the monomer and gave an 85% inhibition efficiency at a concentration of 50 ppm, whereas the monomer gave an efficiency of 73% at 5000 ppm.	58
57	carbon steel	cooling water	sodium octanoate	-	potentiodynamic polarization and weight loss, FTIR	Results revealed that the concentration should not fall below 200 ppm for the tested inhibitor to be effective. The adsorption of inhibitor on the carbon steel surface was found to obey the Langmuir adsorption isotherm model. FTIR spectra revealed that octanoate was adsorbed on the steel surface via its functional group.	59
58	mild steel	cooling water	dextran containing carboxyl groups	-	weight loss	The inhibitor showed moderate corrosion inhibition activity for mild steel, and biodegradability under conditions for cooling water systems.	60
59	carbon steel	aqueous	polyepoxysuccinic acid (PESA)	Zn ²⁺ , sodium gluconate	weight loss	The synergistic effect exists among PESA, Zn ²⁺ and sodium gluconate and the corrosion inhibition efficiency for carbon steel is higher than 99%.	61
60	carbon steel	river water	calcium propionate	Zn ²⁺	mass-loss, polarization, FTIR spectra	The system controls cathodic reaction predominantly. Protective film is formed on the metal surface. Protective film consists of Fe ²⁺ -CP complex Zn(OH) ₂ and Ca(OH) ₂ .	62
61	stainless steel	3M hydrochloric acid	N-cyclohexyl-N'-phenyl thiourea (CPTU)		polarization technique, SEM	The thermodynamic parameters of adsorption deduced revealed a strong interaction and spontaneous adsorption of CPTU on the steel surface. Scanning electron microscopic study (SEM) was done to investigate the surface characterization of inhibited and uninhibited 304 SS specimens.	63
62	carbon steel	CO ₂ -saturated 3 wt.% NaCl solution	2-undecyl-1-sodium ethanoate-imidazole salt (2M2)	thiourea (TU)	electrochemical methods, Langmuir adsorption isotherm	Inhibition efficiency increased with increase in 2M2 concentration but decreased with increase in TU concentration with optimum. The data suggest that the compounds functioned via a mixed-inhibitor mechanism. A synergistic effect was observed between TU and 2M2.	64
63	iron	1.0 M solution of HNO ₃	N-methyl thiourea (MTU), N-propyl thiourea (PTU), and N-allyl thiourea (ATU)	-	weight loss, Tafel polarization and electrochemical impedance spectroscopy, EIS	These compounds revealed a good corrosion inhibition, (ATU) being the most efficient and (MTU) the least. The efficiency order of the inhibitors obtained by experimental results was verified by theoretical analysis.	65

Table 1. (cont.)

No.	Metal	Medium	Inhibitor	Additives	Methods	Findings	Ref
64	mild steel	0.5 M H ₂ SO ₄	acetyl thiourea chitosan polymer (ATUCS)	-	polarization, EIS, SEM	EIS showed that the resistance (R _s) increases slightly with increasing immersion time indicating a slight decrease in corrosion rate of the steel with time. Also, the corrosion rate increases with either increasing temperature or decreasing the polymer concentration. ATUCS has shown very good inhibition efficiency (IE) in 0.5 M sulphuric acid solution reaches to 94.5% for 0.76 mM concentration. IE of this compound has been found to vary with the concentration of the polymer solution, immersion time and temperature.	66
65	ingot iron	dilute HCl solution	allyl-thiourea (ATU)	-	potentiodynamic polarization tests	The phenomenon of desorption appears at the concentration of 100 mg/L, but the variation of the potential E _{des} between is obvious. The inhibition effect of ATU for BNII is limited by comparison with CPII.	67
66	stainless steel	0.5 M H ₂ SO ₄ solution	1-methyl-3-pyridine-2-yl-thiourea (MPT)	-	weight loss and polarization	MPT is of the mixed-type inhibitor. The adsorption of this inhibitor is also found to obey the Langmuir adsorption isotherm. Scanning electron microscopy indicated uniform film on the surface.	68
67	stainless steel	acid	0.004-0.007 M of 1-methyl-3-pyridine-2-yl-thiourea (MPT)	-	potentiostatic polarization measurements.	Corrosion potential (E _{corr}) increases with increasing MPT concentrations, while corrosion current (i _{corr}) decreases. Inhibition efficiency of MPT is slightly more in 1 M H ₂ SO ₄ than in 1 M HCl. The inhibitor functions through adsorption and follows Temkin isotherm in both the acids. Activation energy (E _a) and Gibbs free energy (E _g) for adsorption of MPT are calculated. The values of G _{ads} decreased (attained more negative values) with increasing temperature.	69
68	mild steel	H ₂ SO ₄ solution	1-methyl-3-pyridin-2-yl-thiourea	-	different techniques.	Inhibition efficiency increases with the increase of inhibitor concentration. This compound affects both the anodic dissolution of steel and the hydrogen evolution reaction in 0.5 M H ₂ SO ₄ . The adsorption of this inhibitor is also found to obey the Langmuir adsorption isotherm.	70
69	ordinary steel	aqueous	phosphonate anion (PHOS)	cetyltrimethylammonium bromide (CTAB)	weight loss, polarization curves, EIS	PHOS perform excellently as corrosion inhibitor for ordinary steel in simulated cooling water. The inhibition efficiency of PHOS was increased with increasing both its concentration and water circulation velocity. The inhibition efficiency decreased slightly with temperature as well as hold time immersion under open circuit potential conditions. The adsorption of PHOS on ordinary steel surface obeyed Langmuir's isotherm.	71
70	carbon steel	low chloride aqueous medium	tungstate	N,N-bis(phosphonomethyl) glycine (BPM(G)) and zinc ions	polarisation studies, impedance studies, XPS reflection absorption FTIR	The synergistic action of tungstate has been established through the present studies. System functions as a mixed inhibitor. The surface film is highly protective and it consists of iron, phosphorus, nitrogen, oxygen, carbon, zinc and tungsten in the surface film.	72
71	carbon steel	low chloride environment	2-phosphonobutane-1,2,4-tricarboxylic acid (PBTC)	ascorbate, Zn ²⁺	Polarisation, impedance studies, XPS, FTIR	The synergistic effect of ascorbate has been established from the present studies. In the presence of ascorbate, lower concentrations of PBTC and Zn ²⁺ are sufficient in order to obtain good inhibition. This mixture functions as a mixed inhibitor, predominantly cathodic. An immersion period of 24 h is necessary for the formation of the protective film, with a very high charge transfer resistance. The film is stable even at 60 °C in the presence of the inhibitor in the corrosive environment.	73
72	carbon steel	1 M HCl solution	aminotris-(methylene)phosphonic acid (ATMP)	-	weight loss, polarization, EIS techniques, Tafel polarization	The inhibition efficiency increased with increasing inhibitor concentration. ATMP acts as a mixed inhibitor. It obeyed the Langmuir adsorption isotherm. Corrosion inhibition is mainly controlled by a physisorption process. ATMP have an antibacterial effect against both Gram positive and Gram negative bacteria. The MIC of ATMP against <i>Listeria innocua</i> in a buffered medium (pH 6.5) was of ca. 4-fold higher than MIC measured in unbuffered medium. The antibacterial activity of ATMP is a result of a combined effect of the pH solution and the chemical nature of the used phosphonate.	74
73	carbon steel	aqueous soln. containing 60 ppm of Cl ⁻	diethylenetriaminepenta-methylenephosphonic acid	zinc, sodium gluconate	weight loss, EIS, FTIR, AFM	System functions as a mixed inhibitor. A protective film is formed on the metal surface. It consists of Fe ²⁺ -DTPMP complex, Fe ²⁺ -SG complex and Zn(OH) ₂ .	75
74	high purity polycrystalline zinc	aqueous	1,5-diphosphono-pentane (DPP) and 1,7-diphosphono-heptane (DPH)	-	XRD and XPS, GD-OES	The corrosion inhibition was explained by the formation of insoluble zinc-phosphonate salt on the zinc surface, blocking the zinc dissolution process.	76

Table 1. (cont.)

No.	Metal	Medium	Inhibitor	Additives	Methods	Findings	Ref
75	mild steel	aqueous	1-hydroxyethylidene 1,1 diphosphonic acid (HEDP)	sodium silicate	EIS, Tafel polarization techniques, polarization, SEM	Inhibitors mixtures have shown synergistic effects at lower value of HEDP. The surface homogeneity increases in case of inhibitors mixture application and this provides good protection to mild steel against corrosion in soft water solution.	77
76	steel	1 M HCl	sodium methyl dodecyl phosphonate and sodium methyl (11-methacryloyl-oxyundecyl) phosphonate	-	EIS, polarisation, weight loss measurements	The dissolution process of steel occurred under activation control. The inhibitors tested acted as cathodic inhibitors.	78
77	mild steel	well water	sodium tungstate	Zn ²⁺ , HEDP	weight loss, A.C impedance, polarization	The system works as an anodic inhibitor. Charge transfer resistance increases, double layer capacitance decreases. Hence a protective film is formed on the surface.	79
78	steel	alkaline solution	sodium tartrate, sodium benzoate, sodium glutamate, DMEA and TETA	-	EIS and potentiodynamic tests	Theoretical calculations based on molecular mechanics and molecular dynamics were used to establish which functional groups bind to the passive film, the strength of their binding, the functional groups contributing to their filming, and their evolution with time.	80
79	carbon steel	30 mg l ⁻¹ NaCl + 70 mg l ⁻¹ Na ₂ SO ₄ eq. solution	sodium benzoate	-	polarization curves, EIS	Corrosion inhibition of sodium benzoate in near-neutral aqueous solution was increased as the grain size of iron was decreased from micro to nanocrystalline surface.	81
80	iron	30 mg l ⁻¹ NaCl + 70 mg l ⁻¹ Na ₂ SO ₄	sodium benzoate	-	Tafel polarization curves, EIS	Results obtained suggested that the inhibition effect and corrosion protection of sodium benzoate inhibitor in near-neutral aqueous solutions increased as the grain size decreased from microcrystalline to nanocrystalline. The improvement on the inhibition effect is attributed to the increase of the surface energy.	82
81	steel	alkaline solution	sodium tartrate, sodium benzoate, sodium glutamate, dimethylethanolamine and triethylenetetramine	-	EIS, potentiodynamic tests	The theoretical results showed the presence of favourable interaction energy with the surface of the adsorbed molecules, with repulsive intermolecular interactions, mainly among the anions. The adsorption isotherms confirmed both the presence of a strong physisorption between the inhibitors and the substrate, and of repulsive interactions between the molecules of inhibitors, leading to the formation of a non-homogenous monolayer.	83
82	carbon steel	aqueous	sodium benzoate and sodium- (phenylamino) benzenesulfonate	-	gravimetric method, FTIR	These inhibitors retard the anodic dissolution of low carbon steel by protective layer bonding on the metal surface.	84
83	stainless steel	seawater	sodium benzoate	-	weight loss	The highest corrosion rate is observed for the stainless steel with no inhibitor was added to the seawater. As the concentration of sodium benzoate being increased, the corrosion rate is decreases. Results show that by the addition of 1.0M of sodium benzoate in seawater samples, it giving ≥ 90% efficiencies	85
84	mild steel	sulphuric acid solution	sodium dodecyl benzene sulphonate	hexamethylenetetramine	weight loss, electrochemical impedance and Tafel polarisation measurements	For HA, a monotonous increase in inhibition efficiency is observed as a function of concentration. For SDBS, however, an optimum in the inhibition efficiency is observed for a concentration close to 250 ppm. Upon mixing HA and SDBS, concentration regions showing synergistic and antagonistic inhibition behaviour are identified, and it is concluded that electrostatic interactions between adsorbate ions are likely responsible for both phenomena.	86
85	mild steel	0.5 M H ₂ SO ₄ solution	p-toluene sulphonic acid doped copolymer	-	weight loss, polarization and electrochemical impedance techniques	The inhibition efficiency has been found to increase with increase in inhibitor concentration, solution temperature and immersion time. A strong interaction between inhibitor and mild steel surface. The adsorption of this inhibitor on the mild steel surface obeyed the Langmuir adsorption equation.	87
86	Armco iron	0.5 mol dm ⁻³ H ₂ SO ₄ solution	naphthalenesulfonic acid, 2,7-naphthalenedisulfonic acid and 2-naphthol-3,6-disulfonic acid	-	weight loss, polarization	The inhibitors behave as a cathodic corrosion inhibitors. The inhibitive efficiency, changes with the number of functional groups substituted on benzene ring and increases with concentration.	88
87	aluminium	hydrochloric acid solution	dodecyl sulphonic acid sodium salt, dodecyl benzene sulfonic acid sodium salt and sodium dodecyl sulfate	-	weight loss method	The adsorption of the inhibitor could prevent aluminium from weight loss and the adsorption was according to Langmuir equation. Thermodynamic parameters such as adsorption heat, adsorption free energy were calculated.	89

Table 1. (cont.)

No.	Metal	Medium	Inhibitor	Additives	Methods	Findings	Ref
88	stainless steel, nickel alloys, and refractory metals	methane sulphonic acid		ferric and nitrate ions	weight loss coupon exposure tests and potentiodynamic polarisation measurements	It was found that most of the stainless steels, nickel alloys, and titanium corrode to a considerable extent, whereas Hastelloy G-30, zirconium, and tantalum withstand this environment. The addition of ferric and nitrate ions was found to produce an inhibiting effect.	90
89	steel	cooling water systems	copolymer of acrylic acid-diphenyl amine sulphonic acid	-	constant potential electrolysis, EIS, SEM XRD	AA-DPSA polymer acts as a very good antiscaling inhibitor both in the carbonate and sulphate brines. Copolymer of acrylic acid-diphenyl amine sulphonic acid can be used safely in cooling water industries.	91
90	mild steel	-	poly(styrene sulphonic acid)-doped polyaniline	-	weight loss galvanostatic polarisation studies, electropermeation studies and a.c. impedance	The polymer acts predominantly as an anodic inhibitor and corrosion inhibitor. The adsorption of the compound on the mild steel surface obeys Temkin's adsorption isotherm.	92
91	stainless steel	3% NaCl solution	poly(o-anisidine)-dodecylbenzenesulfonate	-	OCP, polarization technique, EIS	POA-DBSA acts as a corrosion protective coating on steel and reduces the corrosion rate (CR) of steel almost by a factor of 14.5.	93
92	mild steel	HCl	bipyrazolic derivatives	-	functional approach B3L YP/6-31G(d) calculations	The bipyrazole inhibitors exhibited the highest inhibition efficiency. The quantum chemical parameters calculated are, the highest occupied molecular orbital (HOMO), the lowest unoccupied molecular orbital (LUMO), the gap energy (ΔE), the dipole moment (μ), the softness (σ) and the total energy (TE).	94
93	steel	2 wt.% NaCl and 1 wt.% Na ₂ SO ₄	dicyclohexylamine nitrite or sodium dihydrogen ortho phosphate	-	weight loss	Treatment of steel with either dicyclohexylamine nitrite or sodium dihydrogen orthophosphate both at 10 mM concentration for 1 day at room temperature resulted in significant inhibition of corrosion.	95
94	copper	3% NaCl solution	(bipy1); (bipy2); (bipy3); (bipy4); (bipy5); (bipy6)	-	cathodic Tafel plots, polarisation resistance weight loss, EIS	The studied molecules act as mixed-type inhibitors. Detailed study of bipy1 shows that the maximum inhibition efficiency revolves around 99 per cent from 5·10 ⁻⁴ M of inhibitor. This latter adsorbs on the copper surface according to the Frumkin isotherm model. The inhibition efficiency of bipy1 decreases with the rise of temperature in the range 25 - 60°C.	96
95	carbon steel	2.0% NaCl and 1.0% Na ₂ SO ₄	sodium dihydrogen ortho phosphate, dicyclohexylamine nitrite and sodium benzoate	-	electrochemical methods	Sodium dihydrogen orthophosphate had the best performance among the three inhibitors. It was still effective at the end of 180 days of atmospheric exposure. The performances of dicyclohexylamine nitrite and sodium benzoate, on the other hand, were effective in the early stages of the atmospheric exposure. Their inhibition effectiveness deteriorated with further exposure to the atmosphere, being totally ineffective by the end of the exposure period.	97
96	carbon steel		dicyclohexylamine, dicyclohexylamine nitrite	-	polarization and the electrochemical impedance methods	The corrosion rate decreased significantly in the acid vapours at high humidity when a volatile corrosion inhibitor was also present.	98
97	coupled steel trod zinc	aqueous	dicyclohexylamine nitrite	-	mass loss, polarisation and ac impedance measurements	DCHN acts as an anodic inhibitor in the corrosion of mild steel. For zinc, DCHN acts to accelerate corrosion. This is attributed to surface chelation between DCHN and zinc, resulting in the formation of a soluble complex.	99
98	copper	0.5 M sulphuric acid	N-(5,6-diphenyl-4,5-dihydro-[1,2,4] triazin-3-yl)-guanidine	-	weight loss, polarization, EIS	NTG is a cathodic-type inhibitor for copper in 0.5 M H ₂ SO ₄ solutions. Adsorption of NTG on the surface of copper is found to obey the Langmuir adsorption isotherm.	100
99	copper	neutral solution of 3% NaCl	N-(5,6-diphenyl-4,5-dihydro-[1,2,4]triazin-3-yl)guanidine	-	weight loss polarization, EIS, EFM	These studies have shown that NTG was a very good inhibitor and the inhibition efficiency up to 99% in 3% NaCl is obtained. The adsorption of the inhibitor on the copper surface in the acid solution was found to obey Langmuir's adsorption isotherm.	101
100	Armco iron	molar hydrochloric acid (1 M HCl)	polyphosphate derivative of guanidine and urea copolymer	-	EIS	PGUC is an efficient inhibitor and the inhibition efficiency increases with increase in inhibitor concentration. This inhibitor can be used as biocides in aqueous environment. PGUC has a broad inhibitory spectrum against both Gram positive and Gram negative bacteria.	102

Volatile corrosion inhibitors (VCI)

Volatile corrosion inhibitors (VCI) reduce corrosion in closed spaces (package bags), VCI compound is emitted (vaporized) by the material enclosing the space. The vapours condense on the metal surface in form of microscopic crystals, which dissolve in the moisture film present on the surface. The ions of the dissolved VCI displace water molecules from the metal surface and form monomolecular invisible protection film reducing the corrosion rate. Volatile corrosion inhibitors may be added to various package materials: polymer film (e.g. low density polyethylene), paper, foam, powder, oils, etc.). The following compounds are used as Volatile corrosion inhibitors (VCI): cyclohexylamine,⁹⁴⁻⁹⁶ dicyclohexylamine,⁹⁷⁻⁹⁹ guanidine.¹⁰⁰⁻¹⁰²

The choice of inhibitors very much depends on the metal to be protected and the medium with which metal is in contact. The results are summarized in Table 1.

References

- ¹Gowri, S., Sathiyabama, J. and Rajendran, S., *Eur. Chem. Bull.*, **2012**, *1*, 470.
- ²Kavipriya, K., Rajendran, S. and Suriya Prabha, A., *Eur. Chem. Bull.*, **2012**, *1*, 366.
- ³Gogoi, P. K., Barhai, B., *Indian. J. Chem. Technol.*, **2010**, *17*, 291.
- ⁴Appa Rao, B. V., Srinivasa Rao, S., *Mater. Corros.*, **2010**, *61*, 285.
- ⁵Zhang, D. Q., Cai, Q. R., He, X. M., Gao, L. X., Kim, G.S., *Mater. Chem. phys.*, **2009**, *114*, 612.
- ⁶Gopi ,D., Govindaraju ,K. M., Collins Arun Prakash,V., Manivannan, V., Kavitha, L., *J. App. Electrochem.*, **2009**, *39*, 269.
- ⁷Lata, S., Chaudhary, R.S., *Indian .J. Chem. Technol.*, **2008**, *15*, 364.
- ⁸Shao,Y., Jia, G., Meng, T., Zhang, F., Wang, I., *Corros. Sci.*, **2009**, *51*, 371.
- ⁹Amar, H., Benzakour, J., Derja, A., Villemin, D., Moreau ,B., Braisaz ,T., Tounsi, A. *Corros. Sci.*, **2008**, *50*, 124.
- ¹⁰Reou, J. S., Ann ,K. Y., *Mater. chem. Phys*, **2008**, *109*, 526.
- ¹¹Girciene, O., Samuleviciene, M., Sudavicius, A., Ramanauskas, R., *Bull. Electrochem.*, **2005**, *21*, 325.
- ¹²Awad, H. S., Turgoose, S., *Corros.*, **2004**, *60*, 1168.
- ¹³Sreevalsan, K., Anithakumary, V., Shibi, I. G., *Orient. J. Chem.*, **2008**, *24*, 669.
- ¹⁴Varma, P. C. R., Duffy, B., Cassidy, J., *Surf. Coat. Tech.*, **2009**, *204*, 277.
- ¹⁵Groysman, A., Shvarts, I., *Corrosion Conference Series.*, **2006**, 060971-0609710.
- ¹⁶Kumar, Harish, Saini, Vishal, Kumar, Dheeraj, Chaudhary , R.S., *Mater. Lett*, **2008**, 1602.
- ¹⁷Souissi, N., Triki, E., *J.Mater. Sci.*, **2007**, *42*, 3259.
- ¹⁸Jing, G .L., Zhao , H., Wang, X.Y., *Polym. Mater. Sci. Eng.*, **2007**, *23*, 235.
- ¹⁹Mohanani, S., Maruthamuthu, S., Kalaiselvi, N., Palaniappan, R., Venkatachari, G., Palaniswamy, N., Raghavan, M., *Corros.Revie*, **2005**, *23*, 425.
- ²⁰Mehr, M.E., Shahrabi, T., Hosseini, M. G., *Anti-Corros. Method. Mat.*, **2004**, *51*, 399.
- ²¹Kalendova, A., *Anti-Corros.Method.Mat.*, **2003**, *50*, 82.
- ²²Rangel, C. M., de Damborenea, J., de Sa, A. I., Simplicio, M. H., *Br. Corros. J.*, **1992**, *27*, 207.
- ²³Gu, G., Zou, H., Ma, L., Chu, G., Fu, J., Chen, J., *J. Beijing University of Chem. Tech., (Natural Science Edition)*, **2010**, *37*, 20.
- ²⁴Bastos, A. C., Ferreira, M. G. S., Simoes, A.M., *Prog. Org. Coat.*, **2005**, *52*(4), 339.
- ²⁵Zin, I. M., Pokhmurskyi, V. I., Lyon, S. B., Bilyi, L. M., Tymus, M. B., *Mater. Sci*, **2009**, *1*.
- ²⁶Zin, I. M., Lyon,S. B., Bilyi, L. M., Tymus, M.B., *Mater. Sci.*, **2008**, *44*, 638.
- ²⁷Igual Munoz, A., Garcia Anton, J., Guinon, J.L., Perez Herranz, V., *Corros. Sci.*, **2007**, *49*, 3200.
- ²⁸Prosek, T., Thierry, D., Olsson, M., Bexell, U., *Corros.*, **2007**, *63*, 258.
- ²⁹Igual Munoz, A., Garcia Anton, J., Guinon, J.L., Perez Herranz, V., *Corros. Sci.*, **2006**, *48*, 4127.
- ³⁰Slobodyan, Z.V., Mahlatyuk, L. A., Nykyforchyn, H. M., *Mater. Sci.*, **2006**, *42*, 589.
- ³¹Bastos, A.C., Ferreira, M. G. S. and Simoes, A.M., *Corros. Sci.*, **2006**, *48*, 1500.
- ³²Olorunniwo, O.E., Umoru, L. E., Bamigboye, O. R., *J. Appl.Sci.*, **2006**, *6*, 878.
- ³³Baghni, I. M., Lyon, S. B., *Corros. Eng. Scie Tech.*, **2005**, *40*, 165.
- ³⁴Mekhalif, Z., Forget, L., Delhalle, J., *Corros. Sci.*, **2005**, *47*, 547.
- ³⁵Al-Refaie, A. A., Walton, J., Cottis, R. A., Lindsay, R., *Corros. Sci.*, **2010**, *52*, 422.
- ³⁶Al-Refaie, A. A., Cottis, R. A., Lindsay, R., *Impact of molybdate and nitrite anions on the corrosion of mild steel, NACE - International Corrosion Conference Series.*, **2009**, 11.
- ³⁷Moon, B. C., Lee, H., Kim, Y., *Key. Eng. Mater*, **2008**, 385, 605.
- ³⁸Song, H. W., Saraswathy, V., Muralidharan, S., Lee, C.H., Thangavel, K., *J. Appl. Electrochem.*, **2009**, *39*, 15.
- ³⁹Garces, P., Saura , P., Mendez, A., Zornoza, E., Andrade, C., *Corros. Sci*, **2008**, *50*, 498.
- ⁴⁰Zhou, X., Yang, H.Y., Wang, F. H., *Corros.Sci. Prot. Tech*, **2010**, 343.
- ⁴¹Kong, G., Lu, J., Zhang, S., Che, C., Wu, H., *Surf. Coat. Tech.*, **2010**, *205*, 545.
- ⁴²Shen, S.F., *Corros.Sci.Prot.Tech.*, **2009**, *21*, 179.
- ⁴³Chen, Z., Guo, X., Zhang, X., Huang, L., *Mater. Corros.*, **2009**, *60*, 726.
- ⁴⁴Qu, Q., Li, L., Jiang, S., Bai, W., Ding, Z., *J. Appl. Electrochem.*, **2009**, *39*, 569.
- ⁴⁵Sarmiento, E., González-Rodríguez, J.G., Uruchurtu, J., *ECS Transactions.*, **2008**, *151*, 221.
- ⁴⁶Hu, G., Lue, G.C., Wu, X. H., *Corros. Sci. Prot. Tech.*, **2008**, *20*, 25.
- ⁴⁷Lytle, D. A., Schock, M. R., Scheckele, K., *Environ. Sci. Technol.*, **2009**, *43*, 6624.
- ⁴⁸Dartmann, J., Alex, T., Dorsch, T., Schevalje, E., Johannsen, K., *Acta Hydrochimica et Hydrobiologica.*, **2004**, *32*, 25.
- ⁴⁹Li, S., Ni, L., Sun, C., Wang, L., *Corros. Sci.*, **2004**, *46*, 137.

- ⁵⁰Malki Alaoui, L., Kertit, A. S., Bellaouchou, Guenbour, A., Benbachir, A., Hammouti, B., *Electrochim. Acta.*, **2008**, 26,339.
- ⁵¹Edwards, M., Hidmi, L., Gladwell, D., *Corros. Sci.*, **2002**, 44,1057.
- ⁵²Kalendova, A., *Pigment. Resin. Tech.*, **2002**, 31, 381.
- ⁵³Abd El Wanees, S., Abd El Aal Mohamed, A., Abd El Azeem, M., El Said, R., *J. Dispersion. Sci.Technol.*, **2010**, 31,1516.
- ⁵⁴Zheng, Z.G., Yang, H.Y., *Physico - Chimica Sinica.*, **2010**, 26, 2354.
- ⁵⁵Khaled, K.F., *Corros. Sci.*, **2010**, 52, 2905.
- ⁵⁶El Hleem, S. M. A., Ahmed, A. M., El-Naggar, A. E., *J. Dispersion. Sci.Technol.*, **2010**, 31,512.
- ⁵⁷Sauri, A. S. M., Kassim, K., Bahron, H., Yahya, M. H. A., Harun, M. K., *Materials. Res. Innovations.*, **2009**, 13, 305.
- ⁵⁸Manivel, P., Sathiyarayanan, S.,Venkatachari, G., *J. Appl. Polym.Sci.*, **2008**, 110, 2807.
- ⁵⁹Ali, A. H., Abdel Salam,O. E., Waheed, A. F., Abdel-Karim, R., *Corrosion Inhibition of Carbon Steel in Cooling System Media by Non-Toxic Linear Sodium Octanoate,17th International Conference on Nuclear Engineering (ICONE17)*, **2009**, 1, 12.
- ⁶⁰Oyaizu, K., Yamaguchi, A., Hayashi,T., Nakamura,Y., Yoshii, D., Ito, D.Y., Yuasa, M., *Polym. J.*, **2006**, 38, 343.
- ⁶¹Xiong, R. C., Zhou, Q., Wei, G., *Chin.Chem. Lett.*, **2003**, 14, 955.
- ⁶²LeemaRose, A., Noreen Antony, Felicia Rajammal Selva Rani, Peter Pascal Regis, A., Susai Rajendran, *Zastit.Mater.*, **2009**, 50, 187.
- ⁶³Herle, R., Divakara Shetty, S., Achutha Kini, U., Shetty, P., *Chem. Eng.Commun.*, **2011**, 198, 120.
- ⁶⁴Okafor, P. C., Liu, C. B., Liu, X., Zheng,Y.G., Wang, F., Liu, C.Y., Wang, F., *J. Solid State. Electrochem.*, **2010**, 14, 1367.
- ⁶⁵Khaled, K. F., *Appl. Surf. Sci.*, **2010**, 256, 6753.
- ⁶⁶Fekry, A. M., Mohamed, R. R., *Electrochim Acta.*, **2010**, 55, 1933.
- ⁶⁷Shen C. B., Ding, Z. M., Wang,Y., *Mater. Sci. Tech.*, **2009**, 17, 781.
- ⁶⁸Hosseini, S. M. A., Salari, M., Ghasemi, M., *Mater. Corros.*, **2009**, 60, 963.
- ⁶⁹Hosseini,S. M. A., Salari, M., *Indian. J. Chem. Technol.*, **2009**, 16, 480.
- ⁷⁰Hosseini, S. M. A., Azimi, A., *Corros.Sci.*, **2009**, 51, 728.
- ⁷¹Touir, R., Dkhireche, N., Ebn Touhami, M., Sfaira, M., Senhaji, O., Robin, J.J., Boutevin, B., Cherkaoui, M., *Mater. Chem. Phys.*, **2010**, 122, 1.
- ⁷²Rao, B. V. A., Rao, M.V., Rao, S.S., Sreedhar, B., *J. Chem. Sci.*, **2010**, 122, 639.
- ⁷³Appa Rao, B.V., Srinivasa Rao, S., *Mater.Corros.*, **2010**, 61, 285.
- ⁷⁴Labjar, N., Lebrini, M., Bentiss, F., Chihib, N.E., Hajjaji, S.E., Jama, C.,*Mater. Chem.Phys.*, **2010**, 119, 330.
- ⁷⁵Manjula, P., *E-Journal of Chemistry.*, **2009**, 6, 887.
- ⁷⁶Pilbath, A., Bertoti, I., Sajo, I., Nyikos, L., Kalman, E., *Appl. Surf. Sci.*, **2008**, 255,1841.
- ⁷⁷Salasi, M., Shahrabi, T., Roayaei, E., *NACE - International Corrosion Conference Series.*, **2007**,070721-0707214.
- ⁷⁸Benabdellah, M., Dafali, A., Hammouti, B., Aouniti, A., Rhomari, M., Raada, A., Senhaji, O., Robin, J.J., *Chem. Eng. Commun.*, **2007**, 194,1328.
- ⁷⁹Kanimozhi, S.A., Rajendran, S., *Inter. J. Electrochem. Sci.*, **2009**, 4, 353.
- ⁸⁰Diamanti, M.V., Ormellese, M., Perez-Rosales, E. A., Pedeferra, M. P., Raffaini, G., Ganazzoli,F., *NSTI Nanotechnology Conference and Expo, NSTI-Nanotech.*, **2010**, 1 , 689.
- ⁸¹Afshari,V., Dehghanian,C., *J. Solid State Electrochem.*, **2010**, 14,1855.
- ⁸²Afshari,V., Dehghanian, C., *Mater.Chem. Phys.*, **2010**, 24, 466.
- ⁸³Ormellese, M., Perez, E. A., Raffaini, G., Ganazzoli, F., Lazzari, L., *Inhibition mechanism in concrete by organic substances: An experimental and theoretical study, NACE - International Corrosion Conference Series*,**2009**,19.
- ⁸⁴Mohammed, B. A., Mohanael , K.N.,*Monatshefte fur Chemie.*, **2009**,140,1.
- ⁸⁵Seoh, S.Y., Senin, H.B., Nik ,W.N.W., Amin, M. M., *AIP Conference Proceedings*, **2007**, 909, 210.
- ⁸⁶Mirghasem Hosseini, F.L., Stijn Mertens, Mohammed Arshadi, R., *Anti-Corros. Method. Mater.*, **2002**, 49,19.
- ⁸⁷Srivastava, V., Singh, M. M., *J. Appl. Electrochem.*, **2010**, 40, 2135.
- ⁸⁸Vracar ,Lj. M., Drazic, D. M., *Corros. Sci.*, **2002**, 44,1669.
- ⁸⁹Tianpei Zhao., Guannan Mu., *Corros. Sci.*, **1999**, 41, 1937.
- ⁹⁰Gaur, B., Srinivasan, H. S., *Br. Corros. J.*, **1999**, 34, 63.
- ⁹¹Shakkthivel, P., Vasudevan,T., *Desalination.*, **2006**, 197,1 79.
- ⁹²Manickavasagam, R., Jeya Karthik, K., Paramasivam, M., Venkatakrishna Iyer, S., *Anti corros. Methods. Mater.*, **2002**, 49, 19.
- ⁹³Chaudhari, S., Patil, P.P., *Electrochim Acta.*, **2010**, 5, 6715.
- ⁹⁴Laarej, K., Bouachrine, M., Radi, S., Kertit, S., Hammouti, B., *E-Journal of Chemistry.*, **2010**, 7, 419.
- ⁹⁵Kahraman , R., Saricimen, H., Al-Zahrani , M., Al-Dulaijan, S., *J. Mater. Eng.Perform.*, **2003**, 12, 524.
- ⁹⁶Dafali, A., Hammouti, B., Touzani, R., Kertit, S., Ramdani, A., K. *Anti-Corros.Methods.Mater.*, **2002**, 49(2), 96.
- ⁹⁷Malaibari, Z., Kahraman , R., Saricimen , H., Quddus, A., *Anti-Corros.Methods.Mater.*, **2002**, 49, 96.
- ⁹⁸Cano, E., Bastidas, D. M., Simancas, J., Bastidas, J. M., *Corros.*, **2005**, 61, 473.
- ⁹⁹Khamis, E., Oun, S. R., Lyon, S. B., *Br. Corros.J.*, **2001**, 36, 197.
- ¹⁰⁰Khaled, K. F., *App. Sur. Sci.*, **2008**, 255, 1811.
- ¹⁰¹Khaled, K. F., *Mater.Chem. Phys.*, **2008**, 112, 104.
- ¹⁰²Lebrini, M., Bentiss, F., Chihib, N. E., Jama, C., Hornez, J. P., Lagrenee, M., *Corros. Sci.*, **2008**, 50, 2914.

Received: 31.12.2012.

Accepted: 10.01.2013.



PHOTOCYCLISATION OF 2'-HYDROXYCHALCONES INTO 2- PYRAZOLINES UNDER IRRADIATION OF SOLAR ENERGY

Sainath B. Zangade*, Avinash T. Shinde, Shivaji B. Chavan, Shyam S. Mokle
and Yeshwant B. Vibhute ^[a,c]

Keywords: 2'-Hydroxychalcone, 2-pyrazoline, solar energy, photocyclisation

An efficient and facile reaction has been shown between 2-hydroxychalcone with hydrazine hydrate in ethanol in presence of catalytic amount of glacial acetic acid under irradiation of solar thermal energy to afford 2-pyrazoline. Cyclised product established on the basis of IR, NMR, MS, ¹³C NMR and elemental analysis.

*Corresponding Authors

*E-mail: drsbz@rediffmail.com

[a] Laboratory of Organic Synthesis, P.G. Department of Studies in Chemistry, Yeshwant Mahavidyalaya, Nanded (M.S) India.

Introduction

Chalcones (1,3-diaryl-2-propene-1-ones) constitute an important class of naturally occurring flavonoid compounds that exhibit a wide spectrum of biological activities and are well-known intermediates for synthesizing various heterocycles.

Amongst five-membered heterocycles, pyrazolines represent a class of compounds of great importance in heterocyclic chemistry.^{1,2} Substituted pyrazolines are fluorescent compounds with high quantum yields and are used as optical brighteners and whiteners.³

2-Pyrazolines exhibit good characteristics of blue photoluminescence, electroluminescence and as fluorescence.⁴ Among the methods employed in the synthesis of 2-pyrazolines, the condensation of α,β -unsaturated carbonyl compounds with hydrazine and hydroxylamine is commonly used. Recently various modified methods for the preparation of 2-pyrazolines using mercury(II) acetate,⁵ Zn,⁶ KHSO₄.H₂O/SiO₂,⁷ tungstophosphoric acid,⁸ Lewis acid/Lewis base⁹ and porous calcium hydroxyapatite catalyst.¹⁰ The reaction combination of solvent, costly chemicals/catalyst and long reaction time makes these methods economically expensive. Thus utilization of non-toxic chemicals, renewable materials and simple reaction conditions are the key issues of synthetic chemistry.

In view of these observations, we report herein, the synthesis of 2-pyrazolines by the condensation α,β -unsaturated ketone with hydrazine hydrate in ethanol in presence of glacial acetic acid under exposure of sunlight (Scheme-1). The formation of this class of five-membered heterocyclic compounds was characterized by spectroscopic technique.¹³

Methods and Materials

Instrumentation

Reaction of chalcone, hydrazine hydrate afforded a single compound. The progress of reaction was monitored by TLC, using hexane/ethyl acetate as the mobile phase. Melting points were determined in an open capillary tube and are uncorrected. IR spectra were recorded in KBr pellets on a Perkin-Elmer FT-IR Shimadzu spectrometer. ¹H and ¹³C NMR spectra were obtained in DMSO-d₆ on Avance 300 MHz spectrometer using TMS as an internal standard. The mass spectra were recorded on EI-Shimadzu-GC-MS spectrometer. Elemental analyses were performed on a Carlo Erba 106 perkin-Elmer model 240 analyzer.

Typical procedure for synthesis of 2-pyrazolines

A mixture of 2'-hydroxychalcones **1** (0.01 mol) and hydrazine hydrate (0.02 mol) was dissolved in ethanol in 20 ml ground-glass test tube. To this reaction solution a glacial acetic acid (0.001 mmol) was added and the ground-glass test tube was closed with a ground-glass plug, and was supported in an inverted position in beaker and exposed to direct sunlight for 25-30 min. at 43 °C. The progress of reaction was monitored on TLC. After exposure to sunlight, resulting solid product was collected by filtration and recrystallized from EtOH to yield **2**.

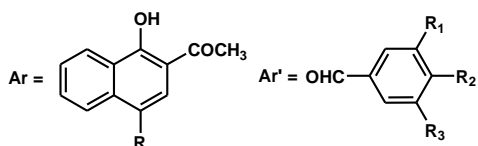
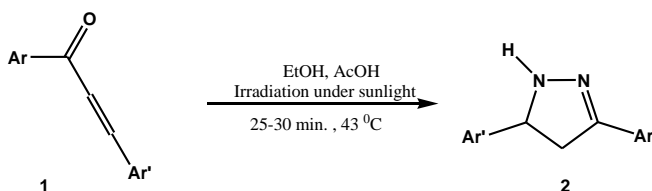
2-[5-(3,4,5-Trimethoxy-phenyl)-4,5-dihydro-1H-pyrazol-3-yl]-naphthalen-1-ol

Crystal appearance: Faint green. Yield: 92 %, M.P.: 192 °C. IR (KBr pellets): 3322 (N-H), 1589 (C=N), 1472, 1542 (C=C), 1232, 1130 (C-N) cm⁻¹. ¹H NMR (300 MHz, DMSO-d₆) δ 12.34 (s, 1H, OH), 7.48-8.37 (m, 8H, Ar-H), 6.87 (s, 1H, NH), 3.21 (dd, *J* = 4.8, 17.5 Hz, 1H, H_A), δ 3.72 (dd, *J* = 11.8, 17.5 Hz, 1H, H_B), δ 4.89 (dd, *J* = 4.8, 11.9 Hz, 1H, H_X), δ 3.80 (s, 3H, OCH₃), 3.42 (s, 6H, OCH₃). ¹³C NMR (DMSO) 154.05 (C of Ar-OH), 153.28 (C of C=N), 148.67 (C of Ar-OCH₃), 148.42 (2C of Ar-OCH₃) 134.13 (Ar-C), 133.19 (Ar-C), 128.23 (Ar-C), 128.36 (Ar-C), 127.41 (Ar-

C), 126.30 (Ar-C), 124.97 (Ar-C), 122.71 (Ar-C), 121.28 (Ar-C), 112.65 (Ar-C), 110.86 (Ar-C), 110.32 (Ar-C), 62.39 (3C of OCH₃), 56.36 (C of CH), 42.37 (C of CH₂). MS m/z: 378 (M⁺, 80 %), 377, 361, 347, 287, 231, 211, 210, 181, 168, 140, 128, 115, 109, 95, 77, 65, 51, 40. Anal.Calcld. for C₂₂H₂₂O₄N₂: C, 69.84; H, 5.82. Found: C, 70.92; H, 5.98.

2-[5-(3,4-Dimethoxy-phenyl)-4,5-dihydro-1H-pyrazol-3-yl]-4-iodo-naphthalen-1-ol

Crystal appearance: Faint green. Yield: 88 %, M.P.: 164 °C. IR (KBr pellets): 3319 (N-H), 1592 (C=N), 1468, 1546 (C=C), 1229, 1134 (C-N) cm⁻¹. ¹H NMR (300 MHz, DMSO-d₆) δ 12.2 (s, 1H, OH), 7.22-8.23 (m, 8H, Ar-H), 6.78 (s, 1H, N-H), 3.23 (dd, *J* = 5.0, 17.5 Hz, 1H, H_A), 3.77 (dd, *J* = 12.0, 17.6 Hz, 1H, H_B), 4.92 (dd, *J* = 5.0, 12.0 Hz, 1H, H_X), 3.40 (s, 6H, OCH₃). ¹³C NMR (DMSO): 154.12 (C of Ar-OH), 153.21 (C of C=N), 148.62 (2C of Ar-OCH₃), 133.27 (Ar-C), 130.46 (Ar-C), 127.30 (Ar-C), 128.78 (Ar-C), 127.46 (Ar-C), 126.34 (Ar-C), 124.80 (Ar-C), 122.50 (Ar-C), 121.25 (Ar-C), 112.70 (Ar-C), 110.94 (Ar-C), 110.28 (Ar-C), 62.43 (2C of OCH₃), 56.39 (C of CH), 42.33 (C of CH₂). ¹³C NMR (DMSO) 146 (C=N), 139-112 (=CH, Ph), 48.62 (-CH), 40.35 (-CH₂). 52.42 (-OCH₃). MS m/z: 474, (M⁺, 65%), 443, 412, 347, 286, 228, 207, 128, 112, 77, 65, 51, 40. Anal.Calcld for C₂₁H₁₉O₃N₂I: C, 53.16; H, 4.00; X (I), 26.73. Found: C, 50.39; H, 4.28; X (I), 26.75.



R: H, I; R₁: OCH₃, H; R₂, R₃: OCH₃.

Result and discussion

In our recent success on different methodology in organic synthesis towards the development of novel heterocyclic compounds,¹¹⁻¹⁶ in present communication we have described the photocyclisation of 2'-hydroxychalcones by the reaction of **1** with hydrazine hydrate in presence of catalytic amount of acetic acid using solar thermal energy to afford 2-pyrazolines **2**. The starting chalcones were prepared by well-known Claisen-Schmidt condensation under solvent-free conditions.¹⁵ The use solar energy can be considered as ideal green route for synthesis of 2-pyrazolines since they are easily available natural source, could be successfully used in place of toxic or expensive chemicals to overcome the activation energy in organic synthesis.

Initially we attempted the condensation of 1-(4-bromo-1-hydroxy-naphthalen-2-yl)-3-(3,4,5-trimethoxy-phenyl)-propanone **1** (0.01 mol) with hydrazine hydrate (0.02 mol) in 15 ml ethanol using glacial acetic acid in combination with solar energy irradiation. The reaction went completion

within 25 min at temperature 43 °C and corresponding product **2** obtained in 92% yield. Their IR spectra show absence of carbonyl absorption band and the appearance of characteristic absorption band for ν C=N at 1592-1588 cm⁻¹ and a band at 1130 cm⁻¹ for C-N. In the ¹H NMR spectrum, an ABX pattern was observable, H_A, H_B and H_X appear as double doublets at δ 3.10–3.30, 3.75–3.80 and 4.90–5.0 ppm with *J*_{AB} = 17.5 Hz, *J*_{AX} = 4.8 Hz, and *J*_{BX} = 11.8 Hz and singlet of 2-H pyrazolines around at δ 6.85 ppm respectively. The ¹³C NMR spectrum revealed the presence of a methylene carbon at δ 42.37 ppm, a methine carbon at δ 56.36 ppm and C=N at 153.28 ppm. The signals at δ 110.3–148.6 ppm show the presence of the aryl groups in the structure.

Conclusion

We have described efficient and simple practical procedure for synthesis of 2-pyrazoline using solar thermal energy. Present method is simple, economically cheaper and consistent with the green chemistry approach because it does not need heating.

Acknowledgement

The authors gratefully acknowledge University Grant Commission (UGC) New Delhi for sanctioning major research grant (No. 38-267/2009). The authors are also thankful to Principal, Yeshwant Mahavidyalaya, Nanded, for providing laboratory facilities and Director Indian Institute of Chemical Technology (IICT), Hyderabad, KTHM College, Nasik for providing necessary instrumental facilities.

References

- Elguero J, In: *Comprehensive Heterocyclic Chemistry*. Karitzky A. R., Ress, C. W., (Eds.) Pergamon: Oxford, **1984**, 5, 167-303.
- Elguero, J., In: *Comprehensive Heterocyclic Chemistry.II* Karitzky A. R., Ress, C. W., Scriven, E. F. (Eds.) Pergamon: Oxford, **1996**, 3, 1-76.
- Wang P., Onozawa-Kamatsuzaki, N., Hameda, Y., Sugihara, H., Arakawa, H., Kasuga, K. *Tetrahedron Lett.*, **2001**, 42, 9199–9201.
- De Silva, A. P., Gunaratne, H. Q. N., Gunlaugsson, T., Huxley, A. J., McCoy, C. P., Rademacher, J. T., Rice, T. E., *Chem. Rev.* **1997**, 97, 1515–1566.
- Lokanatha Rai, K. M., Linganna, N., *Synth. Commun.*, **1997**, 21, 3737-3744.
- Alex K, Tilack A, Schwarz N, Beller, M. *Org.Lett.*, **2008**, 10, 2377-2379.
- Kamal, K. K., Bilal, A. G., Kumar, S., Charanjeet, S. A. *Synth. Commun.*, **2006**, 36, 2727-2735.
- Fazaeli, R., Aliyan, H., Mallakpour, S., Rafiee, Z., Bordbar, M. *Chin. J. Catalysis*. **2011**, 32: 582-588.
- Krishna, P. R., Sekhar, E. R., Morgin, F. *Tetrahedron Lett.*, **2008**, 49, 6768-6772.
- Atir, R., Mallouk, S., Bougrin, K., Soufiaoui, M. *Synth. Commun.* **2006**, 36, 111-120.
- Zangade, S. B., Shinde, A. T., Vibhute, A. Y., Vibhute, Y. B. *Pak. J. Chem.* **2012**, 2, 18-23.

¹²Zangade, S., Mokle, S., Chavan, S., Vibhute, Y. *Orbital Elect. J. Chem.*, **2011**, *3*, 144-149.

¹³Zangade, S. B., Shinde, A. T., Patil, A. M., Vibhute, Y. B. *Eur. J. Chem.*, **2012**, *3*, 208-210.

¹⁴Zangade, S. B., Mokle, S. S., Shinde, A. T., Vibhute, Y. B. *Green Chem. Lett. Rev.* **2013**, *6*, 123-127.

¹⁵Zangade S, Mokle S, Vibhute Y, Vibhute, Y. *Chem. Sci. J.*, **2011**, *article ID:CSJ-13*, 1-6.

¹⁶ Chavan, S., Zangade, S., Vibhute, A., Vibhute, Y. *Eur. J. Chem.* Accepted.

Received: 10.01.2013.
Accepted: 13.01.2013.



EFFICIENT SYNTHESIS OF β -ENAMINONES AND β -ENAMINO ESTERS USING TRIS(HYDROGENSULFATO)BORON OR TRICHLOROACETIC ACID AS CATALYSTS

Zahed Karimi-Jaberi^{[a]*}, Zahra Takmilifard^[a]

Keywords: β -enaminones, β -enamino esters, tris(hydrogensulfato) boron, trichloroacetic acid.

New and efficient methods have been developed for the synthesis of β -enaminones and β -enamino esters in the presence of a catalytic amount of tris(hydrogensulfato)boron or trichloroacetic acid as highly efficient catalysts at 120 °C under solvent-free conditions. Both methods are simple, and provide desired products in good yields and short reaction times.

* Corresponding Authors

Fax: +98 7126224402

E-Mail: zahed.karimi@yahoo.com

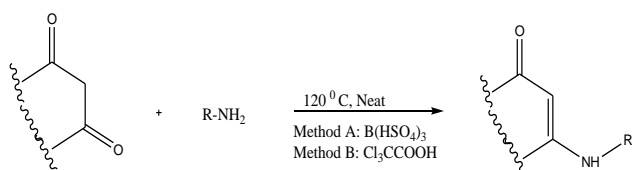
[a] Department of Chemistry, Firoozabad Branch, Islamic Azad University, P.O. Box 74715-117 Firoozabad, Fars, Iran

Introduction

Enaminones and enamino esters are useful intermediates for synthesis of biologically significant heterocyclic compounds, nitrogen containing compounds, and naturally occurring alkaloids.¹⁻⁴ They even served as synthons for γ -aminoalcohol, β -aminoacids which are a class of very stable compounds useful in asymmetric catalysis as a chelating agent.⁵

The most well-known and exploited route for the synthesis of β -enaminones involves the direct condensation of 1,3-dicarbonyl compounds with amines in refluxing aromatic hydrocarbons with azeotropic removal of water.⁶ Some improved procedures have been subsequently reported for this transformation using different catalysts.⁷⁻¹⁴ Although, these approaches are satisfactory for synthesis of enaminones, the harsh reaction conditions, expensive reagents, use of toxic organic solvents and long reaction times limit the use of these methods.

Due to extending our interest in the development of practical, safe, and environmentally friendly procedures for several important organic transformations,¹⁵⁻¹⁹ we now describe a simple and efficient protocol for the synthesis of β -enaminones through the reaction of 1,3-dicarbonyl compounds and amines using catalytic amounts of tris(hydrogensulfato)boron or trichloroacetic acid as catalysts under solvent-free conditions (Scheme 1).



Scheme 1. Synthesis of β -enaminones and β -enamino esters

Experimental

General procedure for the synthesis of β -enaminones

To a mixture of amines (1 mmol), 1,3-diketone (1 mmol) and $B(HSO_4)_3$ (10 mol%) or trichloroacetic acid (20 mol%) was added and the mixture was stirred and heated in an oil bath at 120 °C for appropriate time. Completion of the reaction was indicated by TLC. After completion of the reaction, the reaction mixture was cooled to room temperature. Chloroform (10 mL) was added and the catalyst was recovered by filtration. The solvent was evaporated and the product was isolated in almost pure form. Further purification was carried out by recrystallization from ethanol.

Selected spectral data

Product Table 1, entry 1: ¹HNMR (250 MHz, $CDCl_3$) δ : 1.08 (s, 6H, CH_3), 2.20 (s, 2H, CH_2), 2.34 (s, 2H, CH_2), 5.56 (s, 1H, CH), 7.15 (s, 1H, NH), 7.26-7.34 (m, 5H, ArH) ppm; IR (KBr): 3237, 3062, 2958, 1597, 1571, 1525, 1495, 1446, 1369, 1150, 1124 cm^{-1} .

Product Table 1, entry 2: ¹HNMR (250 MHz, $CDCl_3$) δ : 1.10 (s, 6H, CH_3), 2.22 (s, 2H, CH_2), 2.33 (s, 2H, CH_2), 5.52 (s, 1H, CH), 6.34 (s, 1H, NH), 7.08 (d, 2H, J=8.75 Hz, ArH), 7.28 (d, 2H, J=12.5 Hz, ArH) ppm; IR (KBr): 3241, 2956, 1727, 1596, 1567, 1489, 1364, 1258, 1084, 818 cm^{-1} .

Product Table 1, entry 3: ¹HNMR (250 MHz, $CDCl_3$) δ : 1.06 (s, 6H, CH_3), 2.21 (s, 2H, CH_2), 2.32 (s, 2H, CH_2), 5.53 (s, 1H, CH), 6.43 (s, 1H, NH), 7.02 (d, 2H, J=8.5 Hz, ArH), 7.43 (d, 2H, J=8.75 Hz, ArH) ppm; IR (KBr): 3241, 3173, 3096, 3042, 2955, 1610, 1571, 1524, 1487, 1462, 1401, 1368, 1262, 1147, 1071, 719 cm^{-1} .

Product Table 1, entry 4: ¹HNMR (250 MHz, $CDCl_3$) δ : 1.13 (s, 6H, CH_3), 2.27 (s, 2H, CH_2), 2.39 (s, 2H, CH_2), 5.66 (s, 1H, CH), 6.66 (s, 1H, NH), 7.51-7.57 (m, 2H, ArH), 7.99-8.01 (m, 2H, ArH) ppm; ¹³CNMR (62.5 MHz, $CDCl_3$) δ : 28.22, 32.88, 43.29, 49.94, 99.54, 118.95, 129.72, 139.59

148.81, 160.46, 198.07 ppm; IR (KBr): 3270, 3195, 3099, 2927, 1580, 1537, 1480, 1434, 13550, 1265, 1150 cm^{-1} .

Product Table 1, entry 12: $^1\text{H-NMR}$ (250 MHz, CDCl_3) δ : 1.21-1.26 (m, 6H, CH_3), 1.09 (s, 6H, CH_3), 3.34-3.36 (m, 4H, 2 CH_2), 4.03-4.11 (q, $J=21.25$ Hz, 2 CH_2), 4.47 (s, 2H, CH), 8.64 (s, 2H, NH) ppm; $^{13}\text{C-NMR}$ (62.5 MHz, CDCl_3) δ : 14.59, 19.27, 43.78, 58.47, 83.49, 161.33, 170.61 ppm; IR (KBr) : 3296, 2985, 1649, 1605, 1510, 1457, 1438, 1390, 1339, 1289, 1259, 1224, 1167, 1091, 1066, 1081 cm^{-1} .

Results and Discussion

Initially the reaction of dimedone with aniline in the presence of tris(hydrogensulfato)boron was used as a model reaction and this reaction was optimized using different conditions. It was found that best conditions were solvent-free at 120 $^\circ\text{C}$ using 10 mol% tris(hydrogensulfato) boron and a molar ratio of dimedone/aniline of 1:1.

Tris(hydrogensulfato)boron [$\text{B}(\text{HSO}_4)_3$] was easily prepared by addition of chlorosulfonic acid to boric acid under N_2 atmosphere at room temperature. This reaction was easy and clean, because HCl gas was evolved from the reaction vessel immediately. This catalyst is safe and easy to handle.²⁰ It has been utilized as a catalyst by our group for the synthesis of α,α' -benzylidene bis(4-hydroxycoumarin) derivatives¹⁷ and 2,3-dihydroquinazolin-4(1H)-ones.¹⁸

To study the scope of the reaction, a series of 1,3-dicarbonyl compounds with various anilines under catalytic amounts of tris(hydrogensulfato)boron were applied. The reaction proceeded well with aromatic amines. As shown in Table 1, by this method (Method A), reaction of various aryl amines carrying either electron-donating or electron-withdrawing substituents were successfully reacted with dimedone to produce their corresponding β -enaminones in high yields with short reaction times.

Under the optimized reaction conditions, the reactions of acetyl acetone with aryl amines were examined and very good yields of products were obtained (Table 1, entries 7-8).

The condensation of amines with ethyl acetoacetate was also successfully carried out under the same conditions and the corresponding β -enamino esters were obtained in high yields and short reaction times (Table 1, entries 9-12).

These results encouraged us to exploit the generality and scope of this reaction by using other catalyst such as trichloroacetic acid. Trichloroacetic acid (TCAA) is a readily available and inexpensive reagent and can conveniently be handled and removed from the reaction mixture.¹⁶

Trichloroacetic acid (TCAA) is an efficient catalyst which has been successfully utilized by our group in some reactions, for example, synthesis of 1,4-dihydropyranopyrazoles,¹⁶ tetrahydrobenzoxanthen-11-ones and dibenzoxanthenes.¹⁹ Thus, the remarkable catalytic activities together with its operational simplicity make it the most suitable catalyst for the synthesis of β -enaminones and β -enamino esters. After systematic screening, TCAA was found to be the catalyst of choice. Similarly, the mole ratio of TCAA was studied and found 20 mol% of TCAA to be optimum. The reaction was carried out with amine (1 mmol) and 1,3-dicarbonyl compounds (1 mmol) in the presence of TCAA (20 mol%) and heated at 120 $^\circ\text{C}$ under solvent-free conditions resulted to the formation of the corresponding β -enaminones and β -enamino esters (Scheme 1). The results are compiled in Table 1 (Method B). This protocol is remarkably simple and requires non-hazardous reagents or inert atmosphere.

All products were identified by $^1\text{H-NMR}$, ^{13}C NMR and IR spectroscopic methods and the results were confirmed by comparison with those available in the literature.

Table 1 Synthesis of β -enaminones and β -enamino esters

Entry	R	1,3-diketone	Method A ^a		Method B ^b		m.p. ($^\circ\text{C}$) ^{ref.}
			Time (min)	Yield (%)	Time (min)	Yield (%)	
1	C_6H_5	Dimedone	7	85	7	75	183-184 ²¹
2	4- ClC_6H_4	Dimedone	8	80	8	80	191-194 ²²
3	4- BrC_6H_4	Dimedone	7	83	7	83	159-163 ²¹
4	3- $\text{NO}_2\text{C}_6\text{H}_4$	Dimedone	8	80	8	80	165-170
5	4- $\text{NO}_2\text{C}_6\text{H}_4$	Dimedone	7	82	7	82	191-193 ²²
6	2- $\text{COOH}\text{C}_6\text{H}_4$	Dimedone	7	85	7	85	187-189 ²³
7	$\text{H}_2\text{N}(\text{CH}_2)_2$	Acetylacetone	7	85	7	85	110-113 ²⁴
8	n-butyl	Acetylacetone	7	85	7	85	Oil ⁸
9	n-butyl	Ethyl acetoacetate	7	85	7	85	Oil ⁸
10	Ph- CH_2	Ethyl acetoacetat	10	85	10	85	Oil ²⁴
11	4- ClC_6H_4	Ethyl acetoacetate	7	83	7	83	Oil ⁸
12	$\text{H}_2\text{N}(\text{CH}_2)_2$	Ethyl acetoacetate	8	85	8	85	121-124 ²⁴

^aMethod A: tris(hydrogensulfato) boron; ^b Method B: Trichloroacetic acid

Conclusion

In conclusion, we have developed efficient procedures for a convenient and mild synthesis of various β -enaminones through the reaction of 1,3-dicarbonyl compounds and amines using catalytic amounts of tris(hydrogensulfato) boron or trichloroacetic acid as catalysts under solvent-free conditions. Prominent among the advantages of these new methods are operational simplicity, good yields in short reaction times and easy work-up procedures employed.

References

- ¹Li, G.; Watson, K.; Buckheit, R. W.; Zhang, Y. *Org. Lett.* **2007**, *9*, 2043.
- ²White, J. D.; Lhle, D. C. *Org. Lett.* **2006**, *8*, 1081.
- ³Calle, M.; Calvo, L. A.; Ortega, A. G.; Gonzalez-Nogal, A. M. *Tetrahedron* **2006**, *62*, 611.
- ⁴Felice, E.; Fioravanti, S.; Pellacani, L.; Tardella, P. A. *Tetrahedron Lett.* **1999**, *40*, 4413.
- ⁵Palmieri, G.; Cimorelli, C. *Arkivoc.* **2006**, *6*, 104.
- ⁶Martin, D. F.; Janusonis, G. A.; Martin, B. B. *J. Am. Chem. Soc.* **1961**, *83*, 73.
- ⁷Mohammadizadeh, M. R.; Hasaninejad, A.; Bahramzadeh, M.; Khanjarloo, Z. S. *Synth Commun.* **2009**, *39*, 1152.
- ⁸Gholap, A. R.; Chakor, N. S.; Danil, T.; Lahoti, R. J.; Srinivasan, K. V. *J. Mol. Catal A: Chem.* **2006**, *245*, 37.
- ⁹Bhatte, K. D.; Tambade, P. J.; Dhake, K. P.; Bhanage, B. M. *Catal. Commun.* **2010**, *11*, 1233.
- ¹⁰Kidwai, M.; Bhardwaj, S.; Mishra, N. K.; Bansal, V.; Kumar, A.; Mozumdra, S. *Catal. Commun.* **2009**, *10*, 1514.
- ¹¹Giuseppe, B.; Marcella, B.; Manula, L.; Enrico, M.; Paolo, M.; Letizia, S. *Synlett.* **2004**, 239.
- ¹²Rafiee, E.; Mahdavi, H.; Eavani, S.; Joshaghani, M.; Shiri, F. *Appl. Catal. A: Gen.* **2009**, *352*, 202.
- ¹³Epifan, F.; Genovese, S.; Curini, M. *Tetrahedron Lett.* **2007**, *48*, 2717.
- ¹⁴Datta, B.; Reddy, M. B. M.; Pasha, M. A. *Synth Commun.* **2011**, *41*, 2331.
- ¹⁵Karimi-Jaberi, Z.; Arjmandi, R. *Monatsh. Chem.* **2011**, *142*, 631.
- ¹⁶Karimi-Jaberi, Z.; Reyazoshams, M. M. *Heterocycl. Commun.* **2011**, *17*, 177.
- ¹⁷Karimi-Jaberi, Z.; Nazarifar, M. R.; Pooladian, B. *Chin. Chem. Lett.*, 2012, **23**, 781.
- ¹⁸Karimi-Jaberi, Z.; Zarei, L. *J. Chem. Research*, 2012, **36**, 194.
- ¹⁹Karimi-Jaberi, Z.; Abbasi, S. Z.; Pooladian, B.; Jokar, M. *E. J. Chem.*, 2011, **8**, 1895.
- ²⁰Kiasat, A. R.; Fallah-Mehrjardi, M. *J. Braz. Chem. Soc.* **2008**, *19*, 1595.
- ²¹Sapkal, S. B.; Shelke, K. F.; Shingate, B. B.; Shingare, M. S. *J. Korean. Chem. Soc.* **2010**, *54*, 6.
- ²²Rathod, S. B.; Lande, M. K.; Arbad, B. R.; Gambhire, A. B. *Arab. J. Chem.* **2010**, in Press.
- ²³Tu, S.; Li, G.; Cao, L.; Shao, Q.; Zhou, D.; Xia, M. *J. Comb. Chem.* **2007**, *9*, 1144.
- ²⁴Das, B.; Venkateswarlu, k.; Majhi, A.; Reddy, M, R.; Reddy, k. N.; Roa, Y. K.; Ravikumar, K.; Sridhar, B. *J. Mol. Catal A: Chem.* **2006**, *246*, 276.

Received: 08.01.2013.

Accepted: 16.01.2013.



SELF ASSEMBLING MONOLAYERS OF GLYCINE ON CARBON STEEL

S. Gowri^{[a]*}, J. Sathiyabama^[a], S. Rajendran^[a,b] and J. Angelin Thangakani^[c]

Keywords: Self-assembled monolayers, carbon steel surface, AFM, FTIR, corrosion, deposition method; Glycine

Well-ordered self assembling monolayer's (SAMs) using glycine were formed on the carbon steel surface by immersion method. This leads to ordered, robust monolayers bound to the surface in a bidentate manner. Monolayer formation takes place when carbon steel is immersed in an aqueous solution containing 60ppm of Cl⁻ and 50 ppm of glycine for 5 minutes, and rinsing the physisorbed molecules in distilled water and heating in a hot air oven. The glycine monolayers on iron oxide steel carbon can withstand rinsing with water, concentrated acid and base exposure. Additionally, these monolayers are stable over the course of one week. The formations of monolayers were confirmed by AFM study and FTIR spectra. The results of this study show that glycine monolayers adsorbed on metal surface can reduce electrochemical activity on the surface, often the first step in corrosion.

*Corresponding Authors

*E-mail: divisrigowri@yahoo.in, brigow@yahoo.co.in

- [a] PG and Research Department of Chemistry, Corrosion Research Centre, GTN Arts College, Dindigul-624 005, India.
 [b] Department of Chemistry, RVS School of Engineering and Technology, Dindigul, India. Email: srmjoany@sify.com.
 [c] CEOA Matriculation Higher Secondary School, A Kosakulam, Madurai, India.

Organic acids such as phosphonic,^{13,14-18} carboxylic,^{19,20-23} hydroxamic,²⁴ and sulfuric¹⁶ acids are capable for forming SAMs by chemisorption on stainless steel,^{25,19,26} aluminium,^{20-22,27} titanium^{13,14,17,18} and copper oxide²⁸ surfaces.

Introduction

Nanometer-sized particles are attracting considerable attention because of their unique properties, including optical, electrical, electrochemical, photo-electrochemical and magnetic properties¹⁻³. Noble metals, such as gold and silver, are hot spots of the research because they can be easily prepared and exist steadily. Moreover, we can manipulate these nano-particles according to our will. Much effort has been done in exploring self-assembled (SA) nanoparticles into ordered structures⁴. Specific structures can provide controlled fabrication of nanometer-sized building blocks with distinctive and useful properties⁵. Polymer-stabilized nanoparticles are usually self-assembled into two-dimensional arrays on the substrate⁶. Yiwei Tan et al.⁷ had reported the self-organization of wire-pattern arrays of Ag nanoparticles. Byeong-Hyeok Sohn⁵ had demonstrated a directed self-assembly of two different kinds of nanoparticles on a block copolymer micellar template. These two particles are gold and iron oxide. The self-assembling process has been investigated to improve corrosion inhibition of metals because self-assembled substances are able to react spontaneously on the metal surface and form compact and stable films^[8]. These films can protect metal from corrosion successfully. Iron is a widely used metal with extensive industrial application and the study of its corrosion inhibition has attracted much attention^{9, 10}.

The first work to use self-assembled films on iron for corrosion protection was self-assembling alkanethiols¹¹. But the application of thiol-compounds is limited due to their toxicity¹². Ilona Felhosi et al.^[12] studied the formation of self-assembled films of alkane monophosphonic acids on iron surface and explained its mechanism of corrosion protection.

In the present work, SAMs of glycine were formed on carbon steel surface by immersion coating (immersing metal surface in an aqueous solution containing 60 ppm of Cl⁻, in the absence and presence of 50 ppm of glycine). The modified samples were characterized by FTIR, and atomic force microscopy (AFM). The formation, uniformity, ordering and bonding of the monolayers accomplished by immersion method have been evaluated.

Experimental Section

Material

Very pure glycine of analytical reagent grade was used in the present study.

Preparation of the substrates

Carbon steel substrates (Composition : wt % : 0.026% S, 0.06% P, 0.4% Mn, 0.1% C and the rest Fe) of dimensions 1 x 1 x 0.2 cm were polished to a mirror finish and degreased with trichloroethylene and stored in oven at 100 °C for 1 h or more.

Formation of monolayers

Immersion deposition monolayers

The cleaned substrates were placed in the oven for 24 h. They were then immersed in an aqueous solution containing 60ppm Cl⁻ in the absence and presence of 50ppm of glycine acid for 5 mts and placed in an oven at 100°C for at least 1 h.

Characterization of the monolayers

FTIR

The substrates were studied using a Perkin Elmer 1600 FTIR spectrophotometer. FTIR spectrophotometer was used to analyze the nature of interaction between the molecules of glycine and the substrate and the alkyl chain ordering the νCH_2 peaks as the reference. The film was removed carefully, mixed with KBr and made into pellets. FTIR spectra were recorded.

Atomic force microscopy

The carbon steel specimen immersed in blank and in the inhibitor solution for a period of 5 mts was removed, rinsed with double distilled water, dried and subjected to the surface examination. Atomic force microscopy (Veeco innova model) was used to observe the samples' surface in tapping mode, using cantilever with linear tips. The scanning area in the images was $5\ \mu\text{m} \times 5\ \mu\text{m}$ and the scan rate was 0.6 HZ / second.

Weight-loss method

Carbon steel specimens in triplicate were immersed in 100 mL aqueous solution containing 60 ppm of Cl^- various concentrations for one day. The weight of the specimens before and after immersion was determined using a Shimadzu balance, model AY62. The corrosion products were cleansed with Clarke's solution. The inhibition efficiency (IE) was then calculated using the equation:

$$\text{IE} = 100 [1 - (W_2 / W_1)] \%$$

Where W_1 = corrosion rate in the absence of the inhibitor.

W_2 = corrosion rate in the presence of the inhibitor.

Results

Immersion depositon method

FTIR Spectra

A simple procedure of immersing mild steel into an aqueous solution containing 60 ppm of Cl^- and 50 ppm of glycine for 5 minutes led to spontaneous film formation on the carbon steel surface. There is also possibility of formation of iron-glycine film, in the absence of iron oxide, if there is less corrosion or no corrosion of carbon steel. The samples were characterized by FTIR spectra to determine alkyl chain conformation and head group-substrate bonding^{25, 17}. Position of the CH_2 stretching in the infrared spectrum can be used to determine the ordering of the alkyl chain within a film^{22, 29-31}.

For disordered chains, the frequency of the CH_2 stretching is close to that of a liquid alkane (νCH_2 asym $\sim 2924\ \text{cm}^{-1}$) due to the presence of a gauche conformation in the alkyl chains^{30, 32}. For well-ordered alkyl chains the frequency is shifted to lower wave numbers and is close to that of a crystalline alkyl (νCH_2 asym $\sim 2914 - 2918\ \text{cm}^{-1}$) which is considered to have a high degree of order, with all-trans

conformation throughout the alkyl chain. The FTIR spectrum of pure glycine is shown in Fig 1a. The peaks due to νCH_2 sym appear at $2771\ \text{cm}^{-1}$. The FTIR spectrum of iron oxide film formed on metal surface after immersion in 60ppm Cl^- is shown in Fig 1b. The peaks due to iron oxide appear at $\gamma\text{FeOOH} = 1045, 1590\ \text{cm}^{-1}$; $\alpha\text{FeOOH} = 678\ \text{cm}^{-1}$. The peaks due to Fe_3O_4 are absent. The position of the peaks corresponding to νCH_2 asym and νCH_2 sym after immersion in an aqueous solution containing 60ppm of Cl^- and 50 ppm of glycine for 5 minutes and after rinsing in distilled water to remove any physisorbed material or multilayer's, were $2809\ \text{cm}^{-1}$ and $2722\ \text{cm}^{-1}$, respectively (Fig 1c). This indicates that the film is stable, well ordered and strongly bound to the surface.

The IR spectra further indicate that the organic molecules are bound to the surface in a bidentate manner as determined from the shifting of $\nu\text{C}=\text{O}$ and $\nu-\text{OH}$ stretching of the one carboxyl groups of glycine specifically the $\nu\text{C}=\text{O}$ has shifted from 1590 to $1596\ \text{cm}^{-1}$ and νOH has shifted from 3093 to $3416\ \text{cm}^{-1}$. Similar bidentate interaction has been reported for alkyl phosphonic acid on nickel oxide surface³³ and other organic molecules on other oxides^{25, 19, and 17}.

While FTIR spectroscopy can be used to characterize alkyl chain ordering and binding of the molecules to the surface, it cannot determine film thickness and integrity. Therefore, AFM imaging was used to examine the monolayer at nanometer resolution and to verify that the deposition method produces uniform monolayers.

AFM imaging

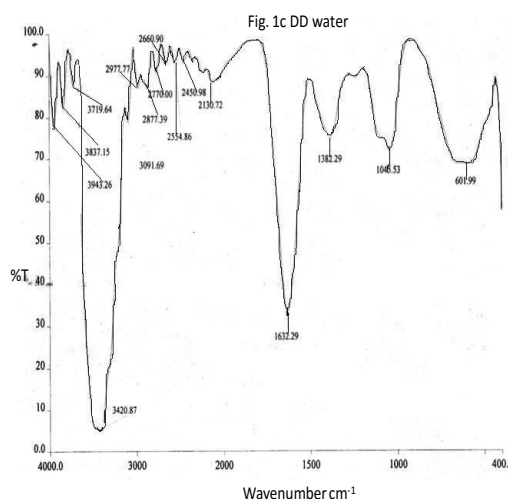
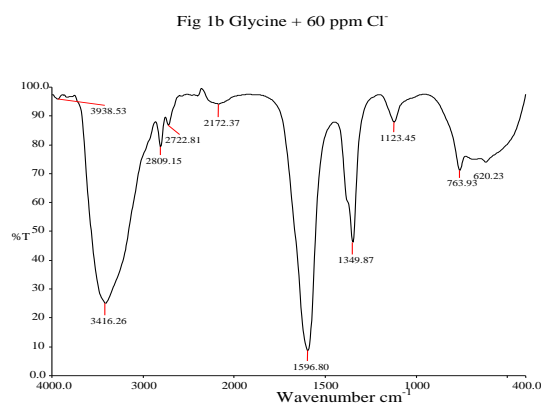
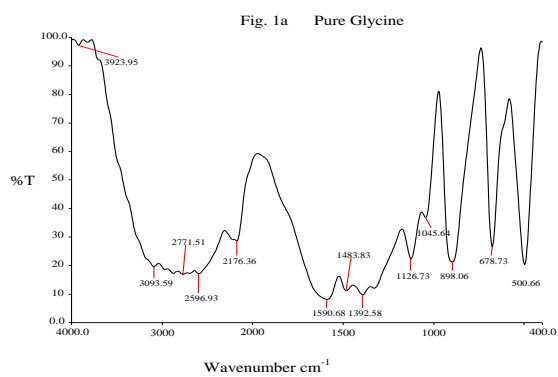
The comparison of the root mean square (rms) roughness of the unmodified substrate to the modified samples is an indicator of the film uniformity. The rms roughness parameter is a measure of the deviations in the surface from the mean plane within the sampling area³⁴.

Modified surfaces with an rms roughness similar to the control surface are considered to be films of monolayer thickness that follow the contour of the surface, while modified surfaces that have much larger rms roughness than the control are multilayer or non-uniform films^{35, 36}.

The iron oxide control samples had an average rms roughness of 12.06 nm (Fig 2a). The control sample of iron oxide is rough in comparison to model surfaces such as gold and silicon^{37, 38}. Modified samples formed by the immersion method (immersed in 60 ppm of Cl^- and glycine had an rms roughness of 4.3806 nm (Fig 2b). The rms roughness of the substrate did not change very much after the adsorption of glycine molecules suggests uniform deposition of the organic molecules on the surface without aggregate or micelle formation. Therefore it is concluded that within the scope of the analysis, the film formed is a single layer of molecules that follows the contour of the underlying substrate.

The rms roughness values of the films (SAMs) formed on metal surface after immersion in various test solutions are given in Table 1.

The IR spectra of the formed films can be seen on Fig.1.



Figur

- glycine
- glycine and 60 ppm chloride
- DD water

Table 1. The rms roughness values of the films (SAMs) formed on metal surface immersed in various test solutions.

Test solution	rms roughness of the films (SAMs), nm
Cl ⁻ 60ppm	12.0558
Cl ⁻ 60ppm + Glycine 50ppm	4.38

The rms value of pure glycine molecule is very low (4.38nm) when compared with the rms value of iron oxide formed in the absence of glycine (12.06 nm). This indicates that glycine molecules are adsorbed on the metal surface before the formation of iron oxide on the metal surface. Suppose glycine molecules adsorbed on iron oxide surface then the rms value will be greater than 12.06. But it is not so. Hence it is concluded that glycine is adsorbed on carbon steel surface and not on iron oxide surface.

Stability of monolayer films

The monolayers formed by deposition method were analyzed for stability. After rinsing in water, the samples were left under atmospheric conditions for one day and analyzed. The monolayers remained ordered and bound to the surface as indicated by the lack of change in the FTIR spectra over one day. Stability to acid and base exposure was tested by rinsing modified substrates 1 M HCl or 1 M NaOH. FTIR spectra taken after these treatments remained unchanged.

Film stability and chain ordering can be dependent on alkyl chain length. In general, stability and order increase as the chain length increases^{39, 40-43}. Therefore, a long chain length (> 11 carbons) is commonly used in the formation of SAMs. Substantial disorder is generally found in films formed by short chain molecules, although ordered monolayers of short chain phosphonic acids have been formed on nitinol, titanium and stainless steel oxide^{25, 17, and 44}. In the present study there are only 3 carbons in the chain (H₂N- CH₂- COOH). However, the monolayer is found to be stable. Further research in this line will confirm the proposed concepts.

These conclusions are confirmed by visual observations also. In the blank experiment (60ppm Cl⁻ only) brown film was observed on the metal. In the presence of 50 ppm of glycine brown film was absent and thin interference films (VIBGYOR colour) were noticed.

Analysis of Weight loss Study

The corrosion inhibition efficiencies of glycine in controlling corrosion of carbon steel in aqueous solution containing 60 ppm of Cl⁻ are given in Table 2. It is observed that the inhibition efficiency increases as the concentration of glycine increases upto 100 ppm. However further increases of concentration of glycine leads to a decrease in IE. This is due to the fact that as the concentration of glycine increases, the iron glycine complex formed on the metal surface goes into solution. Hence IE decreases as the concentration of the glycine increases.

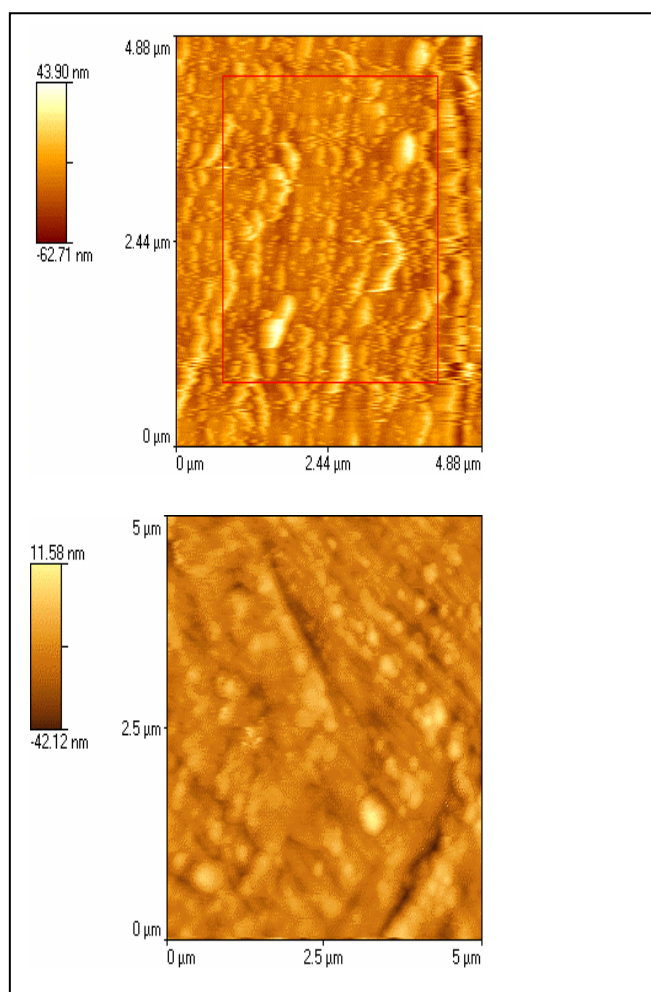


Figure 2. AFM topography images of films formed on carbon steel surface after immerse in in various test solution. Cl⁻ 60ppm; Cl⁻ 60ppm + glycine 50ppm

Discussion

Ordered, complete monolayers of glycine were formed on carbon steel surface. These monolayers were formed using an immersion deposition process. To accomplish monolayer by immersion, a counteraction of 50 ppm of glycine, solution exposure time of 5 minutes and setting temperature of keeping the metal specimens in the oven at 100°C for 1 hr.

Table 2. Inhibition efficiencies of glycine in controlling corrosion of carbon steel in aqueous solution containing 60 ppm of Cl⁻

Glycine (ppm)	Cl ⁻ (60ppm)	
	IE %	CR mmpy
0	-	0.0093
50	70	0.0028
100	75	0.0023
150	65	0.0033
200	60	0.0037

The process of monolayer formation using immersion coating has been described as a sequential process of nucleation, growth and coalescence of densely packed two-dimensional islands, finally covering the entire substrate surface or a large fraction of it^{45, 46-49}.

The average surface coverage for glycine films on iron surface is found to increase monotonically with solution concentration, consistent with a quarter surface density of glycine molecules. It is proposed that the initial islands are nucleated through the adsorption of individual glycine mole from solution^{45, 46, 47}. Therefore a higher concentration of the monomer (100 ppm) in solution leads to more collisions between monomers and subsequent island nucleation becomes more probable leading to a large number of islands on the surface^{46, 50}. For the immersed substrates, increasing the solution concentration leads to the formation of a complete monolayer. When the substrates were heated the bidentate increased, the molecules become thermally mobile and therefore more available for nucleation and / or growth⁵¹.

The molecules in the monolayers formed by immersion method were bound to the carbon steel surface in a bidentate manner. This bonding motif was persistent from deposition through solvent, acid and base rinsing and exposure to atmosphere for one day. A bidentate or monodentate bonding motif is seen between phosphonic acids and various metal oxides such as stainless steel 316L and Zirconium^{25, 17, 44, 52-55}. In the present case, glycine is bonded to carbon steel surface in bidentate manner; since glycine is a monocarboxylic acid and coordination can take place through oxygen atoms of carboxyl groups.

The cause of the differences in bonding motifs has not been determined but may be a function of several factors including oxygen-metal-oxygen distance on the surface, hydroxyl content of the native oxide surface and the coordination sites available on the adsorbate molecules.

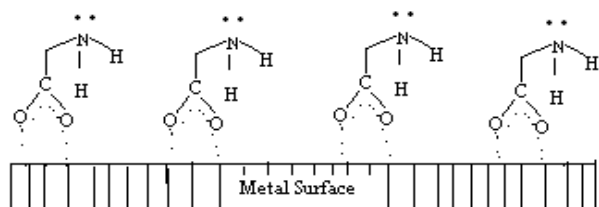
Summary

Well-ordered SAMs using glycine were formed on the oxide of iron carbon steel surface by immersion method. This leads to ordered, robust monolayers bound to the surface in bi dentate manner. Monolayer formation takes place when carbon steel is immersed in an aqueous solution containing 60ppm of Cl⁻ and 50 ppm of glycine for 5 minutes, and rinsing the physisorbed molecules in distilled water and heating in a hot air oven. The glycine monolayers on carbon steel can withstand rinsing with water, concentrated acid and base exposure. Additionally, these monolayers are stable over the course of one week.

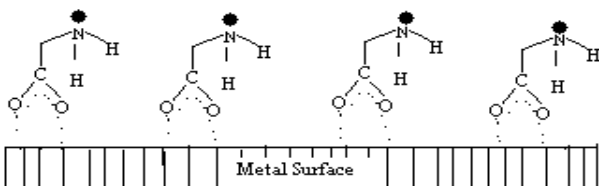
The formations of monolayers were confirmed by AFM study and FTIR spectra. The results of this study show that glycine monolayers adsorbed on metal surface can reduce electrochemical activity on the surface, often the first step in corrosion. Monolayer formation on the carbon steel surface is a significant advance in surface modification of iron oxide and can be used as a building block for future applications in corrosion barriers and electronics.

Scope of the future study

The adsorption of glycine molecule on the carbon steel surface, through the oxygen atoms of the carboxyl group can be represented as follows.



On the nitrogen atom a lone pair of electron is available. On these nitrogen atoms of silver or gold nano particles can be attached if these nanoparticles are generated in *-situ* by suitable methods⁵⁶. Such SAMs containing nano silver or



gold may find applications in biosensors.

● - (Nanometals- Gold or Silver)

References

- ¹Liu, Y.; Juang, L.; *Langmuir* **2004**, *20*, 6591.
- ²Li, X.; Zhang J.; Xu, W.; Jia, H.; *Langmuir*, **2003**, *19*, 4285.
- ³Jana, N. R.; Gearheart, L.; Murphy C. J.; *J. Phys. Chem. B*, **2001**, *105*, 4065.
- ⁴Sun, S.; Murray, C. B.; Weller, D.; Folks, L.; Moser, A.; *science* **2000**, *287*, 1989.
- ⁵Sohn, B. H.; Choi, J. M.; Yoo, S.; Yun, S. H.; *J. Am. Chem. Soc.* **2003**, *125*, 6368.
- ⁶Teranishi, T.; Haga, M.; Shiozawa, Y.; Miyake, M.; *J. Am. Chem. Soc.* **2000**, *122*, 4237.
- ⁷Tan, Y.; Jiang, L.; Li, Y.; Zhu, D.; *J. Phys. Chem. B*, **2002**, *106*, 3131.
- ⁸Wang, C.; Chen, S.; Ma, H.; Qi, C. S.; *J. App. Electrochem.* **2003**, *33*, 179.
- ⁹Lendvay-Gyorik, G.; Meszaros, L.; Meszaros, G.; Lengyel, B.; *Corros. Sci.*, **2000**, *42*, 79.
- ¹⁰Khaled, K. F.; Hackerman, N.; *Electrochim. Acta*, **2003**, *48*, 2715.
- ¹¹Nozawa, K.; Nishihara, H.; Aramaki, K.; *Corros. Sci.* **1997**, *39*, 1625.
- ¹²Felhosi, I.; Teleddi J., Palinkas G., Kalman E., *Electrochim. Acta*, **2002**, *47*, 2335.
- ¹³Gawalt, E. S.; Lu, G.; Bernasek, S. L.; Schwartz J., *Langmuir*, **1999**, *15*, 8929.
- ¹⁴Adden, N.; Gamble, L.J.; Castner, D. G.; Hoffmann, A.; Gross, G.; Menzel, H.; *Langmuir*, **2006**, *22*, 8197.
- ¹⁵Fiurasek, P.; Reven, L.; *Langmuir*, **2007**, *23*, 2857.
- ¹⁶Yee, C.; Kataby, G.; Ulman, A.; Prozorov, T.; White, H.; King, A.; Rafaiovich, M.; Sokolov, J.; Gedanken, A.; *Langmuir* **1999**, *15*, 7111.
- ¹⁷Gawalt, E. S.; Avaltroni, M. J.; Koch, N.; Schwartz, J.; *Langmuir* **2001**, *17*, 5736.
- ¹⁸Zwahlen, M.; Tosatti, S.; Textor, M.; Hahner, G.; *Langmuir* **2002**, *18*, 3957.
- ¹⁹Raman, A.; Gawalt, E.S.; *Langmuir* **2007**, *23*, 2284.
- ²⁰Vanden Brand, J.; Blajiev, O.; Beentjes, P. C. J.; Terryn, H.; De Wit, J. H. W.; *Langmuir* **2004**, *20*, 6308.
- ²¹Lim, M. S.; Feng, K.; Chen, X.; Wu, N.; Raman, A.; Nightingale, J.; Gawalt, E. S.; Korakakis, D.; Hornak, L. A.; Timperman, A.T.; *Langmuir* **2007**, *23*, 2444.
- ²²Allara, D. L.; Nuzzo, R. G.; *Langmuir*, **1985**, *1*, 45.
- ²³Hustak, G.; Domb A. J.; Mandler, D.; *Langmuir*, **2004**, *20*, 7499.
- ²⁴Folkers, J. P.; Gorman, C. B.; Laibinis, P. E.; Buchholz, S.; Whitesides, G. M.; Nuzzo, R. G.; *Langmuir*, **1995**, *11*, 813.
- ²⁵Raman, A.; Dubey, M.; Gouzman, I.; Gawalt, E.S.; *Langmuir*, **2006**, *22*, 6469.
- ²⁶Shustak, G.; Domb, A. J.; Mandler, D.; *Langmuir* **2004**, *20*, 7499.
- ²⁷Brukman, M. J.; Marco, G. O.; Dunbar, T. D.; Boorman, L. D.; Carpick, R. W.; *Langmuir*, **2006**, *22*, 3988.
- ²⁸Sung, M. M.; Sung, K.; Kim, C.G.; Lee, S. S.; Kim, Y.; *J. Phys., Chem., B*, **2000**, *104*, 2273.
- ²⁹Snyder, R. G.; Struss, H. L.; Elliger, C. A.; *J. Phys. Chem*, **1982**, *86*, 5145.
- ³⁰Helmy, R.; Fadeev, A. Y.; *Langmuir*, **2002**, *18*, 8924.
- ³¹Strauss, R. G. S. H.; *J. Phys. Chem.* **1982**, *86*, 5146.
- ³²Nuzzo, R. G.; Dubois, L.H.; Ilang, D. L.; *J. Am. Chem. Soc.* **1990**, *112*, 558.
- ³³Rosalynn Quinones, Aparna Raman and Ellen, S.; Gawalt, *Thin Solid Films*, **2008**, *516*, 8774.
- ³⁴Jerome Workman, J.; Koch, M.; Veltkamp, D.J.; *Anal. Chem.* **2003**, *75*, 2859.
- ³⁵Quinones, R.; Raman, A.; Gawalt, E.S.; *Surf. Interface Anal.* **2007**, *39*, 593.
- ³⁶Faucheux, A.; Gouget-Laemmet, A. C.; Villeneuve, C.H.d.; Boukherroub, R.; Ozanam, F.; Allongue, P.; Chazalviel, J.-N.; *Langmuir* **2006**, *22*, 153.
- ³⁷Ederth, T.; Claesson, P.; Liedberg, B.; *Langmuir* **1998**, *14*, 4782.
- ³⁸Ishizaki, T.; Saito, N.; SunHyng, L.; Ishida, K.; Takal, O.; *Langmuir*, **2006**, *22*, 9962.
- ³⁹Bain, C. D.; Whitesides, G. M.; *Science*, **1987**, *40*, 62.
- ⁴⁰Xiao, X.; Hu, J.; Charych, D. H.; Salmeron, M.; *Langmuir*, **1996**, *12*, 235.
- ⁴¹Touwslager, F. J.; Sondag, A. H. M.; *Langmuir* **1994**, *10*, 1026.
- ⁴²Wolf, K.V.; Cole, D.A.; Bernasek, S.L.; *Anal. Chem.* **2002**, *74*, 5009.
- ⁴³Voue, M.; Rioboo, R.; Adao, M. H.; Conti, J.; Bondar, A. I.; Ivanov, D. A.; Blake, T. D.; DeConinck, J.; *Langmuir*, **2007**, *23*, 4695.
- ⁴⁴Quinones, R.; Gawalt, E. S.; *Langmuir*, **2007**, *23*, 10123.
- ⁴⁵Neves, B. R. A.; Salmon, M. E.; Russell, P.E.; Troughton, J. E. P.; *Langmuir* **2001**, *17*, 8193.
- ⁴⁶Doudevski, I.; Heyes, W. A.; Schwartz, D. K.; *Phys. Rev. Lett.* **1998**, *81*, 4927.
- ⁴⁷Schwartz D. K., *Annu. Rev.* **2001**, *52*, 107.
- ⁴⁸Woodward, J. T.; Ulman, A.; Schwartz, D. K.; *Langmuir*, **1996**, *12*, 3626.
- ⁴⁹Woodward, J. T.; Doudevski, L.; Sikes, H. D.; Schwartz, D. K.; *J. Phys. Chem., B* **1997**, *101*, 7535.
- ⁵⁰Doudevski, I.; Schwartz, D. K.; *J. Am. Chem. Soc.* **2001**, *123*, 6867.

- ⁵¹Neves, B. R. A.; Salmon, M. E.; Rusell, P.E.; Troughton, J. E. B.; *Langmuir*, **2000**, *16*, 2409.
- ⁵²Snyder, R. G.; Struss, H. I.; Elliger, C. A.; *J. Phys. Chem* **1982**, *86*, 5145.
- ⁵³Pawsey, S.; McCormick, M.; De Paul, S.; Graf, R.; Lee, Y.S.; Reven, L.; Spiess, H. W.; Am, J.; *Chem. Soc.* **2003**, *125*, 4174.
- ⁵⁴Schwartz, J.; Avaltroni, M. J.; Danahy, M. P.; Silverman, B. M.; Hanson, E. I.; Schwarzbauer, J. E.; Midwood, K. S.; Gawalt, E. S.; *Mater. Sci. Eng.*, **2003**, *23*, 395.
- ⁵⁵Gao, W.; Dickinson, L.; Grozinger, C.; Morin, F.G.; Reven, I.; *Langmuir*, **1996**, *12*, 6429.
- ⁵⁶Brindha, G.; Suganthi, A.; Rajendran, S.; Satyabama, P. and Robert Kennedy, Z.; *Elixir Nano Tech.*, **2012**, *50*, 10585.

Received: 29.12.2012.

Accepted: 18.12.2012.



APPLICATION OF POLYANILINE /SAWDUST COMPOSITE FOR REMOVAL OF ACID GREEN 25 FROM AQUEOUS SOLUTIONS: KINETICS AND THERMODYNAMIC STUDIES

Reza Ansari^{[a]*} and Hamid Dezhmpanah^[b]

Keywords: Acid green 25, Removal, sawdust, polyaniline, isotherm, kinetics, thermodynamic

This research deals with the application of polyaniline coated onto wood sawdust (PAni/SD) for the removal of anionic or acidic dyes from aqueous solutions. Acid Green 25 (AG25) was selected as test probe throughout of the current investigation as a typical anionic dye. Adsorption experiments were carried out using batch system in order to do equilibrium adsorption isotherm, kinetics and thermodynamic studies. The results indicated that unmodified wood sawdust is a very poor adsorbent for anionic dyes, but when coated by polyaniline (PAni/SD), it is changed into a very efficient adsorbent material for adsorption of AG25 from aqueous solutions. It was found that chemical modification of agricultural wastes such as sawdust with polyaniline is led to a great enhancement in anionic dye removal efficiency. The findings seem to be important for application of the introduced biocomposite of polyaniline as an efficient new nonconventional adsorbent in dye removal technology.

*Corresponding Authors

E-mail: ransari@guilan.ac.ir

Tel: +98-1313243630-4 (Ext. 226)

Fax: +98-131-3233262

[a,b] Chemistry Department, Faculty of Science, University of Guilan, Rasht, Iran, POB: 41635-1914

Introduction

To remove dyes and other colored contaminants from wastewaters, several physical, chemical, physico-chemical and biological such as coagulation and flocculation, membrane separation, different advance oxidation processes, ozonations, electro-coagulation, and adsorption.¹⁻⁵ Among these methods, adsorption currently appears to offer the best potential for overall treatment methods have been developed.⁶ Therefore, in recent years, considerable attention has been devoted to the study of different types of low-cost inorganics, biomaterials and agricultural wastes or byproducts for removal of dyes or other toxic materials such as heavy metals from aqueous solutions.⁷⁻¹⁵ In any adsorption process, the interactions between adsorbent and adsorbates arises from different intermolecular interactions such as Van der Waals forces, hydrophobic forces, H-bonding, ion exchange, dipole-dipole interactions and chemical bonds. However, it has been well established that the biomaterials by themselves or without modification have limited sorption performance. So, in order to enhance their sorption capacity, there is a need to do a suitable chemical modification. The first step in interpreting the adsorption data for describing the performance of a given adsorbent or comparing the performance of two or more adsorbents is to plot an adsorption isotherm that will describe the equilibrium distribution of solute between the solid and liquid phases.

In the present paper sawdust was employed as a very cheap and environmentally friendly substrate for chemical modification (coating) before adsorption experiments. Polyaniline (PAni) was employed for coating or modification of sawdust. Based on our previous study, it has been found that conducting polymers such as polypyrrole,

polyaniline and polythiophene can efficiently improve the sorption capacity of sawdust toward various dyes.¹⁶⁻¹⁹ The effects of different system variables such as adsorbent dose, initial dye concentration, pH of test solution, temperature, and contact time have already been studied and the optimized conditions obtained were used for the current isotherm, kinetics and thermodynamic studies.¹⁸ The current investigation is mainly focused on isotherm, kinetics and thermodynamic studies carried out on the modified sawdust by polyaniline (PAni/SD). Due to the nature of the various reactive functional groups in agricultural wastes (e.g. chelating or ion exchange properties), they are mostly useful for uptake of cationic species such as heavy metal ions or cationic dyes from aqueous solutions.¹⁶ On the other hand unmodified or raw sawdust is a very poor sorbent for removal of anionic dyes. So, the aim of this work is to improve sorption characteristics of sawdust via chemical modification using polyaniline. Sawdust was found a proper choice because it is available as plentiful and almost free of charge. It was also found a suitable substrate for sorption of aniline in acidic media and then for subsequent in-situ polymerization for preparing a novel biocomposite adsorbent for dye removal.

Experimental

Materials and methods

All the chemicals were used were analytical reagents grade and were prepared in distilled water. Sawdust samples (SD) prepared from Narra wood was obtained from a local carpentry workshop. Aniline was obtained from Merck and distilled before use. A single beam Perkin-Elmer UV-Vis spectrophotometer with a 1 cm cell was used for measuring all of absorption data. A Metrohm pH meter (Model 827) with a combined double junction glass electrode was used for pH measurements. pH adjustments were carried out using dilute NaOH and HCl solutions. Acid green dye termed as AG25 (chemical formula= $C_{28}H_{20}N_2Na_2O_8S_2$, MW= 622.58 g mol⁻¹) was employed as a typical anionic

acidic dye for the current investigation (Fig. 1). An accurately weighed quantity (1.0 g) of AG25 was dissolved in double distilled water to prepare stock solution of 100 mg L⁻¹. Experimental solutions of the desired concentrations were prepared by dilution of stock solution with double-distilled water.

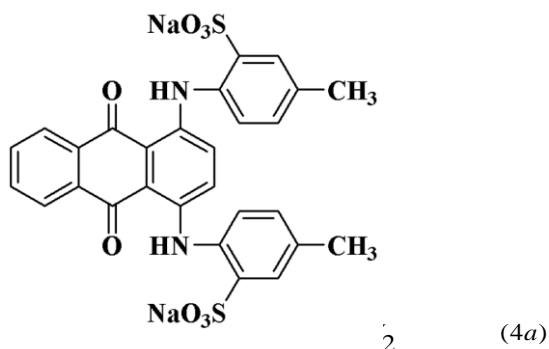


Figure 1. Chemical structure of AG25 dye.

$$m_2 = C_e V_2 \quad (4b)$$

The analysis of test dye solutions for AG25 was carried out spectrophotometry using a UV-vis spectrophotometer at a wavelength corresponding to the maximum absorbance of the dye ($\lambda_{max}=642$ nm). Calibration curve was plotted based on absorbance versus concentration of the dye solution at maximum wavelength of the dye using Beer's law ($A=\epsilon bc$).

Preparation of polyaniline coated sawdust (PAni/SD)

In order to prepare polymer coated onto sawdust (termed as PAni/SD), 10.0 g sawdust (35-50 mesh) immersed in 100 mL of 0.20 M freshly distilled aniline solution for 12 h before polymerization.¹⁸ The excess of the monomer solution was removed by simple decantation. 50 mL of oxidant solution [(0.20 M) (NH₄)₂S₂O₈] was added into the mixture gradually, and the reaction was allowed to continue for 5 h at room temperature. Polymer coated sawdust (PAni/SD) was filtered, washed with sufficient distilled water, and then was dried in an oven at temperature about 60 °C before use.

Adsorption experiments

Batch equilibrium studies were carried out by adding a fixed amount of the sorbent into 250 mL Erlenmeyer flasks containing 50.0 mL of different initial concentrations (20-100 mg L⁻¹) of dye solution at the optimised pH value that has previously been found to be about 2.0.¹⁸ The flasks were agitated in a mechanical shaker at 100 rpm at room temperature for 60 min. At the end of pre-determined time intervals, adsorbent was removed by simple filtration. The filtrates were analyzed for the residual (unadsorbed) concentration of AG25 dye. The following equations were used to calculate the percentage of sorption (φ) and the amount of adsorbed AG25,

$$\varphi = \frac{(C_o - C_e)}{C_o} \times 100 \quad (1)$$

$$\frac{x}{m_1} = \frac{(C_o - C_e)V_1}{m_1} \quad (2)$$

respectively:

where

C_o and C_e are the respective initial (inlet) and equilibrium (outlet) concentrations (mg L⁻¹) of AG25;

$$\xi = \frac{m_2}{m_o} \times 100 \quad (3)$$

X/m_1 is the amount of

AG25 adsorbed onto unit amount of the adsorbent (mg g⁻¹) at equilibrium;

V_1 is the volume of the test solution used in the adsorption experiment (L).

Alternatively, regeneration of the used adsorbent was also examined (Eqs. 3, 4).

where,

ξ is the desorption, in %,

m_o is the initially adsorbed AG25 dye (mg) onto adsorbent

m_2 is the released dye or the concentration of AG25 in the regenerated solution (mg)

V_2 is the volume (L) of the eluent or washing solution.

Adsorption isotherm

In this study in order to facilitate estimation of the adsorption capacities the two well-known equilibrium adsorption models, Freundlich and Langmuir, were employed for the treatments of the equilibrium adsorption data.^{20,21} The Langmuir isotherm is a semi-empirical isotherm derived from a proposed kinetic mechanism. Langmuir assumed that a surface consists of a given number of equivalent sites where a species can stick on the surface of a solid adsorbent through van der Waals' interactions (called physisorption) or through the formation of covalent bonds (called chemisorptions). The Langmuir model is represented by Eq. (5):

$$q_e = \frac{Q_o b C_e}{1 + b C_e} \quad (5)$$

Eq. (5) can be rearranged to linear form:

$$\frac{C_e}{q_e} = \frac{1}{Q_0 b} + \left(\frac{1}{Q_0}\right) C_e \quad (6)$$

where,

q_e is the amount sorbate adsorbed per unit mass of adsorbent (mg g^{-1}),

Q_0 is the maximum amount sorbed (mg g^{-1}) when the monolayer is complete,

b is Langmuir's constant related to the affinity of binding sites and is a measure of the energy or enthalpy of adsorption (L mg^{-1}).

The magnitude of b quantifies the relative affinity that a given solute has for surface adsorption. Like all equilibrium constants, b is temperature dependent. A linearized plot of C_e/q_e against C_e gives Q_0 and b values. Values of Q_0 and b were calculated from the slopes ($1/Q_0$) and intercept ($1/bQ_0$) of the linear plots. Another widely used equation in adsorption processes is the Freundlich equation. The Freundlich isotherm is the earliest known relationship describing the sorption equation. This fairly satisfactory empirical isotherm can be used for non-ideal sorption that involves heterogeneous sorption and is expressed by the following equation:

$$q_e = \frac{x}{m} = k_f C_e^{1/n} \quad (7)$$

Eq. (7) can be rearranged to linear form:

$$\lg \frac{x}{m} = \lg k_f + \frac{1}{n} \lg C_e \quad (8)$$

where,

x/m is the equilibrium adsorption capacity (mg g^{-1}),

C_e is the equilibrium or residual concentration (mg L^{-1}) of AG25 dye in solution, K and n are empirical constants for each adsorbent-adsorbate pair at a given temperature indicating sorption capacity of adsorbent and intensity of adsorption [$(\text{mg g}^{-1} (\text{g L}^{-1})^n)$], respectively.

$1/n$ is the heterogeneity factor and a relatively slight slope and hence a small value of $1/n < 1$ indicates that, the sorption system is favourable and good over entire range of concentration investigated. While values close to or even 1.0 indicate materials with relatively homogenous binding sites. A high value of K_f also indicates a high adsorption capacity of an adsorbent. The adsorption isotherms using both Langmuir and Freundlich equations (linear forms) obtained for removal of AG25 have been depicted in Figs. 2 and 3

respectively.

Figure 2. Langmuir isotherms for the sorption of AG25 by PAni/SD.

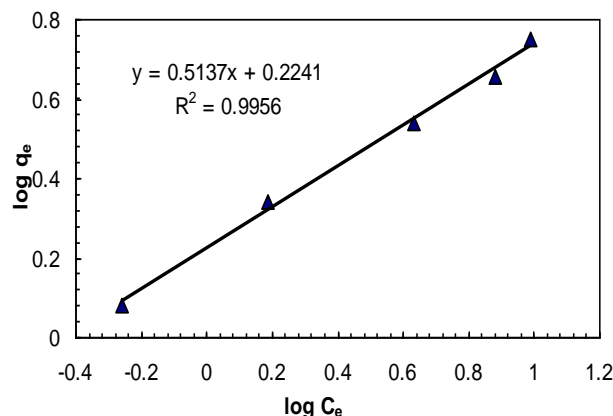


Figure 3. Freundlich adsorption isotherms for the sorption of AG25 by PAni/SD. (Conditions: amount of adsorbent= 0.80 g, $C_0 = 20\text{--}100 \text{ mg L}^{-1}$, time = 60 min, $\text{pH}=2$).

The Langmuir and Freundlich isotherm constants obtained from the related linear equations are summarized in Table 1. The correlation coefficients (R^2) indicate that both Langmuir and Freundlich equations were satisfactory, but the Langmuir isotherm fits the equilibrium data better which confirms chemisorption mechanism during dye removal. The value of n confirms that the adsorption system is suitable. For a suitable adsorption system the value of n is usually between 1 and 10 which implies that the surface of adsorbent is heterogeneous in nature. All the experiments were carried out in triplicate at each condition whose mean values with maximum RSD was less than 1% are presented.

The essential characteristics of a Langmuir isotherm can be expressed in terms of a dimensionless separation, the type of isotherm and is defined by the following equation:

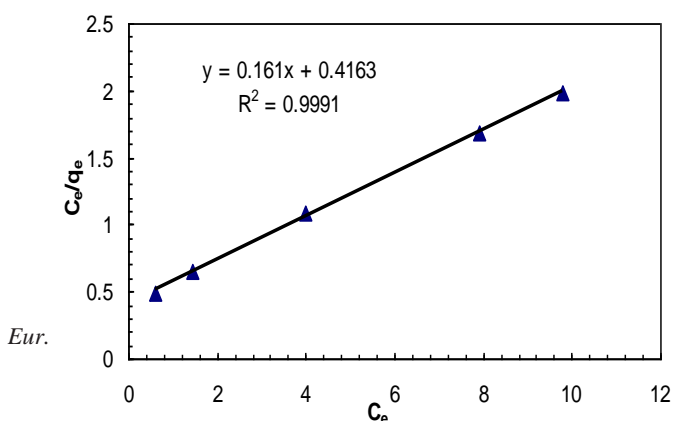
$$R_L = \frac{1}{1 + bC_0} \quad (9)$$

where,

b (L mg^{-1}) is the Langmuir constant and C_0 is the initial dye concentration (mg L^{-1}). The value of R_L indicates the shape of the isotherms to be either unfavorable ($R_L > 1$), linear ($R_L = 1$), favorable ($0 < R_L < 1$) or irreversible ($R_L = 0$).²² As observed, R_L factor value is changing from 0.025 to 0.11 for different dye concentrations of 20–100 (mg L^{-1}) that indicates favourable adsorption, since it is lying between 0 and 1.

Adsorption kinetics

A study of kinetics of adsorption is desirable as it provides information about the mechanism of adsorption, which is important for efficiency of the process. The kinetic data of adsorption can be evaluated using different types of mathematical models, of which the one most widely used is the Lagergren's rate equation.²³ The kinetics of the



adsorption process was analyzed using the pseudo-first-order rate equation as given below (Eq.10):

$$\lg(q_e - q_t) = \lg(q_e) - \frac{K_1 t}{2.303} \quad (10)$$

Freundlich isotherm parameters				Langmuir isotherm parameters		
Adsorbent	K_F (mg g ⁻¹)(g L ⁻¹) ⁿ	n	R^2	Q_o (mg g ⁻¹)	b (L mg ⁻¹)	R^2
PAni/SD	1.67	1.95	0.9952	6.21	0.38	0.9991

Table 1. Freundlich and Langmuir isotherms constants for adsorption of AG25 onto PAni/SD

where,

q_t and q_e (mg g⁻¹) are the amounts of dye adsorbed per unit mass of the adsorbent at time t and at equilibrium, respectively.

k_1 (min⁻¹) is the pseudo-first-order rate constant of adsorption.

As the Eq. (10) shows, there is a linear relationship between $\lg(q_e - q_t)$ and t . The slope of the plot $\lg(q_e - q_t)$ versus t gives the value of K_1 and the value of q_e can be calculated from intercept (Fig.4).

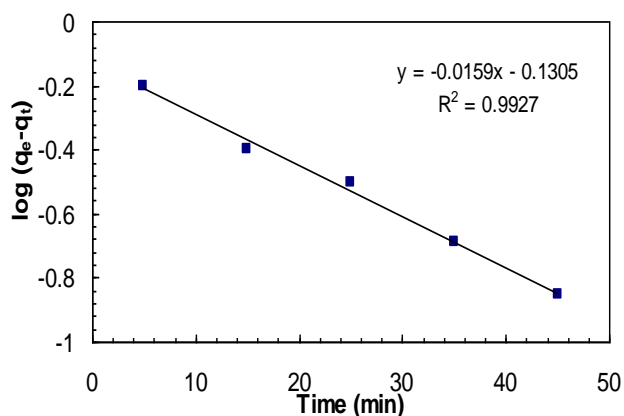


Fig. 4. The pseudo-first-order kinetics for the sorption of AG25 by PAni/SD. (Conditions: $m = 0.80$ g, $C_o = 50$ mg L⁻¹, pH= 2).

Kinetic data were further applied to the pseudo-second-order kinetic model proposed by Ho and McKay.²⁴ The differential equation has the following form:

$$\frac{t}{q_t} = \frac{1}{K_2 q_e^2} + \left(\frac{1}{q_e}\right)t \quad (11)$$

where,

K_2 is the second order rate constant (g mg⁻¹ min⁻¹).

The plot of t/q_t versus t should give straight lines where slopes and intercepts are respectively $1/q_e$ and $1/K_2 q_e^2$ (Fig.5). The values of the rate constant K_2 and of the equilibrium sorption capacity q_e are calculated from these parameters. The values of rate constants and correlation coefficients for these kinetic models are also shown in Table 2.

As the correlation coefficients calculated for the second order kinetic model ($R^2=0.998$) and also the good agreement

of calculated $q_{e2,calc.}$ (3.04) and experimental $q_{e,exp.}$ (2.95) values indicate, the adsorption system follows the pseudo second order kinetic model and a chemisorption mechanism is therefore suggested.

Table 2. Kinetic parameters for the adsorption of AG25 by PAni/SD

First-order kinetic model				Second-order kinetic model		
$q_{e,exp}$ mg g ⁻¹	K_1 min ⁻¹	$q_{e1,calc.}$ mg g ⁻¹	R^2	K_2 mg ⁻¹ min ⁻¹	$q_{e2,calc.}$ mg g ⁻¹	R^2
2.95	0.037	0.74	0.9927	0.12	3.04	0.9981

Adsorption thermodynamics

In understanding better the effect of temperature on the adsorption, it is important to study the thermodynamic parameters such as standard Gibbs free energy change, standard enthalpy, and standard entropy. The Gibbs free energy of adsorption by using equilibrium constant (K_c) is calculated from the following equation.²⁵

$$\Delta G^O = -RT \ln K_c \quad (13)$$

$$\Delta G^O = \Delta H^O - T\Delta S^O \quad (14)$$

Standard enthalpy change (ΔH^O) and standard entropy change (ΔS^O), of adsorption can be estimated from van't Hoff equation given in:

$$\ln K_c = \frac{-\Delta H^O_{ads}}{RT} + \frac{\Delta S^O}{R} \quad (15)$$

where,

T is absolute temperature

R is the gas constant (8.314 J mol⁻¹ K⁻¹),

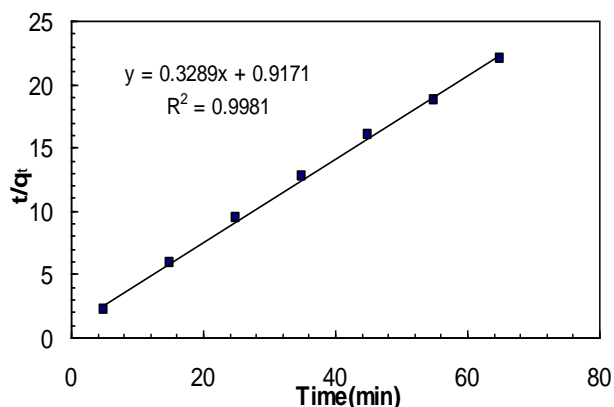
K_c is adsorption equilibrium constant.

The K_c value is calculated from the Eq. (16):

$$K_c = \frac{C_{Ae}}{C_{Se}} \quad (16)$$

where

C_{Ae} is the amount of dye adsorbed on the adsorbent per liter of the solution at equilibrium (mg L^{-1}); C_{Se} is the equilibrium concentration of the dye in the solution (mg L^{-1}).



The plot of $\ln K_c$ against $1/T$ (K^{-1}) should be linear.

Figure 5. The pseudo-second-order kinetics for the sorption of AG25 by PAni/SD. (Conditions: $m=1.0$ g, $C_o = 50 \text{ mg L}^{-1}$, $\text{pH}= 2$).

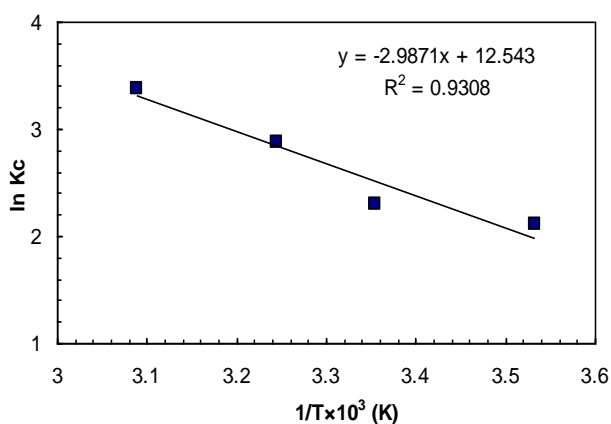


Figure 6. Plot of $\ln k_c$ against reciprocal temperature for the adsorption of AG25 by PAni/SD. (Conditions: $m=0.80$ g, $C_o=50.0 \text{ mg L}^{-1}$, $t = 60$ min, $\text{pH}=2$).

The slope of the van't Hoff plot is equal to, and its intercept is equal to. The van't Hoff plot for the adsorption of AG25 onto PAni/SD is given in Fig. 6.

Thermodynamic parameters obtained are given in Table 3. As shown in the table 3, the negative values of ΔG° at different temperatures indicate the spontaneous nature of the adsorption process. The decrease in ΔG° with rise in temperature indicate that better sorption of dye is obtained at a higher temperature. The positive value of ΔS° also indicates the increased randomness during the uptake of AG25 dye onto PAni/SD particles and reflects the affinity of the PAni/SD for AG25 dye. With displacement of the adsorbed water molecules by the dye molecules, more

translational entropy is gained, thus allowing the prevalence of randomness in the system. Positive value of ΔH° reveals endothermic nature of adsorption and it governs the possibility of physical adsorption. In physisorption ($\Delta H \sim 5 \text{ cal mol}^{-1}$) electrostatic attractions are the basic physical forces in most adsorption reactions (e.g. dipole-dipole, dispersion, London-van der Waals and H-bonding). Chemisorptions ($\Delta H=10-100 \text{ kcal mol}^{-1}$) involve the formation of strong chemical bonds between adsorbates and specific surface locations known as chemically active sites.

Table 3. Thermodynamic parameters for the adsorption of AG25 by PAni/SD

T, K	K_c	ΔG° , kJ	ΔH° , kJ	ΔS° , J K^{-1}
283	8.3	-4.8	+24.8	+104.3
298	9.3	-5.5		
308	18.0	-7.4		
328	29.4	-9.1		

The entropy change ($\Delta S^\circ=104.3 \text{ J/K}$) means that adsorption or removal of anionic dye of AG25 onto PAni/SD corresponds to a increase in entropy and suggests the increased randomness at the solid/liquid interface during adsorption. Hydrophobic interactions are hypothesized to result in greater overall system entropy. So, hydrophobic interactions played a dominant role in the adsorption of AG25 by PAni/SD.

Conclusions

PAni/SD can be simply prepared via direct chemical synthesis of aniline monomer on the surface of biomaterial wastes. The polyaniline/sawdust composite can be efficiently employed for anionic dye removal under acidic conditions. Among the parameters investigated, pH of dye solution has a profound effect on dye uptake by both treated and unmodified sawdust. Both adsorbents are more effective for anionic dye removal under acidic conditions. From the kinetic and thermodynamic investigations, it was found that the AG25 dye removal by PAni/SD is occurred mostly via chemisorption process and the adsorption is spontaneous. Since the enthalpy change is positive, so it could be concluded that the sorption process is endothermic. Positive value of entropy indicates that the entropy and the hydrophobic forces are the driving force for AG25 dye removal by the introduced adsorbent.

Acknowledgment

The authors wish to acknowledge the financial support provided by the Postgraduate Studies of University of Guilan, Iran.

References

- Panswed, J., Wongchaisuwan, S., *Water Sci. Technol.*, **1986**, *18*, 139.
- Ciardelli, G., Corsi, L., *Resour. Conserv. Recycl.*, **2000**, *31*, 189.
- Marechal, M. L., Slokar, Y. M., Taufer, T., *Dyes and Pigments*, **1997**, *33*, 281.

- ⁴ Reynolds, G., Graham N., Perry, R., Rice, R. G., *Ozone Sci. Eng.* **1989**, *11*, 3392.
- ⁵ Alinsafi, A., Khemis, M., Pons, M. N., Leclerc, J. P., *Chem. Eng. Process*, **2005**, *44*.
- ⁶ Mohammad-Khah, A., Ansari, R., *Int. J. Chem. Techn. Res.*, **2009**, *1 (4)*, 859.
- ⁷ Pradhan, J., Das S. N., Thakur R. S., Rao S. B., *J. Coll. Interface Sci.*, **1999**, *217*, 137.
- ⁸ Asyhar, R., Wichmann, H., Bahadir M., Cammenga H. K., *Fresen. Environ. Bull.*, **2002**, *11*, 270.
- ⁹ Dogan, M., Alkan, M., Onganer, Y., *Water Air Soil Pollut.*, **2000**, *120*, 229.
- ¹⁰ Chang, J. S., Chou, C. Y., Lin, C., Lin, P. J., Ho, J. Y., *Water Res.*, **2001**, *35*, 2841.
- ¹¹ Chu, W., *Water Res.*, **2001**, *35(13)*, 3147.
- ¹² Meshko, V. Markovska, L. Mincheva, M. Rodrigues, A. E., *Water Res.*, **2001**, *35 (14)*, 3357.
- ¹³ Wu, F. C. Tseng, R. L., Juang, R. S., *J. Chem. Technol. Biotechnol.*, **2002**, *77*, 1269.
- ¹⁴ Robinson, T., Chandran, B. Nigam, P., *Environ. Int.*, **2002**, *28*, 29.
- ¹⁵ Mall, I. D., Srivastava, V. C., Agarwal, N. K., Mishra, I. M., *Chemosphere*, **2005**, *61*, 492.
- ¹⁶ Ansari, R., and Mosayebzadeh, Z., *J. Iran. Chem. Soc.*, **2010**, *7(2)*, 339.
- ¹⁷ Ansari, R., Mosayebzadeh, Z., *Iranian Polym. J.*, **2010**, *19 (7)*, 541.
- ¹⁸ Ansari, R., Alaie, S., and Mohammad-khah, A., *J Sci Ind Res.*, **2011**, *70*, 804.
- ¹⁹ Ansari, R., Mosayebzadeh Z., keivani M. B., Mohammad-khah A., *J. Adv. Sci. Res.*, **2011**, *2(2)*, 27.
- ²⁰ Freundlich, H. M. F., *Z. Phys. Chem.*, **1906**, *57A*, 385.
- ²¹ Langmuir, I., *J. Am. Chem. Soc.*, **1918**, *40*, 1361.
- ²² Hall, K. R., Eagleton, L. C., Acrivos, A., Vermeulen, T., *Ind. Eng. Chem. Fundament.*, **1966**, *5*, 212.
- ²³ Lagergren, S., *Kung. Sven. Vetenskapsak. Handl.*, **1898**, *24*, 1.
- ²⁴ Ho, Y. S., McKay, G., *Process Biochem.*, **2009**, *34*, 451.
- ²⁵ Lian, L., Guo, L., Guo, C., *J. Hazard. Mater.*, **2009**, *161*, 126.

Received: 10.01.2013.

Accepted: 18.01.2013.



ASSESSMENT OF ABILITY OF THREE CHEMICAL OXIDANTS TO REMOVE HYDROCARBONS FROM SOILS POLLUTED BY BONNY LIGHT CRUDE OIL.

Ozioma Achugasim^[a], Chukwunonye Ojinnaka^[a], Leo Osuji^[a]

Keywords: Permanganates; Persulfates; Fenton's reagent; Bonnylight crude oil; Soil remediation; Chemical oxidants.

Three prominent hydrocarbon groups found in crude oil- Polycyclic Aromatic Hydrocarbon (PAH); Benzene, Toluene, Ethylbenzene and Xylene (BTEX) and Total Petroleum hydrocarbon (TPH) were used to study the ability of three chemical oxidants-Fenton's reagent, potassium permanganate, and potassium persulfate to degrade hydrocarbons in crude oil inundated soils. This was done by spiking soil samples with Bonny light crude oil and subsequently treating the mixture with the different chemical oxidants at acidic, neutral and basic pH media for each of the oxidants. Oil extracts from the treated and untreated soil samples were later analyzed for the three hydrocarbon groups using a gas chromatograph (GC). Treatment with Fenton's reagent proved very efficient in the removal of the hydrocarbons especially at the acidic pH with some components of TPH experiencing complete disappearance. Also the four ringed-PAHs were depleted more than the three ringed- ones at the indicated pHs. For the treatment with potassium persulfate, while the oxidant was good in the removal of BTEX at the different pHs, it was found to be very inefficient for the removal of PAHs. Generally, Four and five ringed-PAHs were degraded more than the three and two ringed-PAHs, an indication that degradation of PAHs by oxidants may be a function of hydrocarbon structure. Treatment with potassium permanganate was found to be pH dependent with most of the depletions occurring at acidic pH. Even though potassium permanganate was not as good as the other oxidants in the removal of aliphatic hydrocarbons(TPH), it was found to be effective in the removal of aromatic hydrocarbon (BTEX and PAH). Also the four ringed-PAHs such as pyrene, benzoanthracene, and chrysene were seriously attacked at all pHs. BTEX was also attacked more at acidic pH with above 90% removal at the acidic pH.

*Corresponding Authors

Tel.: +2348033770425.

E-mail: Ozioma.Achugasim@uniport.edu.ng

[a] Department of Pure and Industrial Chemistry, University of Port Harcourt.

Introduction

The most serious environmental problem facing oil producing provinces especially in the Niger Delta is soil pollution by crude oil. Whenever crude oil is released on the terrestrial environment, it usually overwhelms the soil ecosystem leading to soil contamination/pollution that kills plants and animals giving rise to serious imbalance in the ecosystem.¹ Closely following any incidence of oil spillage are settlement of the affected stakeholders and remediation of the polluted site.² Several methods are used in the remediation of crude oil polluted soils. These methods may be physical, biological or chemical.³ The physical and biological methods have been in use for years while the chemical methods have received attention in the last decade or so.⁴ The chemical method of remediation involves the use of chemicals to convert the contaminants (hydrocarbons) into harmless substances. The chemicals normally used are oxidants. These includes peroxides, ozone, persulfate, Fenton's reagent (hydrogen peroxide plus iron(II) salts), permanganates, perchlorates etc, which act to generate reactive species e.g free radicals that converts the hydrocarbons into innocuous substances. The advantage of chemical methods over other methods mentioned above is that it is very fast and highly efficient. Also it can be bench or pilot tested to determine its applicability for a particular contaminant.⁵⁻⁷

In this research, the ability of Fenton's reagent, Potassium permanganate and potassium persulfate to act as chemical oxidants in the removal of hydrocarbons from crude oil polluted soils is evaluated. Gas chromatography (GC), a time tested method of hydrocarbon determination is employed to monitor the depletion of three broad hydrocarbon groups: BTEX, PAH and TPH providing evidence of remediation or otherwise.^{8,9}

Experimental

Six hundred grams (600 g) of the sieved soil samples were weighed into each of three 1L glass beakers with their pHs adjusted to acidic (pH 5-6.5), basic (pH 7.5-9), and neutral (pH 6.9-7.5) using NaOH and HCl. Each of the soil samples in the three 1 L glass beakers were then spiked with 20 ml of Bonny light crude oil from the Bomu oil field in Rivers state Nigeria. The soil-crude oil mixture in each of the containers were stirred to achieve homogeneity, allowed to stand for one week, and subsequently analyzed for their hydrocarbon contents.

Instrumentation

The amount of the three hydrocarbon components (TPH, BTEX AND PAH) were determined with a high resolution HRGC MEGA 2 series (FISONS instrument) Gas chromatograph (GC) equipped with a flame detector and the peak areas analyzed with an SRI model peak simple chromatography data system. A silica column of (30 m x 0.25µm x 25mm) was used.

TPH was analyzed at a column temperature of 60 °C for 2 minutes to 300 °C programmed at 12 °C min⁻¹ with nitrogen as the carrier gas. Hydrogen and air flow rate were 9 psi and 13 psi respectively. PAH was analyzed at a column temperature of 98°C for 1minute to 300 °C programmed at 80 °C min⁻¹ and air flow rates were 12 psi and 15 psi respectively. BTEX was analysed at the initial temperature of 30 °C for 1 minute then increased to 180 °C at 50 °C min⁻¹ and to 230 °C at 20 °C min⁻¹. Helium was used as the carrier gas.

Results and discussion

The removal of TPH by the three oxidants at acidic soil was encouraging. The striking thing about all the three oxidants is that they are not effective in the removal of the C₁₂-C₁₆ hydrocarbons. The C₉-C₁₁ and the C₁₇-C₂₃ hydrocarbons were almost completely removed especially by Fenton's reagent and potassium persulfate. There was an increased concentration of the C₁₂-C₁₆ hydrocarbons which could be as a result of the oxidative breakdown of the longer chain hydrocarbons to the short chain ones. This is shown in Table 1 and Figure 1.

Table 1. TPH concentration of the acidic soil samples in mg kg⁻¹ after treatment with the different oxidants

Hydrocarbon	Fenton's reagent	Potassium persulphate	Potassium permanganate
C ₉	-	-	-
C ₁₀	-	0.05	-
C ₁₁	-	0.07	0.25
C ₁₂	0.28	0.11	0.39
C ₁₃	0.75	0.42	0.63
C ₁₄	0.46	-	0.74
C ₁₅	0.24	0.65	0.82
C ₁₆	0.16	0.21	0.67
C ₁₇	-	0.01	-
C ₁₈	-	0.01	0.20
C ₁₉	-	0.01	0.05
C ₂₀	-	-	0.16
C ₂₁	-	0.21	0.02
C ₂₂	-	-	0.08
C ₂₃	-	-	0.01

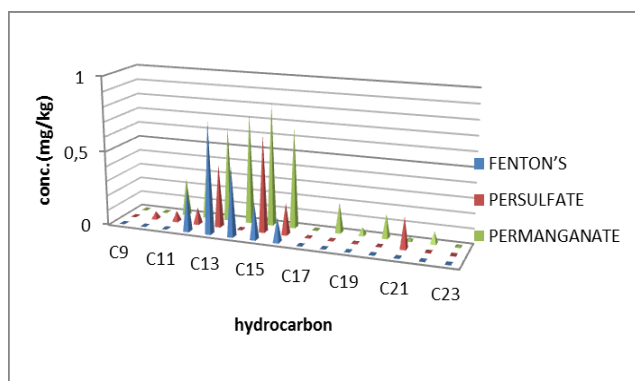


Figure 1. Chart showing the removal of the TPH from the acidic soil sample by the different oxidants

Table 2. TPH concentration of the basic soil samples in mg kg⁻¹ after treatment with the different oxidants

Hydrocarbon	Fenton's reagent	Potassium persulphate	Potassium Permanganate
C ₉	-	0.08	-
C ₁₀	-	0.32	-
C ₁₁	0.29	0.54	0.77
C ₁₂	0.45	0.79	1.66
C ₁₃	0.88	1.23	1.32
C ₁₄	1.04	-	0.88
C ₁₅	0.79	0.98	0.97
C ₁₆	0.24	0.62	0.84
C ₁₇	-	0.11	0.38
C ₁₈	-	-	0.23
C ₁₉	0.01	-	0.16
C ₂₀	-	-	0.11
C ₂₁	0.01	-	0.35
C ₂₂	-	-	0.10
C ₂₃	0.01	-	0.02

This trend is seen in acidic and basic soils but was not pronounced at the neutral soil. It may be suggested that the removal of crude oil aliphatic hydrocarbons from polluted soils using any of the three oxidants may not be pH dependent (Figure 1-3 and Table 1-3).

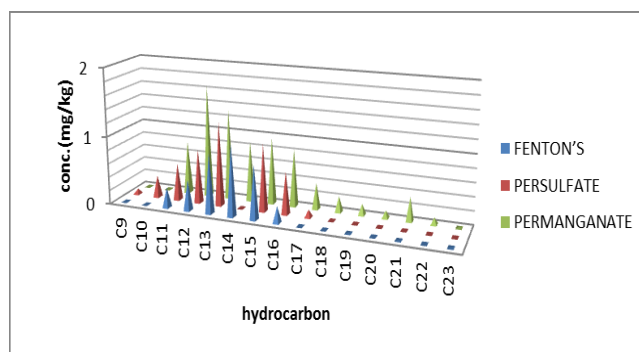


Figure 2. Chart showing the removal of the TPH from the basic soil sample by the different oxidants

The removal of PAH by the three oxidants at different pH proved to be interesting. Fenton's reagent and potassium permanganate were found to be very effective in the removal of PAHs at the acidic, neutral and basic pHs (Figures 4 and 5; table 4 and 4and 5) It is very clear that potassium persulfate is not a very good oxidant for the removal of PAHs from soils at all pHs. From the charts, this work shows that Fenton's reagent was the best oxidant for the removal of PAHs at the different pHs (probably due to the different mechanisms at work at the acidic and basic pHs). The removal of BTEX by the three oxidants at the different pHs gave mixed results. At acidic pH, Fenton's reagent proved to be effective for all the components except o-xylene. Potassium permanganate and persulfate were good for all except ethylbenzene (Figure 8).

At the neutral pH, efficiency of hydrocarbon (BTEX) removal by the three oxidants were reduced as only persulfate gave any reasonable removal as can be deduced from the chart. The removal at basic pH was good for Fenton's reagent and persulfate. This may be an indication that potassium permanganate may not be a good oxidant for the removal of BTEX from crude oil polluted soils. Other much stronger oxidizing permanganates like aluminum permanganate¹⁰ may be studied.

Table 3. TPH concentration of the neutral soil samples in mg kg⁻¹ after treatment with the different oxidants

Hydrocarbon	Fenton's reagent	Persulphate	Permanganate
C ₉	-	-	0.59
C ₁₀	-	0.38	0.54
C ₁₁	0.32	0.66	0.72
C ₁₂	0.57	0.89	0.94
C ₁₃	0.96	-	1.21
C ₁₄	-	1.08	0.60
C ₁₅	1.33	0.75	1.06
C ₁₆	0.84	0.32	0.79
C ₁₇	0.21	0.05	0.27
C ₁₈	0.01	0.05	0.21
C ₁₉	0.05	0.05	0.19
C ₂₀	-	0.03	-
C ₂₁	0.22	0.04	0.48
C ₂₂	0.01	0.02	0.07
C ₂₃	0.02	0.01	0.05

Table 4. PAH concentration of the acidic soil samples in mg kg⁻¹ after treatment with the different oxidants

PAH	Fenton's reagent	Persulfate	Permanganate
Acenaphthene	0.19	17.85	1.65
Phenanthrene	-	6.25	0.87
Anthracene	0.13	4.87	-
Fluoranthene	0.18	1.55	-
Pyrene	-	0.89	-
Benanthracene	-	18.47	-
Naphthalene	-	-	-
Chrysene	-	-	-
Fluorene	-	11.17	0.62
Dibenzothiophene	-	-	1.43
Acenaphthylene	0.11	1.93	0.74

Table 5. PAH concentration of the neutral soil samples in mg kg⁻¹ after treatment with the different oxidant

PAH	Fenton's reagent	Persulfate	Permanganate
Acenaphthene	0.32	33.18	2.87
Phenanthrene	0.59	6.4	0.36
Anthracene	0.73	11.87	0.54
Fluoranthene	-	3.06	0.22
Pyrene	-	1.53	-
Benanthracene	-	4.29	-
Naphthalene	-	2.23	0.99
Chrysene	-	-	-
Fluorene	-	19.99	0.73
Dibenzothiophene	-	-	2.03
Acenaphthylene	0.11	3.5	1.92

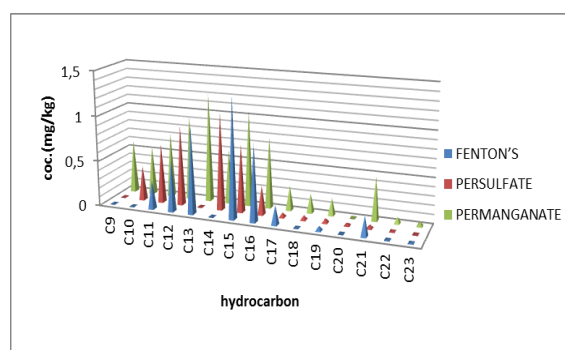
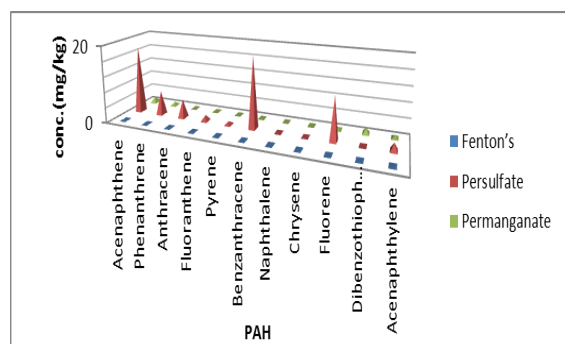
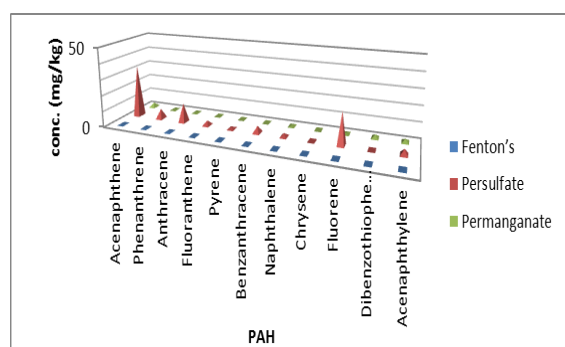
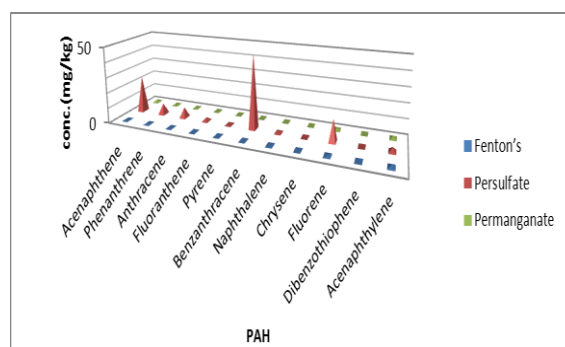
**Figure 3.** Chart showing the removal of the TPH from the neutral soil sample by the different oxidants**Figure 4.** Chart showing the removal of the PAH from the acidic soil sample by the different oxidants**Figure 5.** Chart showing the removal of the PAH from the neutral soil sample by the different oxidants**Figure 6.** Chart showing the removal of the PAH from the basic soil sample by the different oxidants

Table 6. PAH concentration of the basic soil samples in mg kg⁻¹ after treatment with the different oxidants

PAH	Fenton's reagent	Persulfate	Permanganate
Acenaphthene	0.28	24.09	1.97
Phenanthrene	0.65	7.30	0.79
Anthracene	-	6.91	1.10
Fluoranthene	-	2.43	0.44
Pyrene	0.09	1.12	0.13
Benanthracene	-	48.12	-
Naphthalene	0.47	1.87	-
Chrysene	-	-	0.05
Fluorene	0.88	14.21	1.63
Dibenzothiophene	-	-	-
Acenaphthylene	1.33	2.76	1.67

Table 7. BTEX concentration of the acidic soil samples in mg kg⁻¹ after treatment with the different oxidants

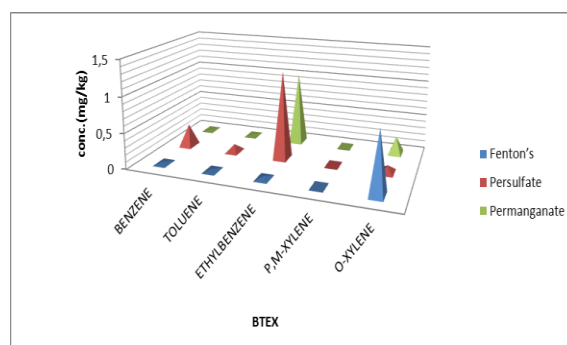
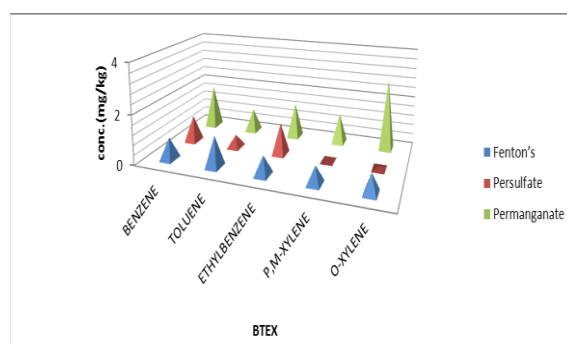
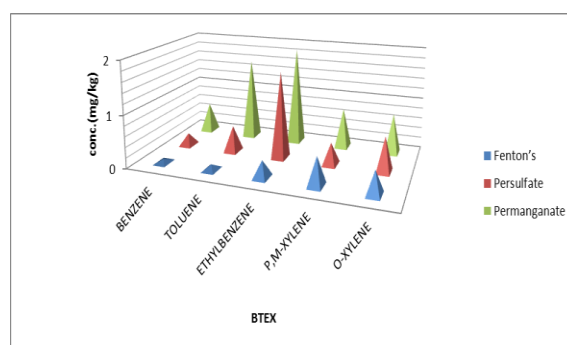
BTEX (mg kg ⁻¹)	Fenton's reagent	Persulfate	Permanganate
Benzene	0.022	0.320	0.006
Toluene	0.021	0.109	0.009
Ethylbenzene	0.034	1.237	1.022
p-Xylene	-	-	-
m-Xylene	-	-	-
o-Xylene	0.854	0.101	0.244

Table 8. BTEX concentration of the neutral soil samples in mg kg⁻¹ after treatment with the different oxidants

BTEX (mg kg ⁻¹)	Fenton's reagent	Persulfate	Permanganate
Benzene	0.887	1.072	1.773
Toluene	1.230	0.516	0.956
Ethylbenzene	0.762	1.262	1.422
p- and m-Xylene	0.699	0.009	1.209
o-Xylene	0.763	0.102	2.902

Table 9. BTEX concentration of the basic soil sample in mg kg⁻¹ after treatment with the different oxidants

BTEX (mg kg ⁻¹)	Fenton's reagent	Persulfate	Permanganate
Benzene	0.069	0.236	0.566
Toluene	0.103	0.500	1.573
Ethylbenzene	0.321	1.656	1.884
p- and m-Xylene	0.533	0.413	0.763
o-Xylene	0.435	0.660	0.763

**Figure 7.** Chart showing the removal of the BTEX from the acidic soil sample by the different oxidants**Figure 8.** Chart showing the removal of the BTEX from the neutral soil sample by the different oxidants**Figure 9.** Chart showing the removal of the BTEX from the basic soil sample by the different oxidants

Conclusion

This work has shown that Fenton's reagent, Potassium permanganate and potassium persulfate are good oxidants for management of Bonny light crude oil polluted soils. The results show that the oxidants especially Fenton's reagent and potassium persulfate will work well in sites polluted by light crudes that are dominated by aliphatic hydrocarbons and one-ring aromatics. The research also highlighted that potassium persulfate may not be well suited for the remediation of sites polluted by heavy crudes or asphaltic crudes that are dominated by polycyclic aromatic hydrocarbons. Potassium permanganate was found to be effective in the removal of aromatic hydrocarbon at acidic pH. Fenton's reagent was shown to be very effective in the

removal of all hydrocarbons from Bonny light crude oil polluted soils especially at acidic pH medium.

Acknowledgements

The authors are thankful to Amni International Petroleum company for the GC analysis of the many soil samples.

References

- ¹Osuji, L. C., Egbuson, E. J. and Ojinnaka, C. M. *Chem. Ecol.* **2005**, *21*(1), 1.
- ²Osuji, L. C. *Afr. J. Interdiscip. Stud.*, **2002**, *3*, 11.
- ³*Environmental Business*, **2010**. <http://www.vironbusines.com>
- ⁴Karpenko, O., Lubenets, V., Karpenko, E. and Novikov, V. *Chem. Technol.*, **2009**, *3*(1), 41
- ⁵Liang, C., Bruell, C. J and Sperry, K. L. *Soil and Sediment Contam.*, **2003**, *12*(2), 207
- ⁶Watts, R. J., *Remediation A*, **1992**, 413.
- ⁷Scullion, J., *J. Plant Natural Soil Sci.*, **2006**, *164*, 631.
- ⁸Osuji, L. C. and Achugasim, O., *Chem. Biodiversity*, **2007**, *4*, 424.
- ⁹Osuji, L. C. and Achugasim, O. *J. Appl. Sci. Environ. Manag.* **2010**, *14*(2), 17.
- ¹⁰Kótai, L., Keszler, A., Pato, J., Holly, S., Banerji, K. K., *Ind. J. Chem. Sect. A. Inorg. Bio-Inorg. Phys. Theor. Anal. Chem.* **1999**, *38*(9), 966., Kótai, L., Banerji, K. K. *Synth. React. Inorg. Metal-Org. Chem.* **2001**, *31*(3), 491., Kótai, L., Sajó, I. E., Gács, I., Sharma, P. K., Banerji, K. K., *Z. Anorg. Allgem. Chem.* **2007**, *633*(8), 1257., Kótai, L., Gács, I., Sajó, I. E., Sharma, P. K., Banerji, K. K., *Trends Inorg. Chem.*, **2009**, *11*, 25-104.

Received: 15.12.2012.
Accepted: 12.01.2013.